UNLIKE INTERACTIONS IN SIMULATED METHANE CLATHRATE HYDRATES

Matthew Lasich

Submitted in fulfillment of the degree of Doctor of Philosophy in Engineering, School of Engineering, University of KwaZulu-Natal

June 2014

Supervisor: Prof. D. Ramjugernath

Co-supervisors: Prof. A.H. Mohammadi, Prof. K. Bolton, and Prof. J. Vrabec

COLLEGE OF AGRICULTURE, ENGINEERING AND SCIENCE

DECLARATION 1 - PLAGIARISM

I, Matthew Lasich, declare that:

1. The research reported in this thesis, except where otherwise indicated, is my original research.
2. This thesis has not been submitted for any degree or examination at any other university.
3. This thesis does not contain other persons' data, pictures, graphs or other information, unless specifically acknowledged as being sourced from other persons.
4. This thesis does not contain other persons' writing, unless specifically acknowledged as being sourced from other researchers. Where other written sources have been quoted, then:

a. Their words have been re-written but the general information attributed to them has been referenced

b. Where their exact words have been used, then their writing has been placed in italics and inside quotation marks, and referenced.

5. This thesis does not contain text, graphics or tables copied and pasted from the Internet, unless specifically acknowledged, and the source being detailed in the thesis and in the References sections.

Signed ……

Matthew Lasich

As the candidate's supervisor I agree/do not agree to the submission of this thesis

Signed ……

Prof. Deresh Ramjugernath

COLLEGE OF AGRICULTURE, ENGINEERING AND SCIENCE

DECLARATION 2 - PUBLICATIONS

DETAILS OF CONTRIBUTIONS TO PUBLICATIONS

Paper I: M. Lasich, A.H Mohammadi, K. Bolton, J. Vrabec, D. Ramjugernath, On the application of binary correction factors in lattice distortion calculations for methane clathrate hydrate, Philosophical Magazine 94 (2014) 974-990.
Contribution: I designed the study with suggestions from Prof. Mohammadi. I performed the calculations and wrote the manuscript with suggestions from Profs. Ramjugernath, Mohammadi, Bolton and Vrabec.

Paper II: M. Lasich, A.H Mohammadi, K. Bolton, J. Vrabec, D. Ramjugernath, Phase equilibria of methane clathrate hydrate from grand canonical Monte Carlo simulations, Fluid Phase Equilibria 396 (2014) 47-54.
Contribution: I designed the study and performed the simulations and calculations. I wrote the manuscript with suggestions from Profs. Ramjugernath, Mohammadi, Bolton and Vrabec.

Paper III: M. Lasich, A.H Mohammadi, K. Bolton, J. Vrabec, D. Ramjugernath, Influence of unlike dispersion interactions in modeling methane clathrate hydrate, Fluid Phase Equilibria 381 (2014) 108-115.
Contribution: I designed the study with suggestions from Prof. Vrabec. I performed the simulations and calculations. I wrote the manuscript with suggestions from Profs. Ramjugernath, Mohammadi, Bolton and Vrabec.

Signed …… ……
Mr. Matthew Lasich Prof. Deresh Ramjugernath

…… ……
Prof. Amir Hossein Mohammadi Prof. Kim Bolton

……
Prof. Jadran Vrabec

ACKNOWLEDGEMENTS

I would like to thank my supervisor Prof. Deresh Ramjugernath, and my co-supervisors Profs. Amir H. Mohammadi, Kim Bolton and Jadran Vrabec for their guidance and support during the preparation of this thesis and associated scientific publications. I would also like to thank my friends and co-workers in the Thermodynamics Research Unit at the University of KwaZulu-Natal for providing a stimulating working environment. Thanks are also due to the South African Research Chairs Initiative of the Department of Science and Technology and National Research Foundation as well as the Swedish International Development Cooperation Agency and the NRF's Focus Area and Thuthuka Programmes. I also owe thanks to the CSIR Centre for High Performance Computing in Cape Town and the University of Borås in Sweden for allowing me to use their computing resources and Stiftelsen FöreningsSparbanken for financing the latter's facilities. Lastly, I would like to thank my friends, my family, and Heike for their support during my time as a doctoral student.

ABSTRACT

Clathrate hydrates are an ice-like substance consisting of networks of water molecules, held together by hydrogen bonds, enclosing trapped gas molecules. Natural gas clathrate hydrates (in which the trapped gas species is chiefly methane) are of interest in the field of offshore gas exploitation, where they frequently form blockages in natural gas pipelines. Knowledge of the phase equilibria of methane clathrate hydrate can thus reduce the overall monetary cost of natural gas extraction.

Computer simulation of molecular systems is useful to understand fundamental mechanisms, and serves as a complementary method to laboratory experiments in the study of chemical systems. The Lennard-Jones potential is frequently used to describe intermolecular interactions in molecular simulations. Correction factors are often applied to the Lennard-Jones potential, although the effect of these correction factors on the behaviour of simulated molecular systems is not fully understood.

This thesis examines the effect of Lennard-Jones correction factors on simulated methane clathrate hydrates using three different computational approaches: lattice distortion theory, grand canonical Monte Carlo simulations (which emulate gas adsorption into the clathrate lattice), and direct estimation of the heat of dissociation coupled with the Clausius-Clapeyron equation. In addition, the use of the results of grand canonical Monte Carlo simulations to infer phase equilibria was demonstrated in this thesis.

The application of Lennard-Jones correction factors in lattice distortion calculations was found to not be viable, due to the extreme sensitivity of the perturbation potential (the quantity of interest in this theory) to changes in the values of the correction factors. Unlike interactions were found to weakly influence methane adsorption into the clathrate hydrate crystal, and so the application of correction factors in grand canonical Monte Carlo simulations is demonstrated to be ineffectual. The direct estimation of the heat of dissociation was shown to be viable when matching to calorimetric data, and the inference of phase equilibria by coupling the Clausius-Clapeyron equation with this approach was shown to yield agreeable results.

TABLE OF CONTENTS

LIST OF TABLES

LIST OF FIGURES

CHAPTER ONE: INTRODUCTION AND BACKGROUND

1.1. OUTLINE OF THE PRESENT STUDY

This thesis examines the application of binary correction factors to the Lennard-Jones (LJ) potential between the water molecules that constitute the hydrate lattice and enclathrated methane molecules. A special focus is given to the unlike dispersion interaction, due to polarizability issues which will be discussed further on in the text. In particular, the effect of such correction factors on phase equilibria and structure of clathrate hydrates is studied. This is significant, since the application of binary correction factors is frequently employed to fit a desired simulated property to its experimental counterpart in order to refine the molecular force fields being used [1-6]. Even though fitting LJ correction factors to experimental data is commonplace, the response of simulated systems to changes in these parameters is not well studied in most cases, and has not been investigated in any detail for clathrate hydrates. Numerous difficulties can arise, such as the 'best fit' binary correction factor not fitting all properties sufficiently well, or the need to employ multiple, heterogeneous correction factors [3].

It should be noted that in this thesis, phase equilibria of clathrate hydrates were not simulated directly, but were estimated using properties obtained via molecular simulations. Calculation of phase equilibria was undertaken using the statistical mechanical van der Waals-Platteuw theory (vdWP) [7] which is a standard approach [8]. Various parameters estimated via molecular computations were then used in the subsequent phase equilibrium calculations. This can reduce the need for experimental measurements in some cases, or improve the estimation of phase equilibria using standard techniques.

Lattice distortion theory [9] is attractive, especially when it comes to LJ parameter fitting, because only two calculations are required. Therefore, this approach was investigated in chapter two. The use of lattice distortion theory to adjust or correct calculated phase equilibria is established in the literature [9], and so the theory was used as is. The response of the properties of the simulated methane hydrate to changes in the unlike LJ parameters was the subject of investigation. Moreover, the behavior of the calculated perturbation potential was investigated, to ascertain the feasibility of using this approach to fit LJ correction factors. The perturbation potential is the quantity of interest in lattice distortion theory, and was estimated using lattice calculations.

Grand canonical Monte Carlo (GCMC) simulations are another approach to simulating clathrate hydrate systems. An advantage is that the occupancies of the cages within the hydrate lattice are found directly. However, adsorption isotherms fitted to the results of GCMC simulations had not previously been

employed to estimate clathrate hydrate phase equilibria. Therefore, chapter three covers the use of simulated adsorption isotherms to predict clathrate hydrate phase equilibria. The sensitivity of this approach to the force fields used was also examined.

Chapter four covers the behavior of simulated adsorption isotherms and associated phase equilibria to changes in the unlike LJ dispersion term, ε_{ij}. This information can be of great use in trying to compare phase equilibria calculated from GCMC simulations to experimental data in order to fit LJ binary correction factors. Additionally, chapter four considers a direct calculation of the heat of dissociation coupled with a phase equilibrium calculation derived from the Clausius-Clapeyron equation. The effect of ε_{ij} on properties determined from this approach is also investigated. A drawback of the second method is that the occupancy behavior cannot be studied directly, although the calculation of phase equilibria is greatly simplified.

Lastly, chapter five outlines the main findings of the thesis, and places the findings of the three separate studies in context, both in terms of the behavior of LJ correction factors in general and in relation to the findings of the three studies themselves. The influence of unlike LJ interactions on the properties of simulated clathrate hydrate systems are discussed. Conclusions are drawn, and suggestions are made as to the directions that future work may take.

1.2. HISTORY OF GAS HYDRATE RESEARCH

The earliest investigations of gas hydrates took place in the first half of 19th century [10], with chlorine hydrate being studied early on [11]. Gas hydrates containing light hydrocarbons such as methane (CH_4), ethane (C_2H_6), and propane (C_3H_8) were reported towards the end of the 19th century [12]. Around the turn of the 20th century, the equilibrium temperatures at atmospheric pressure of several different gas hydrate systems were reported [13].

The earliest encounters with gas hydrates in industry came in the form of pipe blockages during the production and transportation of natural gases [14]. To this day, gas hydrates are a leading concern in deep water off-shore oil and gas exploitation [8,15]. Therefore knowledge of the conditions under which hydrates remain stable is of relevance to the oil and gas industries.

1.3. DESCRIPTION OF GAS HYDRATE STRUCTURES

Gas hydrates, also known as clathrate hydrates, consist of a network of hydrogen-bonded water molecules forming a ‘host’ cage-like structure around ‘guest’ gas molecules. The water molecules form

a three-dimensional lattice with cavities which may be occupied by gas molecules. All of the cages do not necessarily need to be occupied for the hydrate to be stable at a given set of thermodynamic conditions. For this reason, they are known as 'non-stoichiometric' hydrates, as opposed to the stoichiometric hydrates of salt species.

There are three gas hydrate structures commonly found in nature or in industry; namely, structure I (sI), structure II (sII), and structure H (sH). Other structures are also possible, such as the amorphous clathrate hydrate consisting of irregularly sized polyhedral 'cages' [16], although the three aforementioned structures are most often encountered [17]. These different structures consist of various combinations of five types of hydrogen-bonded water cages. The sI and sII hydrates are most frequently encountered, as they may form from pure gases. The sH hydrate, however, requires a combination of a small gas species (such as CH_4) along with a large gas species (such as cyclopentane), in order to stabilize the differently-sized cages within the gas hydrate lattice. Figure 1.1 illustrates the different hydrate structures, along with examples of common hydrate-forming gases for each type of hydrate structure. Table 1.1 displays a summary of the crystalline structures of the sI, sII, and sH gas hydrates.

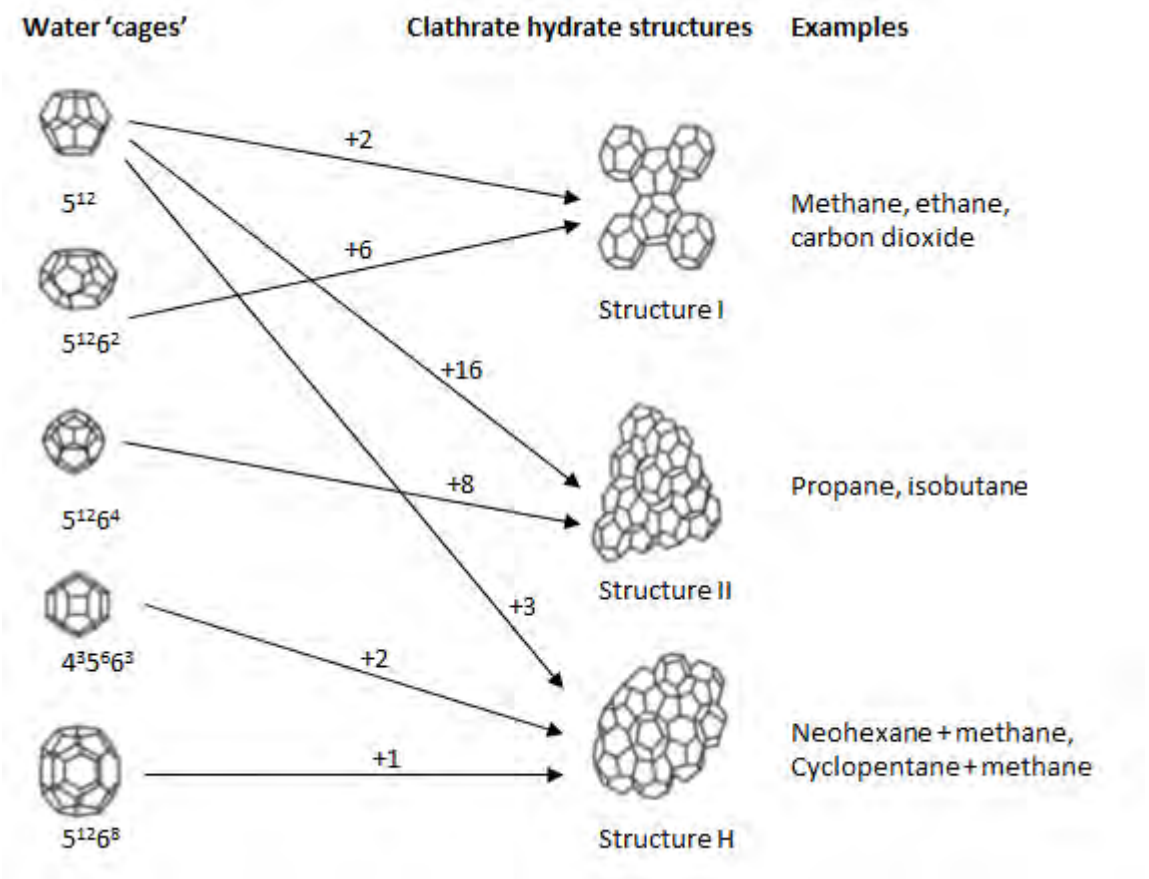

Figure 1.1. Diagram of the three common gas hydrate structures. The structure I and structure II unit cells contain two types of cages, whereas the structure H unit cell consists of three types of cages.

Hydrate structure	sI		sII		sH		
Crystal system	Primitive cubic		Face-centered cubic		Hexagonal		
Space group	*Pm3n*		*Fd3m*		*P6/mmm*		
Cavity type	Small	Large	Small	Large	Small	Medium	Large
Cavity description	5^{12}	$5^{12}6^2$	5^{12}	$5^{12}6^4$	5^{12}	$4^3 5^6 6^3$	$5^{12}6^8$
Cavities/unit cell	2	6	16	8	3	2	1
Cavity radius (Å)	3.95	4.33	3.91	4.73	3.91	4.06	5.71
H_2O/unit cell	46		136		34		
Unit cell formula	$2S{\cdot}6L{\cdot}46H_2O$		$16S{\cdot}8L{\cdot}136H_2O$		$3S{\cdot}2M{\cdot}1L{\cdot}34H_2O$		

Table 1.1. Structural properties of the structure I, II, and H gas hydrates. Small, medium, and large cavities are denoted by S, M, and L, respectively [18].

1.4. POTENTIAL USES OF GAS HYDRATES

Apart from their occurrence as a nuisance in oil and gas exploitation, gas hydrates also hold several potential uses for the future. Natural gas hydrates, consisting mostly of methane hydrate, are found all over the world in the deep ocean, as well as in the permafrost of the tundra regions [8]. If these deposits were exploited, a vast energy reservoir could be unlocked, albeit in the form of a fossil fuel. The quantity of natural gas in these deposits is staggering: approximately 10^{16} m^3 [19,20]. Moreover, some estimates suggest that more organic carbon reserves may be present in the form of naturally-occurring methane hydrates than in all other forms of fossil fuels [21].

Gas hydrates can also be used for energy storage, in the form of a hydrogen (H_2) storage medium [22]. This is largely due to the fact that the storage medium (essentially just water) is relatively cheap and abundant, and transport and storage of hydrogen fuel may be less dangerous when using gas hydrates as opposed to pressurized gas canisters. The challenge associated with gas hydrates as a hydrogen storage medium lies in its relatively low storage capacity of approximately 4 wt % of H_2 at moderate pressure conditions [23]. The storage capacity and formation pressure can be made more practical by using 'hydrate promoter' chemicals, as demonstrated in the literature (e.g., [24]).

Additional uses for gas hydrate technology include gas scrubbing [25] and carbon dioxide sequestration medium [26]. In such scenarios, an industrial flue gas could be cleaned by using a pressure vessel as a hydrate reactor. A hydrate promoter or blend of promoters can then be added to the hydrate + gas system to form the hydrate closer to ambient conditions. Such processes, once perfected for industrial application, may have lower energy and material costs to reduce industrial emissions, as compared to current processes (such as gas absorption). Alternatively, gas hydrates could be used for gas-phase

industrial separations, using the principles outlined above. The same potential benefits of lower material and energy costs may also apply here.

Water desalination is another potential future use for gas hydrates [27]. Desalination is well-known to be an energy-intensive procedure, and perhaps, a more cost-effective process making use of gas hydrates can be implemented in the future.

A potential application for gas hydrates which may result in widespread use of associated technologies is industrial separation processes. Prominent studies from the literature include oil + gas mixtures [28,29], and ionic liquid mixtures [30,31]. In these cases, gas hydrate technology can have a lower energy cost than conventional methods that employ heat addition. A larger overview of potential gas hydrate applications can be found in the literature [32].

1.5. MOLECULAR SIMULATIONS

Before going into details on molecular simulation of clathrate hydrates (see section 1.7), it is instructive to first discuss molecular simulation itself. Briefly, molecular simulation involves simulating the interactions of typically several hundred molecules, and examining the behaviour of the system itself, as well as any derived properties (such as enthalpy). Simulations must account for the different types of interactions that can occur between molecules, such as the purely electrostatic, as well as the weaker London 'dispersion' forces. In addition, interactions occurring within the molecules themselves should also be accounted for, such as bond stretching or bending. However, intramolecular interactions are not always significant for the purposes of molecular simulations, and their application depends upon the sizes of the molecules being considered. In the case of the studies presented in this thesis, intramolecular interactions were not considered at all, due to the small sizes of the molecules involved (i.e., water and methane).

Molecular simulation is an established tool for investigating the behaviour of chemical systems of interest to industry [33]. Simulating systems at the molecular level may reveal information which may be inaccessible at the macroscopic scale, whilst also allowing for any conceivable set of thermodynamic conditions to be investigated.

A significant drawback of simulations, however, lies in the 'force fields' used to represent intermolecular and intramolecular interactions. Such force fields account for both the electrostatic interactions (using the electrostatic pair potential function), and the van der Waals forces (usually described by the LJ potential energy function [34]). These only approximate the behaviour of real molecules, and cannot readily take into account, for example, quantum mechanical considerations

without considerably increasing the computational cost of the simulation.

Shortcomings of particular sets of force fields may be found in the literature, such as for the polyethylene + water system [1]. A correction can be applied to a particular type of interaction (e.g., electrostatic or van der Waals) between specific interaction sites (e.g., water-methyl). In the case of the aforementioned study, corrections were applied by comparing phase equilibrium data for alkanes and water, and adjusting the water-methyl dispersion energy term.

In another study [35], the excess chemical potential of methane in liquid water was used as the reference property to correct the force fields. In this case too, the correction was applied to the unlike dispersion term of the LJ potential. In summary then, while simulations are indeed useful, they should not replace laboratory experiments entirely. Instead, they may be employed in a complementary fashion, with laboratory experiments being used to develop a set of reference data to correct the force fields. The corrected force fields may then be used to investigate other sets of conditions thereafter, thus reducing research costs by eliminating the need to carry out extensive laboratory measurements.

There are two broad categories of molecular simulation approaches [33]: molecular dynamics (i.e., Newtonian motion), and Monte Carlo (random sampling). Molecular dynamics (MD) yields information about the dynamic, or time-dependent properties of the system. Essentially, MD involves the simulation of an initial molecular configuration undergoing motion according to the forces acting upon the particles due to the electrostatic and van der Waals forces these particles exert upon each other. This approach is generally useful when studying the transport (i.e., heat, momentum and mass transfer) characteristics of a system or, in the case of gas hydrates, to investigate the nucleation process in much greater detail than is possible in the laboratory. Monte Carlo (MC) methods [36] are most useful when the equilibrium (e.g., phase equilibrium) properties of a system are being investigated. In essence, MC simulations involve the application of random moves to each particle of the molecular system, until equilibrium is attained. Once the system is stable, properties of the system may be studied through the application of tiny, random fluctuations to the system. These fluctuations may influence the energy, volume, or composition of the system, and thus the behaviour of the system under equilibrium may be studied.

A concluding remark of significance on MD versus MC simulations is derived from the ergodic hypothesis [37]. This hypothesis states that for an isolated system evolving over time according to the laws of mechanics, in which the relative frequency at which any permitted microstate will be reached is the same, the properties averaged over a succession of temporal states will be the same as the ensemble averages. In other words, properties averaged over time at equilibrium (obtained from MD) will be same as the average over a large number of randomly selected states (obtained via MC).

Therefore, in principle, one could employ either MD or MC simulations to determine equilibrium properties.

Ultimately, if an MC simulation is allowed to proceed for a sufficiently large number of MC steps, the average values of the system properties will be the same as for an MD simulation at equilibrium. Usually though, MD simulations take significantly longer than MC simulations to reach equilibrium, and so MC simulations are often employed instead of MD simulations to determine equilibrium properties. It can also be noted here that there are other options for calculating properties from molecular-level computations besides MC and MD simulation, which are frequently undertaken within the context of pair potentials. For example, quantum chemistry and lattice dynamics calculations can also yield information about the properties of matter.

1.6. INTERMOLECULAR INTERACTIONS

In the present study, all intermolecular interactions were considered to fall under two categories: electrostatic and van der Waals (which, as modeled in this study, encompasses an attractive dispersion term as well as repulsion at close intermolecular ranges). The electrostatic potential energy $U_{e\text{-}}$ between two point charges i and j is given by [38,39]:

$$U_{e\text{-}} = q_i \, q_j \, / \, (\, 4 \, \pi \, \varepsilon_0 \, r_{ij} \,) \qquad (1.1)$$

where q is the value of the electrostatic charge and r_{ij} is the separation between the interacting sites. The van der Waals interactions were described using the aforementioned LJ potential:

$$U_{LJ} = 4 \, \varepsilon_{ij} \, [\, (\, \sigma_{ij} \, / \, r_{ij} \,)^{12} - (\, \sigma_{ij} \, / \, r_{ij} \,)^{6} \,] \qquad (1.2)$$

where ε_{ij} (the energy or dispersion parameter) is the depth of the potential energy well, and σ_{ij} (the size parameter) is the distance r_{ij} at which U_{LJ} is zero. For unlike interactions, the Lorentz and Berthelot combining rules [40,41] are commonly used for the size and dispersion terms, respectively. These rules can be summarized, in a generalized form, as follows:

$$\sigma_{ij} = 0.5 \, l_{ij} \, (\, \sigma_{ii} + \sigma_{jj} \,) \qquad (1.3)$$

$$\varepsilon_{ij} = k_{ij} \, (\, \varepsilon_{ii} \, \varepsilon_{jj} \,)^{0.5} \qquad (1.4)$$

In the original forms of these combining rules, parameters l_{ij} and k_{ij} are not considered at all. However,

in the case that a correction is applied to the unlike interactions, then it can be seen that the original Lorentz-Berthelot rules are merely special cases where correction factors are set to unity. Figure 1.2 illustrates the LJ potential between both like and unlike molecules, for the case in which one species has size and dispersion terms which have double the magnitude of the other.

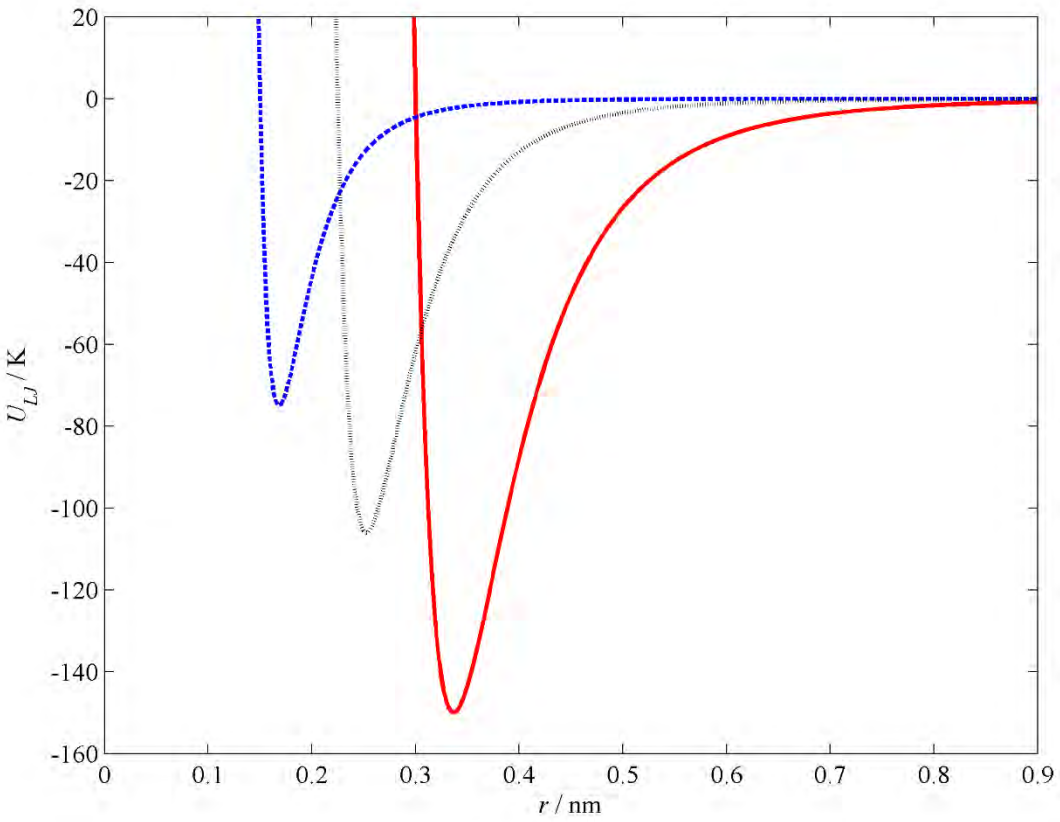

Figure 1.2. LJ potential (U_{LJ}) for two LJ particles; ε_{11} = 150 K, σ_{11} = 0.3 nm, ε_{22} = 75 K, and σ_{22} = 0.15 nm. (-) like interactions for species 1, (- -) like interactions for species 2, (···) unlike interaction between 1 and 2.

In the case of clathrate hydrate systems, it was shown [42] that the unaltered Lorentz-Berthelot rules are inadequate to describe the gas + water interactions, in general. Haslam and co-workers [42] suggested the use of correction factors (e.g., l_{ij} and k_{ij}) to adjust the unlike LJ interactions to more accurately describe clathrate hydrates. The merits of various combining rules (the Lorentz-Berthelot rules are merely one from a set of many), and the deficiencies of the Lorentz-Berthelot rules for studying phase equilibria has also been discussed in the literature [43]. The topic of combining rules in clathrate hydrate systems has not been studied in any detail in the literature as yet, apart from two limited studies [35,44]. In the former investigation [35], k_{ij} was determined (for a single force field combination) from the excess chemical potential of dilute gaseous methane in liquid water, and applied to direct coexistence MD simulations of methane hydrate. In the latter study [44], the effects on cage occupancy of deviations to the standard Lorentz-Berthelot rules were examined for the argon hydrate system along

the dissociation pressure curve. It should be noted here that in experimental work and equation of state modeling, interaction parameters such as k_{ij} are often included in mixing or combining rules such that the mixture property of interest is multiplied by $(1 - k_{ij})$. In this thesis, and the associated publications, the correction factor is a ratio of the unlike interaction to the reference Lorentz/Berthelot case, where applicable.

It can be noted that there are many other combining rules, and a discussion of 11 of them may be found in the literature [45]. However, the net result of any set of combining rules as simply the unlike interaction between particles, and thus it is convenient to compare to a common reference (and since the Lorentz and Berthelot rules are ubiquitous in molecular simulation, they make a very convenient reference). Moreover, a recent study [46] has shown that for a large set of different combining rules, the difference in unlike interactions never deviated more than about 8 % from the unlike energy term determined by the Berthelot rule, and no more than 1 % from the unlike size term determined by the Lorentz rule. Therefore, while there are many different sets of combining rules, they deviate less from the Lorentz and Berthelot rules than was achieved by application of the correction factors k_{ij} and l_{ij} in this thesis.

1.7. SIMULATIONS OF CLATHRATE HYDRATES IN THE LITERATURE

As stated in the preceding subsections, there are several different approaches to molecular simulations. For clathrate hydrate systems, various methods have been used, with varying degrees of success, both in terms of the simulated systems' approximation to physical reality, and in terms of the amount of useful information which each methodology yields.

MD simulations can provide useful information on the physical mechanisms at work during hydrate formation [47-53]. In addition, certain equilibrium properties can be investigated using MD simulations, such as lattice constants [54,55], distortion energies [9,56,57], or even thermodynamic stability [2]. It should be stated, however, that use of MD simulations to determine thermodynamic stability does not yield information about the quantity of adsorbed gas, and is therefore of no use in estimating adsorption isotherms or molecular storage capacity.

Tanaka was the first to use the grand canonical ensemble to simulate clathrate hydrates [58]. Much subsequent work on a variety of clathrate hydrate systems has followed [18,44,59-62]. Such simulations provide information about the equilibrium quantity of adsorbed gas in the clathrate hydrate phase, thus providing adsorption isotherms. This information is useful for analyzing the phase behavior of solid + gas systems, such as clathrate hydrates in equilibrium with the gas phase.

First principles approaches, such as quantum chemistry or density functional theory, have also been used to investigate clathrate hydrate systems [63-65]. First principles calculations are rigorous, and can provide useful information about electronic structure, storage capacity, or thermodynamic stability. Such calculations, however, are computationally much more expensive and in cases in which simple molecular mechanics force fields can provide an equally realistic description of the physical system, the less computationally expensive approach is preferred.

It should also be noted that one of the aforementioned studies [64] used both quantum chemistry and molecular mechanics lattice calculations to study clathrate hydrates and water ice. Lattice calculations can provide information about the vibrational spectra and lowest energy structures of crystalline systems, and have been used by several researchers to investigate clathrate hydrates [66-69]. Knowledge of the vibrational spectra and crystal structures is of interest in understanding the fundamental physics of clathrate hydrates, although information about gas adsorption and thermodynamic stability is not obtained by this approach.

Thus it is apparent that not all of the possible information about the physical properties of clathrate hydrate systems can be readily obtained by means of a single type of calculation. In terms of the variety of quantities which can be studied, first principles calculations are the most attractive option, but their vast computational cost precludes their general use at present. Molecular mechanics force fields, when used in a combination of methods, are therefore an attractive approach to studying clathrate hydrate systems. Computational methods in general, however, should be considered as complementary tools, to be used in conjunction with laboratory experiments [70]. Molecular simulations can, however, provide insight into the physical mechanisms behind phenomena observed in the laboratory. This is afforded by the ability to manipulate the molecular properties of the matter being simulated. This can enable the study of hypothetical chemical species which do not exist in reality, but which can show the physics at work behind processes such as adsorption, nucleation, or structural configuration. In addition, thermodynamic conditions which can be, at the very least, infeasible in the laboratory can be studied without much effort.

1.8. BACKGROUND TO LATTICE DISTORTION THEORY

It was known for some time before the lattice distortion theory of Zele and co-workers [9] that guest gas molecules may distort the host water crystal in clathrate hydrate systems [71-75]. This observation was contradictory to one of the assumptions of the vdWP theory [7] so often used to describe clathrate hydrate phase equilibria: The guest species does not influence the host water-water interactions. Zele and co-workers therefore developed a model which applied a guest-dependent correction to the vdWP calculation which accounted for the effect of the adsorbed gas species on the water-water interactions:

Lattice distortion theory.

In vdWP and lattice distortion theory, the macroscopic quantity of interest is the so-called 'reference potential'; this is the difference between the chemical potential of water in the hydrate phase and the chemical potential of water in a hypothetical empty hydrate crystal, at a predefined reference point. The reference point usually employed is the ice point of water (i.e., T = 273.15 K and P = 0 MPa). The chemical potential of water in the hypothetical empty clathrate hydrate is considered as the reference state when analysing both the liquid and hydrate phases by means of vdWP theory. This reference state is identical for all guest gas species in the original vdWP theory. With lattice distortion theory, Zele and co-workers proposed that the reference state should be guest-dependent, by incorporating a perturbation term to account for the distortion of the hydrate structure. In this way, the lattice of the reference state distorts to the same extent as the lattice of the real hydrate.

Zele and co-workers noted, however, that in the case of expansion of the lattice, the crystal would become destabilised, a factor which should be compensated for by an increase in the guest-host interactions. This increase would result in the chemical potential of water in the filled lattice becoming equal to the chemical potential of water in the other water-containing phase at equilibrium (ice below the ice point, and liquid water above it). Therefore, the reference chemical potential should increase due to presence of a large guest gas species, which would be due to both the interaction energy itself as well as entropy. As discussed in Chapter Two, this change in the reference chemical potential was described in terms of properties which were readily determined by molecular-level computations.

1.9. BACKGROUND TO GCMC SIMULATIONS

GCMC simulations fall under the broad category of 'random sampling' MC simulations (see section 1.5 above). In such simulations, random moves are applied to a system of particles in order to determine equilibrium properties. It is clear that for such simulations, not all variables (e.g., P, N, T, V, etc) can be held fixed simultaneously, and each set of fixed variables constitutes an ensemble. For example, the canonical ensemble holds the number of particles (N), the volume (V) and the temperature (T) fixed, while the isothermal-isobaric ensemble holds the N, the pressure (P) and T fixed. Each ensemble can be appropriate in a particular context; for instance, if the density of a fluid as a function of temperature and pressure is of interest, the isobaric-isothermal ensemble can yield V as an output in terms of inputs N, P and T.

In the grand canonical ensemble, the chemical potential (μ), V and T are fixed. For a multicomponent system, the chemical potential of one of the species is often held fixed. Using this information, it is possible to visualize a binary system in the grand canonical ensemble as a rigid box with a set number

of particles of species A at a specified temperature, with a variable number of particles of species B that vary depending on the chemical potential of species B. It is apparent that such an ensemble may be useful to determine the relationship between the molar composition of a system and the chemical potential of one of its constituents.

Associated with each type of ensemble in MC simulations is a particular set of random moves that are applied to the molecules constituting the system. For the isobaric-isothermal ensemble, for instance, particles may be translated, rotated or swapped, and the simulation box itself may have its volume changed in order maintain the predefined pressure. In grand canonical system, particles may be translated or rotated, but since the volume is fixed, volume changes are not allowed. Sticking with the aforementioned reference to a system consisting of particles from species A and B, creation and destruction moves may be applied to species B in the grand canonical ensemble. In other words, a molecule of species B in the simulation box may be randomly destroyed, or a new particle of species B may be randomly inserted into the system. It is clear that the translation and rotation moves mimic the thermal motion of molecules, whilst the creation and destruction moves mimic adsorption and desorption, respectively.

In order to determine whether or not a random move is accepted or not, the internal energy of the system for the current random move needs to be compared to the internal energy of the system one step prior (i.e., ΔU). For all moves, if the system possesses a lower energy than for the previous step, the move is accepted. However, if the system's internal energy increases after application of a random move, the change in internal energy needs to be assessed to determine a probability of acceptance. This is achieved by computing the probability of acceptance of said move (Π):

$$\Pi = \exp(-\Delta U / kT) \tag{1.5}$$

In eq. (1.5) above, k is Boltzmann's constant. The probability determined by computing Π is then compared to a randomly generated fractional number, and if it is less than this random number, the move is accepted. If it is not, the move is rejected. This scheme is known as the Metropolis importance sampling scheme [36], and is a type of random walk MC simulation, which is commonly used to determine the equilibrium properties of complex system.

With regard to MC methods and ensembles generally, there are indeed a variety of methods which have been used in the past to simulate phase equilibria of various systems, prominent among these being the Gibbs ensemble method developed by Panagiotopoulos [76]. This technique directly simulates phase equilibrium by considering a system of phases at equilibrium as a set of interconnected simulation boxes, in which particles may be exchanged between boxes in order to replicate the transfer of

molecules between phases that occurs naturally. However, in order to study clathrate hydrate phase equilibrium in this manner, three simulation boxes would be required: Gaseous methane, liquid water/ice (depending on whether the system temperature is above/below the ice point), and the hydrate phase itself. In situations where the probability of swapping particles is very low (such as in a dense solid phase), the Gibbs ensemble approach becomes prohibitively expensive, computationally speaking. In fact, in the literature, only a single study employing this method for clathrate hydrate systems was found [77]. An alternative direct approach is direct coexistence MD, which, as stated previously, has been used in the past to study clathrate hydrate systems [2]. However, this method yields the phase equilibrium alone, and no information regarding the cavity occupancy can be obtained. Yet another approach, which can employ either MD or MC simulations is that of thermodynamic integration, which was used to study methane clathrate hydrate in the literature [78]. However, this technique requires simulations to be performed in an iterative manner, and thus dozens of simulations are needed to obtain a single phase coexistence point. Therefore, GCMC simulations are most appropriate, computationally speaking, to directly study clathrate hydrate occupancy behaviour and indirectly infer phase equilibria.

1.10. UNLIKE LENNARD-JONES INTERACTIONS

While the Lorentz and Berthelot combining rules, as discussed above, are widely used to describe the unlike interactions in molecular simulations, they have shortcomings in certain scenarios. For the case of dilute, approximately spherical, non-polar particles surrounded by hydrogen-bonded water molecules, an additional polarizability contribution should be considered in the unlike interactions [34,79,80]. This additional energy contribution arises from the self-organisation of the water molecules in the presence of a particle which exhibits little to no hydrogen bonding. Only recently have any studies considered analyzing the response of clathrate hydrate systems to changes in the unlike LJ interactions [35,44].

It may be noted that explicit-atom models of methane have been used in the literature to study clathrate hydrate systems [81-85]. Such models are computationally costly, however, and a previous study [35] found that features such as polarizability can be easily capture by modification to the unlike interactions between water and a united-atom methane model. It can also be noted here that previously [83], the intramolecular degrees of freedom of both methane and water were included to determine any effects on the properties of simulated clathrate hydrates, as compared to rigid molecules for methane and water. It was found [83] that the internal energies and structural properties were very similar whether molecules were considered to be flexible or rigid, which implied that the internal degrees of freedom of the molecules constituting the clathrate hydrate lattice may not significantly affect the occupancy behaviour.

In practice, this polarizability contribution can be covered in an effective way through the application of a binary correction factor k_{ij} to the Berthelot combining rule, as shown in Equation (1.4). Determination of this correction factor was undertaken for the case of dilute methane in water [35], where it was found to be $k_{ij} = 1.07$. In other words, the numerical energy cross-parameter value obtained from the Berthelot combining rule was increased by 7 % to account for the polarizability contribution. In fitting the results of simulations to available experimental data, the adjustment of k_{ij} can therefore be interpreted as the addition of unlike intermolecular energy contributions arising from electrostatics which are not explicitly accounted for by the electrostatic parameterization of the molecular force fields.

The unlike size correction factor l_{ij}, while not usually used to fit phase equilibrium data (a previous study [45] found that for LJ mixtures, k_{ij} was sufficient to fit vapour-liquid equilibrium data), can significantly influence the radial distribution function of a simple mixture [86,87]. Therefore, l_{ij} can be used to adjust for steric effects, or to account for the 'effective' size of a species in a mixture, which may be different than for the pure species due to attractive forces pulling molecules closer together in the mixture, for instance. In such a case, k_{ij} can only effectively describe the strength of the intermolecular interactions, and not the distance at which they occur. General discussions on the topic of unlike LJ interactions can be found in the literature [1,3,42,43,88].

With regard to the use of k_{ij} and l_{ij} in this thesis, it is necessary to discuss the applicability of either correction factor to the techniques employed to study clathrate hydrates. As stated previously, l_{ij} can encompass effects altering the effective sizes of molecules in mixtures, whilst also significantly altering the radial distribution function. Therefore, if the molecular structure is of interest, it can be useful to implement adjustment of l_{ij}. In this thesis, structural properties were only relevant when the employing lattice-based methods covered in Chapter Two, and hence was only considered in Chapter Two. The use of the grand canonical ensemble to study adsorption of gas into the clathrate hydrate lattice suggests that is not useful to incorporate size effects, because the simulation box possesses a fixed volume. Therefore, in such a case, fitting to a physical measurement of the unit cell size would be futile. Moreover, and as stated previously, an earlier study [46] found that combining rules did not vary significantly in terms of the net estimate of the unlike size term for argon clathrate hydrate. Thus it was determined that investigation of l_{ij} in the context of adsorption simulations may not possess significant practical value. With regard to k_{ij}, however, the wide range of possible unlike dispersion values, depending upon the chosen combining rule (see [46]), meant that there was significant practical interest in analysing the influence of k_{ij} on simulated clathrate hydrates. A concluding remark on the use of correction factors across a variety of methods is related to the emergent complexity arising from atomistic computations of molecular systems. Since all of the constituent molecules are described using similar force fields, and interact in fundamentally similar ways, it may expected that similar trends are observed when the unlike interactions are changed.

REFERENCES

[1] E.L. Johansson, Simulations of Water Clustering in Vapour, Hydrocarbons and Polymers, Doctoral thesis, Chalmers University of Technology, Göteborg, Sweden, 2007.

[2] M.M. Conde, C. Vega, J. Chem. Phys. 133 (2010) 064507.

[3] S. Moodley, E. Johansson, K. Bolton, D. Ramjugernath, Mol. Simulat. 38 (2012) 838-849.

[4] A.Z. Panagiotopolous, in: K.P. Johnston, J.M.L. Penninger (Eds.), Supercritical Fluid Science and Technology, American Chemical Society, Washington D.C., 1989, pp. 39—51.

[5] A.M.A. Dias, H. Carrier, J.L. Daridon, J.C. Pàmies, L.F. Vega, J.A.P. Coutinho, I.M. Marrucho, Ind. Eng. Chem. Res. 45 (2006) 2341-2350.

[6] S. Moodley, Monte Carlo Molecular Simulation of Binary Fluid-Phase Equilibrium Using Heterogeneous Mixing Parameters, Doctoral thesis, University of KwaZulu-Natal, Durban, South Africa, 2012.

[7] J.H. van der Waals, J.C. Platteeuw, Adv. Chem. Phys. 2 (1959) 1-59.

[8] E.D. Sloan, C.A. Koh, Clathrate Hydrates of Natural Gases, CRC Press, Boca Raton, United States, 2008.

[9] S.R. Zele, S.-Y. Lee, G.D. Holder, J. Phys. Chem. B 103 (1999) 10250-10257.

[10] H. Davy, Phil. Trans. Royal Soc. London 101 (1811) 155-162.

[11] M. Faraday, Quart. J. Sci. Lit. Art. 15 (1823) 71-74.

[12] P. Villard, Compt. Rend. 106 (1888) 1062-1063.

[13] R. de Forcrand, Compt. Rend. 135 (1902) 959-961.

[14] E.G. Hammerschmidt, Ind. Eng. Chem. 26 (1934) 851-855.

[15] E.D. Sloan, Hydrate Engineering, SPE Inc., Richardson, United States, 2000.

[16] B.C. Barnes, A.K. Sum, Curr. Opin. Chem. Eng. 2 (2013) 184-190.

[17] Institute of petroleum engineering, Heriot Watt University, http://www.pet.hw.ac.uk/research/hydrate/images/hydrates/structures_large.jpg (date accessed: 30 June 2010).

[18] N.I. Papadimitriou, I.N. Tsimpanogiannis, A.K. Stubos, Monte Carlo Simulations of Methane Hydrates, 7th International Conference on Gas Hydrates, Edinburgh, United Kingdom, 2011.

[19] P. Englezos, Ind. Eng. Chem. Res. 32 (1993) 1251-1274.

[20] P. Englezos, J.D. Lee, Korean J. Chem. Eng. 22 (2005) 671-681.

[21] J.S. Booth, M.M. Rowe, K.M. Fischer, Offshore Gas Hydrate Sample Database, U.S. Geological Survey, Open-File Report 96-272, Denver, United States, 1996.

[22] W.L. Mao, H.K. Mao, A.F. Goncharov, V.V. Struzhkin, Q. Geo, J. Hu, J. Shu, R.J. Hemley, M. Somayazulu, Y. Zhao, Science 297 (2002) 2247-2249.

[23] H. Lee, J.W. Lee, D.Y. Kim, J. Park, Y.T. Seo, K. Zeng, I.L. Moudrakovski, C.I. Ratcliffe, J.A. Ripmeester, Nature 434 (2005) 743-746.

[24] A.T. Trueba, L.J. Rovetto, L.J. Florusse, M.C. Kroon, C.J. Peters, Fluid Phase Equilib. 307 (2011) 6-10.

[25] P.G. Brewer, C. Friederich, E.T. Peltzer, F.M. Orr, Science 284 (1999) 943-945.

[26] S.-P. Kang, H. Lee, Env. Sci. Tech. 34 (2000) 4397-4400.

[27] H. Kubota, K. Shimizu, Y. Tanaka, T. Makita, J. Chem. Eng. Jpn. 17 (1984) 423-429.

[28] K.K. Østergaard, B. Tohidi, A. Danesh, R.W. Burgass, A.C. Todd, T. Baxter, Ann. N.Y. Acad. Sci. (2000) 832-842.

[29] L.R. Dorsett, SPE Gas Technology Symposium, Dallas, Texas, 1989, 239-246.

[30] A. Eslamimanesh, F. Gharagheizi, A.H. Mohammadi, D. Richon, Chem. Eng. Sci. 66 (2011) 3039-3044.

[31] K. Tumba, P. Reddy, P. Naidoo, D. Ramjugernath, A. Eslamimanesh, A.H. Mohammadi, D. Richon, J. Chem. Eng. Data 56 (2011) 3620-3629.

[32] A. Eslamimanesh, A.H. Mohammadi, D. Richon, P. Naidoo, D. Ramjugernath, J. Chem. Thermo. 46 (2012) 62-71.

[33] K.E. Gubbins, Fluid Phase Equilib. 83 (1993) 1-14.

[34] J.E. Lennard-Jones, Proc. Phys. Soc. 43 (1931) 461-482.

[35] H. Doherty, A. Galindo, C. Vega, E. Sanz, J. Chem. Phys. 125 (2006) 074510.

[36] N. Metropolis, A.W. Rosenbluth, M.N. Rosenbluth, A.H. Teller, E. Teller, J. Chem. Phys. 21 (1953) 1087-1092.

[37] L. Boltzmann, Vorlesungen über Gastheorie, J. A. Barth, Leipzig, Germany, 1898.

[38] C.A. de Coulomb, Hist. de l'Acad. des Sci. (1785) 569-577.

[39] C.A. de Coulomb, Hist. de l'Acad. des Sci. (1785) 578-611.

[40] H.A. Lorentz, Ann. Phys. 12 (1881) 127-136.

[41] D.C. Berthelot, Compt. Rend. 126 (1898) 1703-1706.

[42] A.J. Haslam, A. Galindo, G. Jackson, Fluid Phase Equilib. 266 (2008) 105-128.

[43] J. Delhommelle, P. Millie, Mol. Phys. 99 (2001) 619-625.

[44] N.I. Papadimitriou, I.N. Tsimpanogiannis, I.G. Economou, A.K. Stubos, Influence of combining rules on the cavity occupancy of clathrate hydrates: Monte Carlo simulations and van der Waals-Platteeuw-theory-based modeling, Thermodynamics 2013 conference, Manchester, United Kingdom, 2013.

[45] T. Schnabel, J. Vrabec, H. Hasse, J. Mol. Liq. 135 (2007) 170-178.

[46] N.I. Papadimitriou, I.N. Tsimpanogiannis, I.G. Economou, A.K. Stubos, Mol. Phys. 112 (2014) 2258-2274.

[47] P.M. Rodger, T.R. Forester, W. Smith, Fluid Phase Equilib. 116 (1996) 326-332.

[48] L.A. Báez, P. Clancy, Ann. N.Y. Acad. Sci. 715 (1994) 177-186.

[49] C. Moon, P.C. Taylor, P.M. Rodger, J. Am. Chem. Soc. 125 (2003) 4706-4707.

[50] C. Moon, R.W. Hawtin, P.M. Rodger, Faraday Discuss. 136 (2007) 367-382.

[51] H. Nada, J. Phys. Chem. B 110 (2006) 16526-16534.
[52] J. Vatamanu, P.G. Kusalik, J. Phys. Chem. B 110 (2006) 15896-15904.
[53] J. Zhang, R.W. Hawtin, Y. Yang, E. Nakagava, M. Rivero, S.K. Choi, P.M. Rodger, J. Phys. Chem. B 112 (2008) 10608-10618.
[54] W. Cheng, H.-Y. Zhou, Chinese Phys. Lett. 19 (2002) 609-612.
[55] W. Cheng, H.-Y. Zhou, Chinese Phys. Lett. 20 (2003) 1-4.
[56] M.S. Sudhakar, Prediction of Gas Hydrates Equilibria Using Molecular Dynamics Simulation, Masters dissertation, Texas A&M University-Kingsville, Kingsville, United States, 2006.
[57] K.S. Jatkar, Phase Equilibrium of Gas Hydrates using Molecular Dynamics Simulation, Masters dissertation, Texas A&M University-Kingsville, Kingsville, United States, 2009.
[58] H. Tanaka, Fluid Phase Equilib. 144 (1998) 361-368.
[59] K. Katsumasa, K. Koga, H. Tanaka, J. Chem. Phys. 127 (2007) 044509.
[60] N.I. Papadimitriou, I.N. Tsimpanogiannis, A.Th. Papaioannou, A.K. Stubos, Mol. Simulat. , 34 (2008) 1311-1320.
[61] N.I. Papadimitriou, I.N. Tsimpanogiannis, C.J. Peters, A.Th. Papaioannou, A.K. Stubos, J. Phys. Chem. 112 (2008) 14206-14211.
[62] N.I. Papadimitriou, I.N. Tsimpanogiannis, A.K. Stubos, J. Chem. Phys. 131 (2009) 044102.
[63] N.I. Papadimitriou, I.N. Tsimpanogiannis, A.K. Stubos, Colloids Surf. A: Physicochem. Eng. Aspects 357 (2010) 67–73.
[64] A. Lenz, L. Ojamäe, J. Phys. Chem. A 115 (2011) 6169-6176.
[65] H.K. Srivastava, G.N. Sastry, J. Phys. Chem. A 115 (2011) 7633-7637.
[66] P.K. Chattaraj, S. Bandaru, S. Mondal, J. Phys. Chem. A 115 (2011) 187-193.
[67] J. Baumert, C. Gutt, V.P. Shpakov, J.S. Tse, M. Krisch, H. Requardt, M. Müller, W. Press, S. Janssen, Phys. Rev. B 68 (2003) 174301.
[68] J. Baumert, C. Gutt, J.S. Tse, M. Krisch, H. Requardt, M. Müller, W. Press, Phys. Rev. B 72 (2005) 054302.
[69] M. Jing, S. Dong, J. Nat. Gas Chem. 14 (2005) 238-242.
[70] Industrial fluid properties simulation collective, http://www.fluidproperties.org, 2010 (date accessed: 6 August 2013).
[71] J.E. Bertie, S.M. Jacobs, J. Chem. Phys. 77 (1982) 3230-3232.
[72] M.J. Hwang, G.D. Holder, S.R. Zele, Fluid Phase Equilib. 83 (1993) 437-444.
[73] J.S. Tse, B.M. Powell, V.F. Sears, Y.P. Handa, Chem. Phys. Lett. 215 (1993) 383-387.
[74] H. Tanaka, K. Kiyohara, J. Chem. Phys. 98 (1998) 4098-4109.
[75] T. Ikeda, O. Yamamuro, T. Matsuo, K. Mori, M.S. Torii, T. Kamiyama, F. Izumi, S. Ikeda, S. Mae, J. Phys. Chem. Solids 60 (1999) 1527-1529.
[76] A.Z. Panagiotopoulos, Mol. Phys. 61 (1987) 813-826.

[77] M. Keisuke, O. Ryo, A.K. Sum, K. Yasuoka, Gibbs ensemble Monte Carlo simulations for methane, liquid water and methane/hydrate phase equilibrium, 6th International Conference of Gas Hydrates, Vancouver, 2008.

[78] L. Jensen, Experimental Investigation and Molecular Simulation of Gas Hydrates (Ph.D. Thesis), Technical University of Denmark, 2010.

[79] B. Guillot, Y. Guissani, J. Chem. Phys. 99 (1993) 8075-8094.

[80] D.J. Paschek, J. Chem. Phys. 120 (2004) 6674-6790.

[81] A.A. Chialvo, M. Houssa, P.T. Cummings, J. Phys. Chem. B 106 (2002) 442-451.

[82] H. Jiang, K.D. Jordan, C.E. Taylor, J. Phys. Chem. B 111 (2007) 6486-6492.

[83] F. Castillo-Borja, R. Vázquez-Román, U. Bravo-Sánchez, Mol. Simulat. 34 (2008) 661-670.

[84] H. Jiang, E.M. Myshakin, K.D. Jordan, R.P. Warzinski, J. Phys. Chem. B 112 (2008) 10207-10216.

[85] H. Jiang, K.D. Jordan, J. Phys. Chem. C 114 (2010) 5555-5564.

[86] D. Boda, D. Henderson, Mol. Phys. 106 (2008) 2367-2370.

[87] M. Rouha, I. Nezbeda, Fluid Phase Equilib. 277 (2009) 42-48.

[88] D.-M. Duh, L. Mier-y-Teran, Mol. Phys. 90 (1997) 373-379.

CHAPTER TWO (BASED ON PAPER I): ON THE APPLICATION OF BINARY CORRECTION FACTORS IN LATTICE DISTORTION CALCULATIONS FOR METHANE CLATHRATE HYDRATES

ABSTRACT

The lattice distortion theory of Zele and co-workers is an attractive method for amending calculated phase equilibria of clathrate hydrates, since only two molecular computations are required. The perturbation energy between the empty and loaded clathrate hydrate lattice is the quantity of interest. The effect of binary correction factors applied to the Lorentz and Berthelot combining rules for the intermolecular interaction between gas and water particles is investigated. There are clear trends for the perturbation energy and lattice constant in terms of the binary correction factors, although there is significant sensitivity to the force field parameterization of the gas species.

2.1. INTRODUCTION

2.1.1. CLATHRATE HYDRATES

Clathrate hydrates consist of hydrogen-bonded networks of water molecules trapping gas particles in a crystal lattice. Superficially, this material resembles ice and is found in natural deposits in the deep ocean and in permafrost in the tundra [1]. In clathrate hydrate systems, water can be considered as the "host" species, and the enclathrated gas as the "guest" species.

Three different clathrate hydrate structures are found in natural or industrial settings: Structure I (sI), structure II (sII), and structure H (sH). The distinguishing characteristics of these structures are the ratios and types of cavities present in the crystal lattice at the nanometer scale. These cavities are essentially "cages" in which gas particles are enclosed by water molecules, with oxygen atoms forming the vertices of these polygonal cages. The relative sizes of the cavities (i.e. small, medium and large) are used as references within the unit cell. A brief summary of clathrate hydrate crystal structures is presented in Table 2.1 [2]. The sI and sII structures are most common, since these can form with a single gas species. The sH clathrate hydrate, however, requires a small gas species (such as methane) and a large gas species (such as cyclopentane) to simultaneously stabilize the small and large cages, respectively. Thus, the sH structure can only form in the presence of specific gas mixtures that usually

do not occur in the natural environment.

Clathrate hydrate structure	sI		sII		sH		
Crystal system	Primitive cubic		Face-centered cubic		Hexagonal		
Space group	*Pm3n*		*Fd3m*		*P6/mmm*		
Cavity type	Small	Large	Small	Large	Small	Medium	Large
Cavity description	5^{12}	$5^{12}6^2$	5^{12}	$5^{12}6^4$	5^{12}	$4^35^66^3$	$5^{12}6^8$
Cavities/unit cell	2	6	16	8	3	2	1
Cavity radius (nm)	0.395	0.433	0.391	0.473	0.391	0.406	0.571
H_2O/unit cell	46		136		34		
Unit cell formula	$2S\cdot6L\cdot46H_2O$		$16S\cdot8L\cdot136H_2O$		$3S\cdot2M\cdot1L\cdot34H_2O$		

Table 2.1. Table summarizing the crystalline structures and properties of the structure I, II, and H clathrate hydrates [2]. The small, medium, and large cavities are denoted in the unit cell formula by S, M, and L, respectively.

2.1.2. LATTICE DISTORTION (LD) THEORY

Phase equilibrium calculations for clathrate hydrate systems often use thermodynamic models based on the theory of van der Waals and Platteeuw (vdWP) [1,3], which employs the Lennard-Jones-Devonshire cell model to describe interactions between enclathrated gas molecules and the host water network. The vdWP theory has several shortcomings related to assumptions made in its original formulation [4-14]: No interactions between particles of the guest gas species, and fixed spatial positions of the water molecules. One attempt at amending the vdWP theory is the LD theory of Zele and co- workers [15]. LD theory includes a term for distortion of the host lattice, which was not accounted for in the original vdWP theory. The present paper seeks to examine the effects of a further adjustment to LD theory through the use of binary correction factors to the Lennard-Jones (LJ) potential describing the intermolecular interactions between water and methane.

2.1.3. BINARY CORRECTION FACTORS

The cross-interactions between LJ sites are often accounted for by the Lorentz [16] and Berthelot [17] (L-B) combining rules. However, these simple rules cannot always adequately account for all of the complexities of interactions between unlike LJ sites, and thus a binary correction factor (k_{ij}) can be introduced into the dispersion term (ε_{ij}) for the cross-interaction between unlike sites i and j, through a variant of the Berthelot rule:

$$\varepsilon_{ij} = k_{ij} (\varepsilon_{ii} \varepsilon_{jj})^{0.5} \quad (2.1)$$

It should be noted that the Berthelot rule can be considered as a special case of a more general combining rule which considers the ionization potentials and the molecular size parameters when calculating the unlike intermolecular LJ well in depth [18,19]. When considering this general combining rule, the Berthelot rule arises when the two particles are of a similar size and similar ionization potential. Therefore, it can be expected that the unmodified Berthelot rule can be insufficient when describing the interactions between water and gas molecules in the clathrate hydrate phase [20].

In addition, another binary correction factor (l_{ij}) can be applied to account for the cross-interaction in the size term (σ_{ij}) of the LJ potential, using a modified form of the Lorentz rule:

$$\sigma_{ij} = 0.5\, l_{ij} \left(\sigma_{ii} + \sigma_{jj} \right) \qquad (2.2)$$

The binary correction factors kij and lij can be determined in a systematic manner provided that experimental data, with calculated data such as structural energies, are available for comparison. In the context of LD theory, the most useful data type for comparison is dissociation pressure data, as these are computed via the phase equilibrium calculations described above. In the present study, kij was held fixed at unity, while lij was varied and vice versa.

Previous studies have investigated binary correction factors applied to intermolecular
LJ potentials in clathrate hydrate systems; determination of these factors can be indirect, using the excess chemical potential of dilute methane in water [21] or through direct coexistence of molecular dynamics simulations [22]. In both of these prior studies, however, a binary correction factor was only applied to the dispersion term of the LJ potential. It was found that increasing the binary correction factor for this term by 7% improved the fit of the molecular simulations to the experimental measurements.

It should be noted that the aforementioned studies used significantly more computations than the present contribution. Since LD theory requires only two computations per gas species, it is an attractive option if computational costs are to be reduced. Therefore, it is desired to assess the usefulness of LD theory in the context of binary correction factors applied to the intermolecular LJ potential between the guest gas species and the water lattice.

2.2. THEORY AND METHODS

2.2.1. LD AND VAN DER WAALS-PLATTEEUW THEORY

The phase equilibrium criterion of interest here is the equality between the chemical potential of liquid water (μ_W^L) and water in the hydrate phase (μ_W^H):

$$\mu_W^L = \mu_W^H \tag{2.3}$$

For convenience, both of these quantities are expressed relative to the chemical potential of water in the hypothetical empty hydrate (μ_W^β):

$$\Delta\mu_W^L = \mu_W^\beta - \mu_W^L = \Delta\mu_W^H = \mu_W^\beta - \mu_W^H \tag{2.4}$$

The empty hydrate is considered, even though it does not exist in nature, because it represents a useful reference state. The difference between the chemical potential of water in the empty hydrate and water in the loaded hydrate ($\Delta\mu_W^H$) can be calculated in terms of the fractional occupancy (θ) of the gas species enclathrated in the hydrate [3]:

$$\Delta\mu_W^H = - R\,T \Sigma_j [\ \nu_j \ln (1 - \Sigma_i\ \theta_{ij})\ ] \tag{2.5}$$

The index *i* refers to the gas species, *j* is a reference to the cavity type (i.e. small, medium, large), νj is the ratio of cavities of type j to water molecules in the hydrate unit cell, and θ_{ij} is the fractional occupancy of cavity type *j* by gas species *i*. The fractional occupancy is often described in terms of a Langmuir-type adsorption isotherm.

The difference between the chemical potential of water in the hypothetical empty hydrate and the chemical potential of water in liquid water ($\Delta\mu_W^L$) can be expressed as the difference between two pure phases at reference conditions of T_R = 273.15 K and zero absolute pressure. The chemical potential difference at these conditions is the so-called "reference potential", $\Delta\mu^0$. Appropriate corrections (f) for the actual temperature, pressure, and gas solubility of the system in question are then applied [23]:

$$(\Delta\mu_W^L) / (R\,T) = (\Delta\mu^0) / (R\,T_R) + f \tag{2.6}$$

The corrections necessary to account for temperature, pressure, and solubility shall not be elaborated upon here, since the quantity of interest in LD theory is the reference potential, $\Delta\mu^0$. The other quantities

are elaborated upon in the literature [23].

LD theory attempted to introduce an adjustment to the reference potential to account for the distortion of the host water lattice by the guest molecules. This correction becomes especially significant for large molecules, such as cyclopentane or tetrahydrofuran (both of which can be found in clathrate hydrate systems). This correction takes the form of a perturbation potential, $\Delta(\Delta\mu^0)$ [15]:

$$\Delta(\Delta\mu^0) = \Delta U_H - T_R \Delta S \tag{2.7}$$

ΔU_H is the change in the energy of the host lattice due to the distortion associated with enclathration of gas molecules, and $T_R \Delta S$ represents the entropic effect of expansion. The host energy consists of a summation of static and vibrational contributions, details of which are given in the following sections. This entropic term can be calculated as [15]:

$$T_R \Delta S = T_R (\beta / \kappa) \Delta V_H \tag{2.8}$$

β and κ are the thermal expansivity and the isothermal compressibility of the hydrate, respectively, and ΔV_H is the change in molar volume of the host lattice due to the distortion associated with the presence of the guest species. ΔU_H and ΔV_H can be readily determined from molecular-level computations, whereas β and κ can be found in the literature [24,25]. The entropic term is, however, negligible compared to the other contributions to the perturbation energy [15].

The left-hand side of Equation (2.7) is a perturbation term which can be added to the (unperturbed) reference potential to produce a "perturbed" reference potential ($\Delta\mu^*$), which can then be used instead of the reference potential when evaluating Equation (2.6) [15]:

$$(\Delta\mu^*) = \Delta\mu^0 + \Delta(\Delta\mu^0) \tag{2.9}$$

The LD theory of Zele, Lee, and Holder showed that there is indeed a distortion of the host lattice, and that the trends obtained from their simulations were the same as for their empirically determined perturbed reference potentials [15]. It should be noted that for relatively small changes in the lattice constant (i.e. for cell constants in the region of approximately up to 101% of the "fixed" value of the vdWP theory) [15], the results of the previous molecular simulations agreed favourably with the values obtained empirically.

2.2.2. STATIC ENERGY

As stated above, the host energy consists of static and vibrational contributions. The static contribution is usually significantly larger than the vibrational contribution. Therefore, it can be reasonable to neglect the vibrational contributions altogether (i.e. $U_{STATIC} >> U_{VIB}$). This is discussed below for the system studied in this work.

The General Utility Lattice Program of Gale and Rohl [26] was used in this study. In order to determine the static contribution, a geometry optimization was undertaken to obtain the lowest energy configuration, which is the most stable. Optimization was performed using the steepest descent method, similar to previous computations [27]. An energy-minimized crystal lattice structure [28] was used as the starting point for this study. Only the sI structure was considered, since it is well known that methane clathrate hydrate occurs in this form [1]. The lattice optimization was undertaken at zero absolute temperature and zero absolute pressure, and the static energy was determined at this configuration. The spatial coordinates of the energy-minimized lattice associated with each value of the binary correction factors were used as the starting point for the next calculation, such that the calculations proceeded in an incremental fashion. For example, the set of spatial coordinates $\{x\}$ of m water molecules obtained from the minimized structure for the base value of $k_{ij} = 1$ would be used as the starting point for $k_{ij} = 1.01$, and so forth. This helps to avoid the problem of the lattice optimization locating a local minimum structure, as opposed to the desired global minimum structure [28]. A preliminary series of computations that did not follow this incremental procedure showed that local minima were obtained in many of the optimisations; and hence, an erratic and non-monotonic function for ΔU_H as a function of k_{ij} was obtained. The results of these initial calculation attempts can be seen in Figure 2.1, wherein it is also apparent that the nonincremental approach did not yield minimum energy structures. The increments chosen were determined in an ad-hoc fashion, depending on the results of the minimization calculation.

2.2.3. VIBRATIONAL ENERGY

The spatial coordinates of the water molecules were subsequently processed to compute the vibrational contribution to the host energy. This was achieved by means of a vibrational partition function calculation at the reference conditions. This incorporates the effect of temperature, which was not done in the calculation of the static contribution.

The collective vibrational excitations in the elastic crystal lattice are calculated by considering the reciprocal lattice of the clathrate hydrate crystal. This was achieved by computing the force matrix (using the potential energy between sites) and the Hessian matrix to determine the vibrational frequencies. The electrostatic charges on the atoms were included using the Born effective charges

[29,30]. Once the vibrational frequencies were calculated, the vibrational partition function ($Z_{VIB.}$), vibrational energy ($U_{VIB.}$) and vibrational entropy ($S_{VIB.}$) were computed over m vibrational modes [31]. These are shown below:

$$Z_{VIB.} = \Sigma_m \Sigma_k \exp(- h\omega / 2k_BT) / (1 - \exp(- h\omega / k_BT)) \quad (2.10)$$

$$U_{VIB.} = \Sigma_m \Sigma_k w_k (0.5\, h\omega + h\omega / (\exp(h\omega / k_BT) - 1)) \quad (2.11)$$

$$S_{VIB.} = R \ln Z_{VIB.} + RT (\partial \ln Z_{VIB.} / \partial T) \quad (2.12)$$

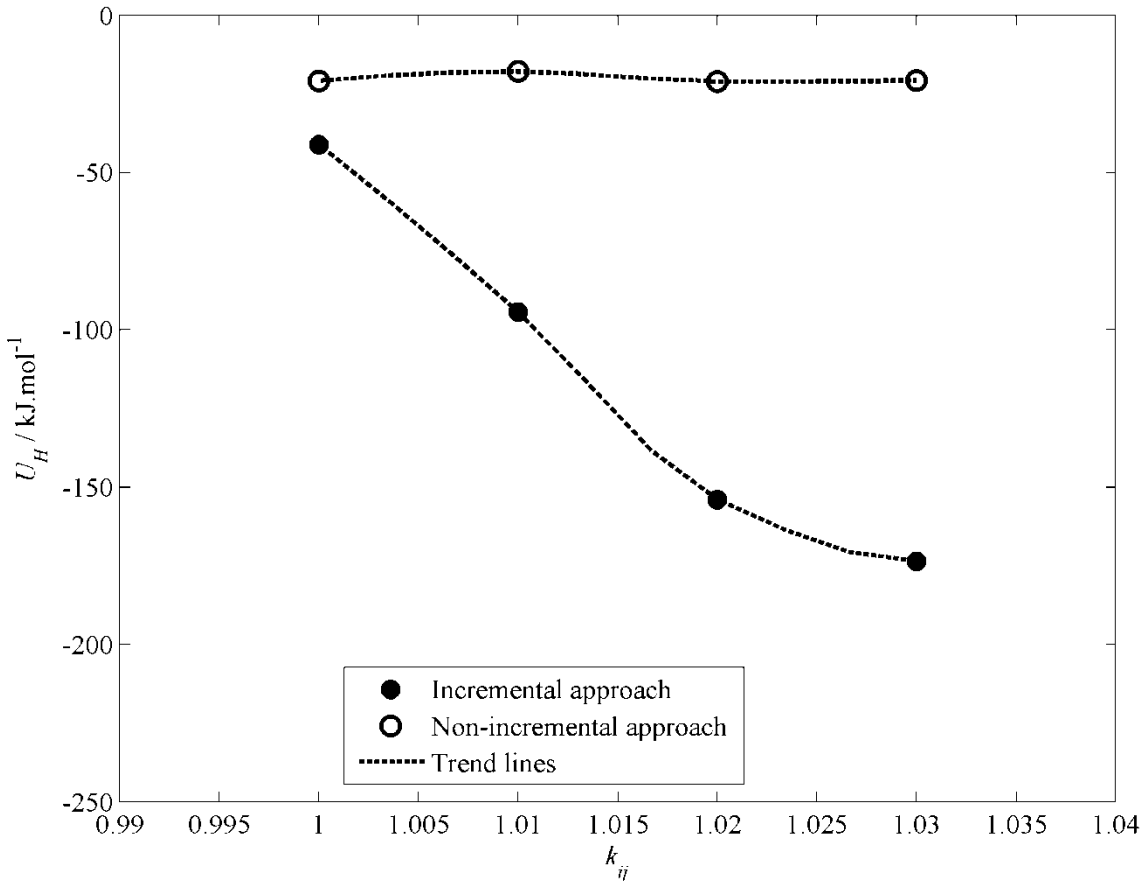

Figure 2.1. Comparison of lattice energies of the empty sI methane clathrate hydrate calculated using incremental and non-incremental approaches in k_{ij}.

In Equations (2.10) and (2.11), ω is the relevant vibrational frequency, and in Equation (2.11), w_k is the weight of each point in reciprocal space, such that the sum of all weights is unity. The calculation of the host energy is the sum of the static and vibrational contributions.

2.2.4. INTERMOLECULAR POTENTIALS

The Simple Point Charge (SPC) force field [32] was used to represent water molecules, and a united atom particle with an intermolecular LJ potential [33] was used for methane. The LJ parameters (εii and σii) of the methane–methane intermolecular interactions are adjusted using [34] the critical temperature (T_C = 190.6 K) and critical pressure (P_C = 4.61 MPa) of methane [35]. The force field parameters are shown in Table 2.2. Ewald summation [36] accounted for electrostatic interactions of the system, and a cutoff radius of 1 nm was used for LJ interactions.

The aforementioned force fields provide adequate descriptions of pure water [15] and methane [34] systems, and therefore the present study focuses on the cross-interaction terms applicable to the clathrate hydrate phase only. Moreover, a previous study [37] has found a significant phase dependence on binary correction factors between unlike LJ interactions, further motivating this approach.

Molecular species	Non-bonded interactions (Lennard-Jones)	Charges	Bond angle
SPC water [21]	ε_O / k_B = 78.21 K	q_O = -0.82 e	$\alpha_{(H\text{-}O\text{-}H)}$ = 109.47 °
	σ_O = 0.3166 nm	q_H = +0.41 e	
United atom LJ methane [23,24]	ε_{CH4} / k_B = 145.27 K		
	σ_{CH4} = 0.3821 nm		

Table 2.2. Force field parameters used in this study.

2.3. RESULTS AND DISCUSSION

2.3.1. LATTICE VIBRATIONS

Figures 2.2 and 2.3 show that there is no significant dependence of the phonon densities of state on k_{ij} or l_{ij}. This suggests that adjusting the size or dispersion terms of the unlike LJ interaction does not significantly influence the vibrations of the clathrate hydrate lattice.

Averaging across all computations, vibrational energy amounted to 10.5 ± 0.4 kJmol^{-1}. This value was approximately constant, regardless of whether the host lattice was distorted or not, which can be expected since lattice vibrations are largely dependent upon temperature. Since the differences in host energy are of interest in this study, the vibrational term can be ignored, since it is approximately constant for the distorted and undistorted lattices.

As expected, it was found that $U_{STATIC} >> U_{VIB.}$ in all cases investigated in this study. Therefore, any influence of k_{ij} or l_{ij} on the vibrational energy would have to be profound for it to influence the results

of this study. Moreover, since the vibrational contribution is significantly smaller than the static contribution, it can be neglected in perturbation energy calculations.

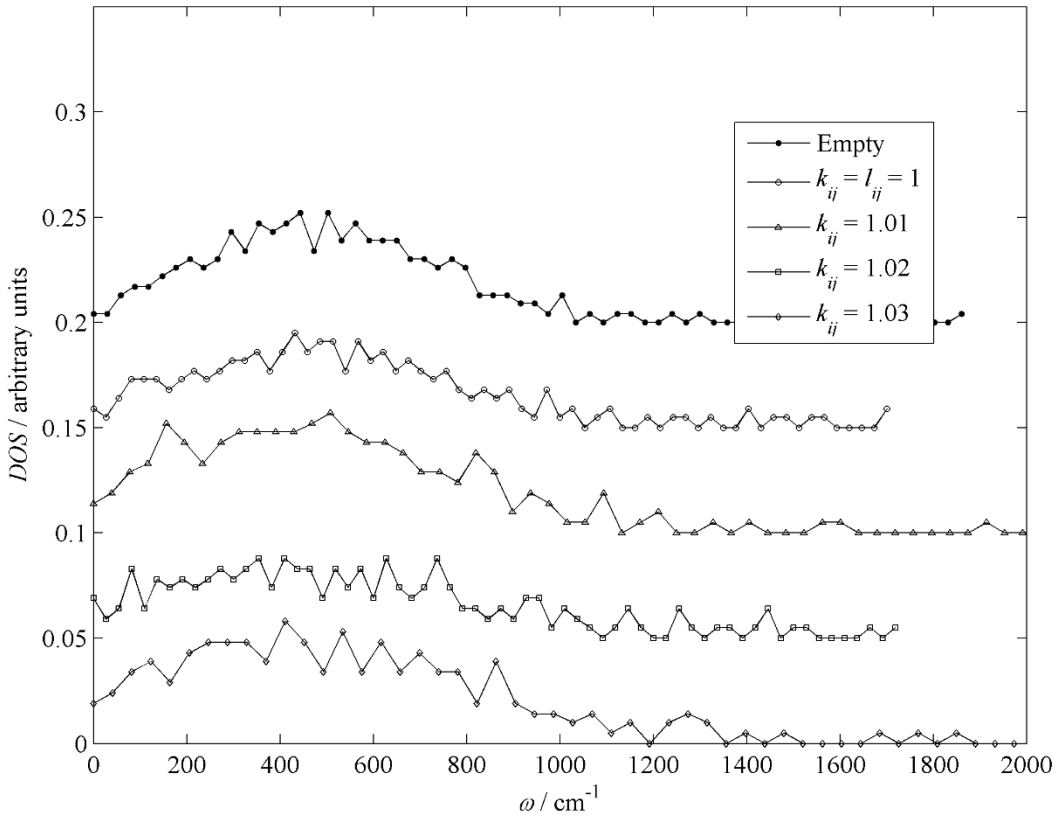

Figure 2.2. Influence of LJ dispersion correction factor (k_{ij}) on phonon DOS of sI methane clathrate hydrate over the vibrational frequency (ω). Each plot is shifted upward from the curve below by 0.05 units for clarity.

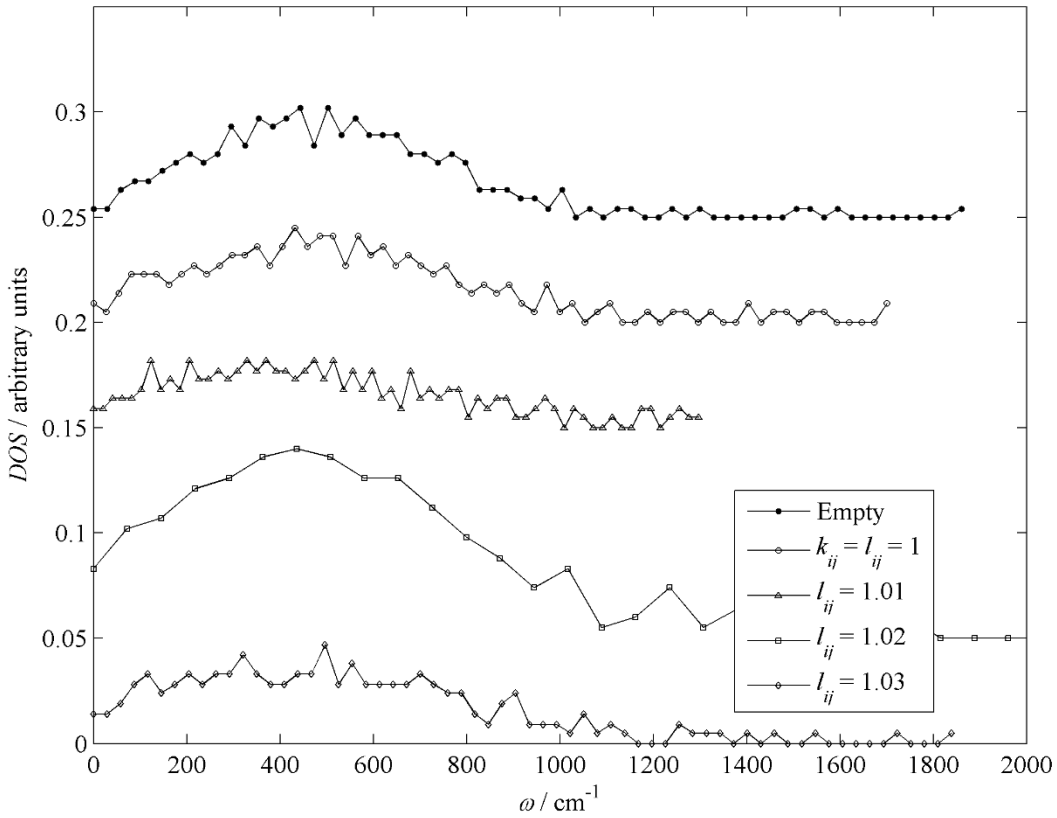

Figure 2.3. Influence of LJ size correction factor (l_{ij}) on phonon DOS of sI methane clathrate hydrate over the vibrational frequency (ω). Each plot is shifted upward from the curve below by 0.05 units (except l_{ij} = 1.01, which is shifted up by 0.1 units) for clarity.

2.3.2. EFFECT OF BINARY CORRECTION FACTORS ON THE PERTURBATION ENERGY

The phonon density of states (DOS) was also used to determine the entropic term for the lattice configurations in Equation (2.7), $T_R \Delta S$. On average, it was found that $T_R \Delta S$ was two to three orders of magnitude lower than ΔU_H. This concurs with previous observations [15], and therefore the entropic contribution was neglected in the presentation of the results.

The result of interest from the computations is the perturbation potential energy of the hydrate lattice, represented by ΔU_H in Equation (2.7). This quantity can be determined directly by calculating the energy of the empty hydrate lattice (which has been optimized at the conditions of interest, namely T = 273.15 K and P = 0 MPa) and comparing it to the energy of the water molecules in the loaded lattice at the same conditions, as per the original LD theory. The host energy of the empty lattice was −84.6 kJ mol^{-1}.

Figure 2.4 shows that the perturbation energy decreases with an increase in both k_{ij} and l_{ij}. It is also clear

that the desired value for the perturbation potential (~20 J mol^{-1}) results in values of k_{ij} = 1.002 ± 0.009 and l_{ij} = 1.015 ± 0.011 obtained through quadratic and linear fitting, respectively. For comparison, k_{ij} = 1.07 was previously obtained for methane + water cross-interactions [21]. It should be noted, however, that different water and methane force fields were used in Ref. [21]. The desired value of the perturbation energy was determined from the experimental phase equilibrium data [38,39] by applying the method of Parrish and Prausnitz [40] and making use of the Peng–Robinson cubic equation of state [41] for the vapour phase fugacity.

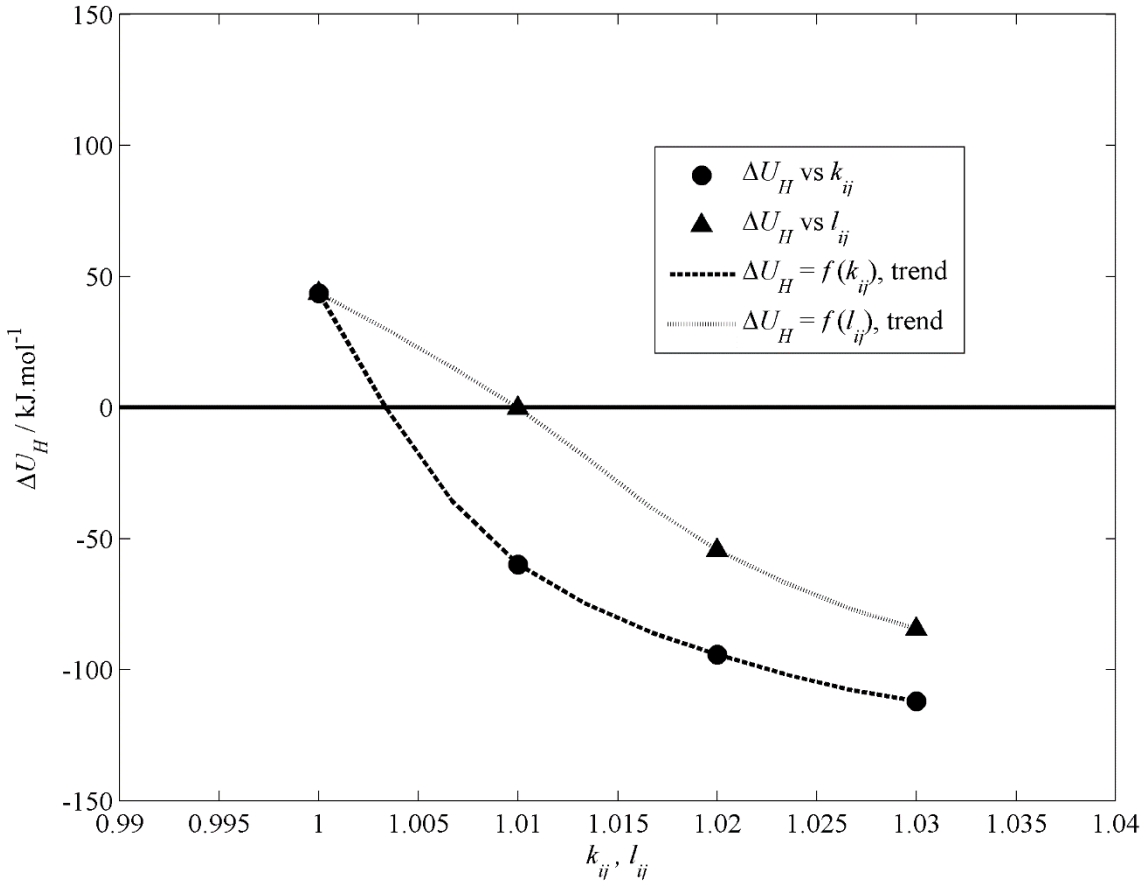

Figure 2.4. Effect of k_{ij} and l_{ij} on ΔU_H. The solid horizontal line is the value of ΔU_H calculated from experimental phase equilibrium data (≈20 J mol^{-1}). The trends are fitted as guides for the eye.

Figure 2.4 also reveals that the perturbation energy is extremely sensitive to changes in the value of either binary correction factor, especially if the order of magnitude of the perturbation energy is considered relative to the aforementioned desired value. This may also be evidenced in the aforementioned values obtained for k_{ij}, compared to the literature [21]. For both of the values mentioned above, changes of less than 1% the binary correction factors result in changes of the order of 50–100 kJ mol^{-1}. These changes are more than three orders of magnitude larger than the desired value of the perturbation energy.

Another point to be noted is the degree of sensitivity of the perturbation energy to changes in the binary correction factors relative to each other. Figure 2.4 shows that ΔU_H is slightly more sensitive to changes in k_{ij} than l_{ij}. However, the difference is not very large, given that $\Delta U_H \approx 20$ J mol^{-1} is achieved over a range of 1–1.011 for k_{ij} or l_{ij}, due to the pronounced sensitivity of the perturbation energy to both parameters. Therefore, adjustment of either the size or dispersion terms of the cross-interaction between water and methane will change the perturbation potential approximately equally.

It can also be seen in Figure 2.4 that the L – B rules without binary correction factors (i.e. $k_{ij} = l_{ij} = 1$) result in values for the perturbation potential which would provide a poor fit to the experimental data. The aforementioned lack of suitability of an unmodified Berthelot rule [18–20], coupled with the results shown in Figure 2.4 suggest that the LD theory used in this study can produce results which fit the experimental data when binary correction factors are employed.

A cause for lack of robustness in determination of the binary correction factors can arise from shortcomings in the force fields used (namely SPC for water and a united atom LJ force field for methane in this study). However, the SPC force field has been used in the original LD study with some success. The united atom LJ force field for methane in this study is similar to other united atom methane force fields [21] which have been used successfully for clathrate hydrate studies, such as the united-atom OPLS force field [42] or the transferable potentials for phase equilibrium (TraPPE) [43]; in fact, the force field used in this study is almost identical to the two aforementioned force fields. Therefore, it cannot simply be a shortcoming of the employed force fields which has resulted in the sensitivity to the binary correction factors.

It is expected that an increase in the binary correction factors lead to a larger (more negative) value for the perturbation energy. This is because increasing the binary correction factors increases the strength of the methane–water interactions (for k_{ij}) or the equilibrium distance between the methane and water molecules (for l_{ij}). As discussed below with reference to Figure 2.5, this results in a larger expansion of the clathrate when methane is present. Since, the perturbation energy is the energy of this expanded structure relative to the structure in the absence of methane, there is a larger perturbation energy for larger binary correction factors (the negative sign arises merely because the energy of the pure clathrate is subtracted from the expanded substrate and not vice versa).

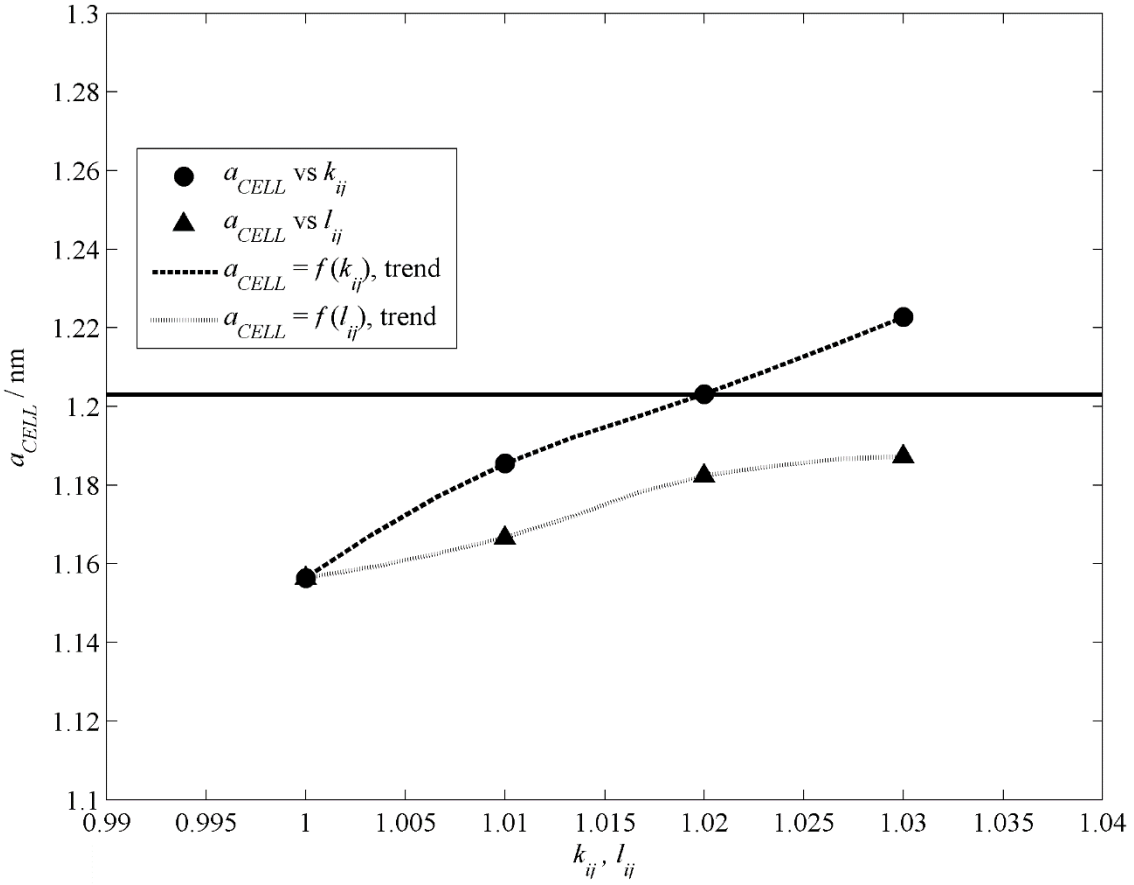

Figure 2.5. Effect of k_{ij} and l_{ij} on a_{CELL}. The solid horizontal line is the experimental value of a_{CELL} (1.203 nm) [15]. The trends are fitted as guides for the eye.

2.3.3. EFFECT OF BINARY CORRECTION FACTORS ON THE CELL CONSTANT

The relationship between the lattice or cell constant of the clathrate hydrate unit cell and the binary correction factors, is shown in Figure 2.5. The experimental lattice constant is generally accepted to be 1.203 nm [15], and is also considered in this analysis. In this case, it can be seen that setting k_{ij} = 1.020 ± 0.014 reproduces the experimental lattice constant. This is different to the value of k_{ij} found when fitting to the perturbation potential. Moreover, whilst the value of l_{ij} fitted to the experimental lattice constant was not determined, it is apparent that it will be greater than 1.03 (provided the trend observed in Figure 2.5 continues), which also differs to the value required for l_{ij} to reproduce the desired perturbation energy. Therefore, the value of the binary correction factors for the size and energy parameters of the LJ potential fitted to the experimental data varies according to the type of experimental data which are being considered.

Figure 2.5 also shows that there is an approximately linear trend of the cell constant with changes in the binary correction factors. In this case, however, increasing the binary correction factors result in an

increase of the cell constant. It can also be seen that the cell constant is more sensitive to variations of k_{ij} than l_{ij}. This can be due to the size of the methane molecule relative to the diameter of the cavities in the sI clathrate hydrate. In nature, methane is known to occupy both the small and large cavities [1] due to its small size. Therefore, larger changes to the size term of the LJ cross-interaction are required to perturb the crystal lattice significantly from the configuration of the empty clathrate hydrate as compared to the dispersion term. It can then be deduced that the intermolecular energy between the gas species and water plays a more significant role in the distortion of the clathrate hydrate lattice than the molecular size of the gas species, at least for approximately spherical gas species.

The dependence of the perturbation energy on the lattice constant is shown in Figure 2.6. Here, it can be seen that these two quantities are related in an approximately linear fashion, with increases in the lattice constant resulting in larger negative values of the perturbation energy. This is to be expected, as Figures 2.4 and 2.5 both suggest that increasing the strength of the intermolecular LJ potential results in more negative perturbation energies and an increase in the lattice constant. This is due to the greater deviation in the size of the crystal unit cell as compared to the empty lattice, which is the chosen reference state in LD theory.

A further point illustrated in Figures 2.4, 2.5, and 2.6 is that k_{ij} or l_{ij} cannot be fitted simultaneously to match the experimental value for the lattice constant and the perturbation energy. This is evidenced by the perturbation energy (≈ -100 kJ mol^{-1}) which corresponds to the experimental lattice constant (1.203 nm). Therefore, it can be supposed that the experimental or calculated quantity which is desired should be carefully selected (depending on the property of interest), since the results of the computations do not yield results which are quantitatively similar to experimental results for all data types.

2.3.4. FORCE FIELD SENSITIVITY

The error limits of the calculated perturbation energies and lattice constants (see Figures 2.7, 2.8, and 2.9) have been estimated by analysing their sensitivity to uncertainties in the critical properties used to calculate the LJ parameters of methane (standard deviations for experimentally measured critical temperature and pressure from an aggregated data-set are σ_{Tc} = 0.3 K and σ_{Pc} = 0.03 MPa [44], respectively). Although the LJ potential is only an approximation of the intermolecular interaction for methane, LD theory in this study is being examined within the context of LJ-type gas molecules distorting the water lattice of clathrate hydrates. For real gases, LJ parameters can be readily estimated using critical properties, and thus some measure of the allowed values of the perturbation energy and lattice constant, k_{ij} and l_{ij} are necessary, since there are a large number of data-sets which researchers can use to obtain T_C and P_C. The ranges between the upper and lower limits in Figures 2.7, 2.8, and 2.9 represent the possible allowed values for ΔU_H, a_{CELL}, k_{ij}, and l_{ij} for the SPC water + united atom LJ

methane sI clathrate hydrate system. The values for k_{ij} and l_{ij} obtained in this study clearly lie within the bounds of the error limits.

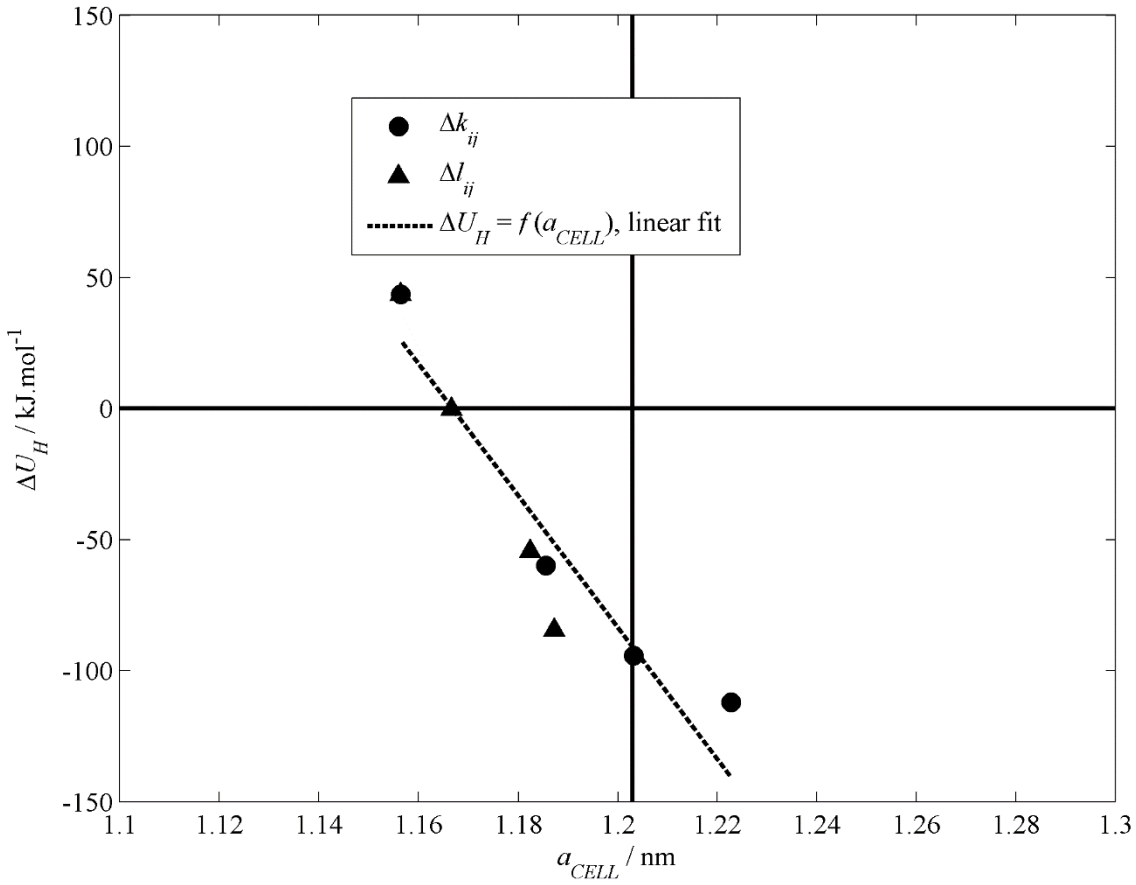

Figure 2.6. General trends for ΔU_H vs. a_{CELL} determined by separately changing k_{ij} and l_{ij}. The horizontal solid line represents the value of ΔU_H determined from experimental phase equilibrium data (≈20 J mol^{-1}), and the vertical solid line represents the experimental lattice constant (1.203 nm) [15]. The dashed line is a linear trend fitted as a guide for the eye.

To determine the error limits, the LJ parameters of methane were recalculated for every combination of addition/subtraction of each of σ_{Tc} and σ_{Pc} . For each set of reevaluated LJ parameters for methane, the lattice energies were recalculated and compared to the values obtained using the mean critical properties. The maximum deviations were then considered as the limits of allowed values of ΔUH, a_{CELL}, k_{ij}, and l_{ij}.

Plausible values for the binary correction factors can also be considered for the entire allowed range of possibilities afforded by the error limits. If the ranges allowed by the error limits are considered, then fairly large ranges are found: $0.999 \leq k_{ij} \leq 1.021$ and $1.003 \leq l_{ij} \leq 1.029$.

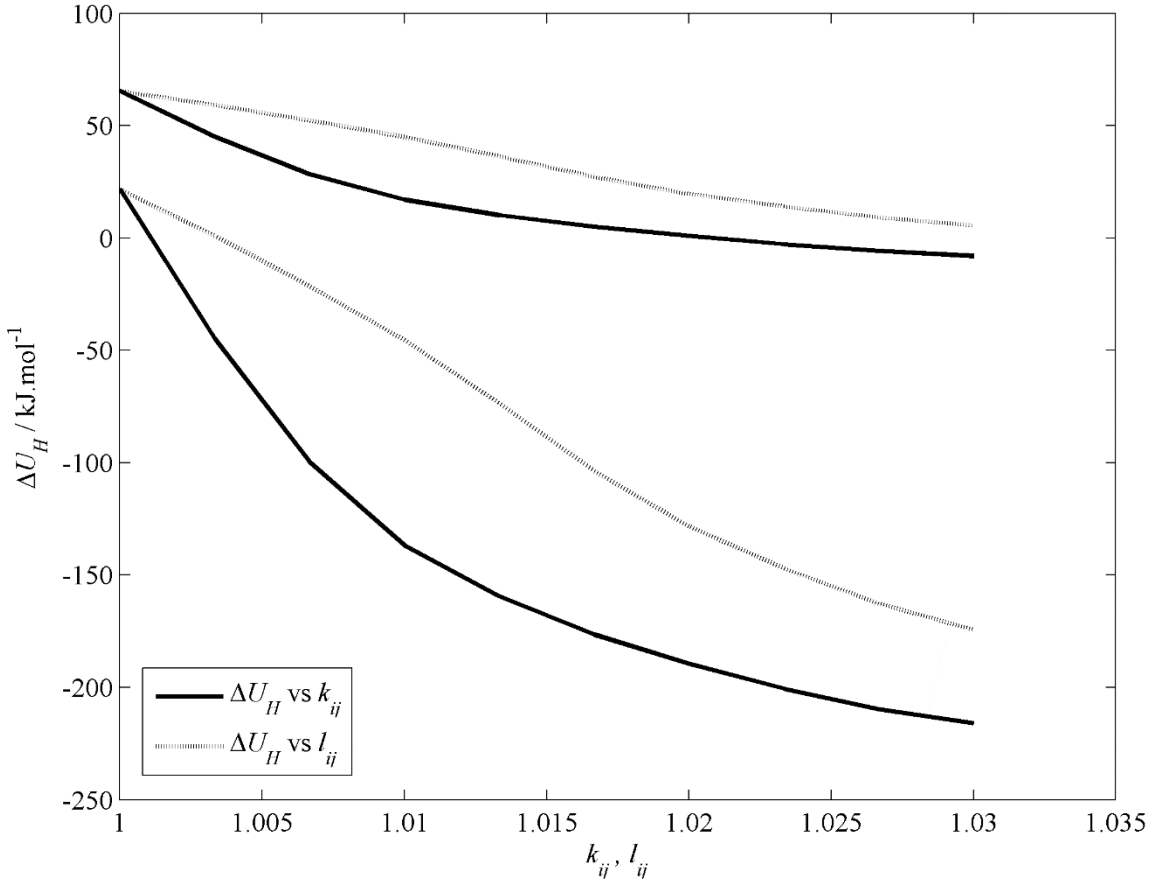

Figure 2.7. Estimates of allowed limits of ΔU_H.

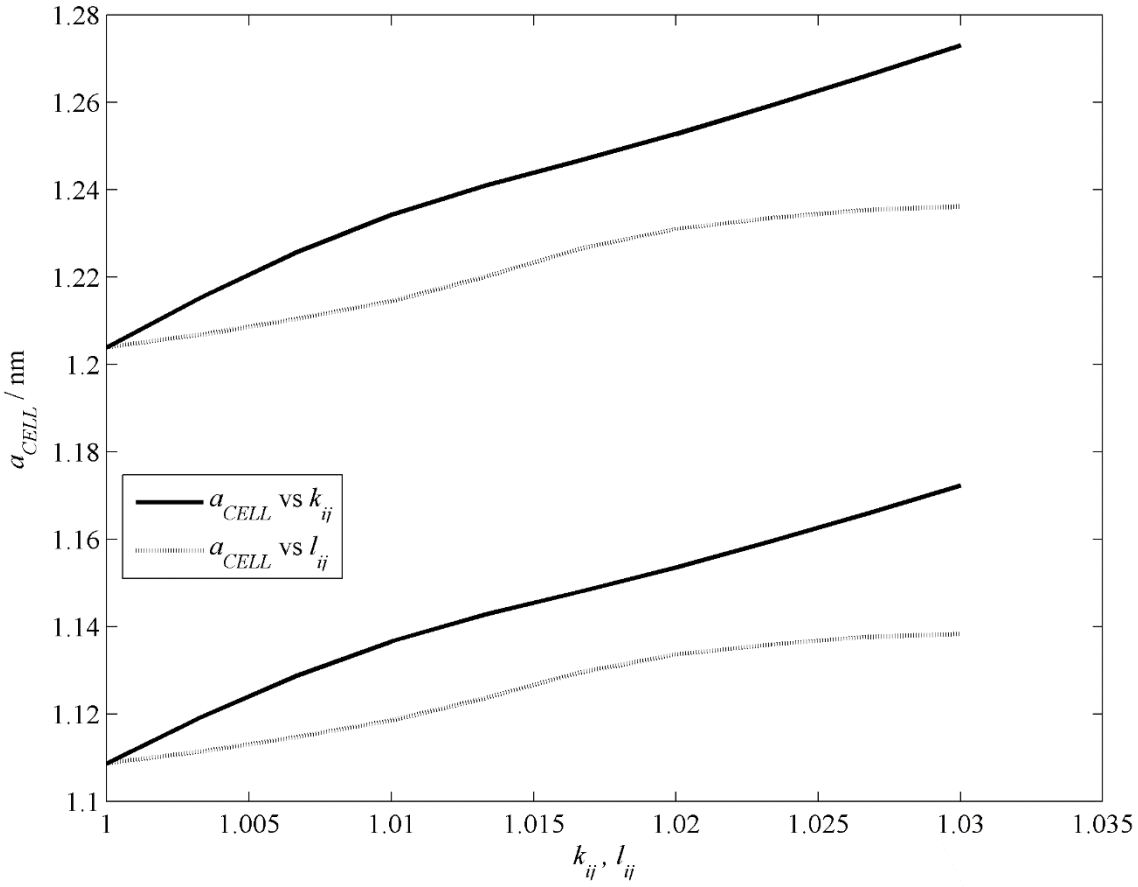

Figure 2.8. Estimates of allowed limits of a_{CELL}.

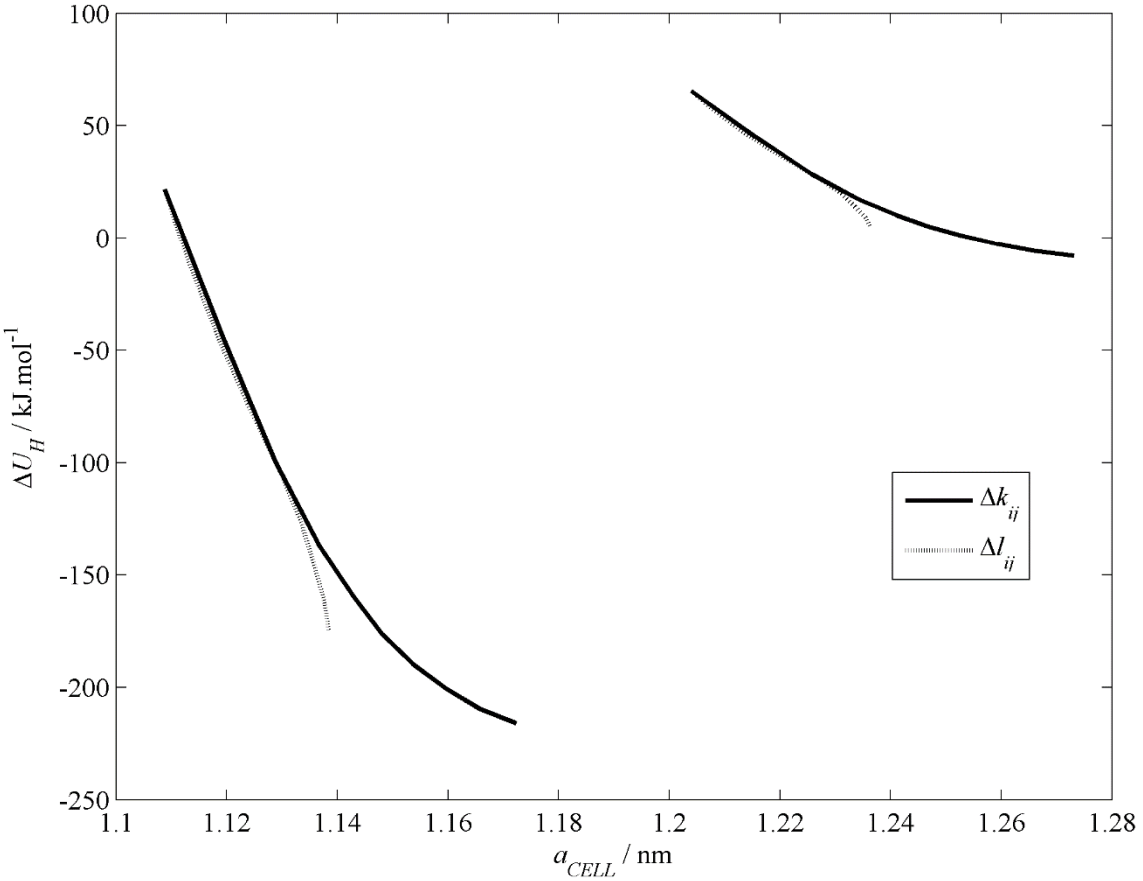

Figure 2.9. Estimates of allowed limits of ΔU_H and a_{CELL} determined by separately changing k_{ij} and l_{ij}.

It should be stated here that these 'allowed limits' do not reflect any tolerances related to inaccuracies or uncertainties in experimental data. Instead, they illustrate and further emphasize the sensitivity of the lattice-based calculations used in this study to changes in the LJ parameters for the adsorbed gas.

2.3.5. GENERAL TRENDS

It is important to consider how the force fields used in this study compare with other force fields which have been used to describe clathrate hydrate systems. The parameters of the SPC force field are very similar to the parameters of the extended SPC (SPC/E) force field [45] as well as the TIP4P force field [46]. The similarities of computations performed for clathrate hydrates using both the SPC/E and TIP4P force fields have been established in the literature [2,47,48]. As stated previously, the parameters of the united atom LJ force field used in this study for methane are very similar to the LJ parameters of other commonly used methane force fields (such as the OPLS-UA and TraPPE force fields). Thus, using the similarities evident in the parameters used for both the water and methane molecules in this study, it can be presumed that a similar response of the perturbation energy and lattice constant to LJ binary

correction factors can be valid for water + LJ clathrate hydrates in general, when using optimized lattice structures.

However, even though the trends observed in this study can be very similar to other united atom methane force fields, the sensitivity of ΔU_H and a_{CELL} to σ_{Tc} and σ_{Pc} should be considered. This sensitivity suggests that any combination of k_{ij} and l_{ij} obtained for a particular force field combination does not have general applicability, since the values obtained for k_{ij} or l_{ij} are specific to the particular LJ parameterization of methane. Thus, although ΔU_H and a_{CELL} can behave similarly as a function of k_{ij} or l_{ij} for each force field combination, the actual values of k_{ij} and l_{ij} can be very different.

An additional factor to consider when determining the general application of the results of this study is the structure forming capacity of the various water force fields. The structure forming capacity describes the capability of a force field to form ordered water dimers, trimers, tetramers, and so on. For pure water, this can be expressed as the frequency of occurrence of each geometric structure as a function of temperature. If results of this study were to have general application, it is important to consider how SPC water compares to other simulated species when forming regular, geometric networks.

A recent study [49] on the structure-forming capacity of SPC, SPC/E, TIP3P [50], TIP4P, TIP4P-Ew [51], TIP4P/2005 [52], and TIP5P [53] water force fields found that the capability of each of these water force fields to form ordered structures was qualitatively the same. Similar quantitative results were obtained for these water force fields if a "temperature shift" was applied. Hence, if the system temperature was adjusted, then all of the force fields form the same quantity of ordered structures, and the amount of each type of structure exhibits almost an identical temperature dependence. Therefore, since a great number of water force fields behave in the same way when forming ordered structures, it can be concluded that the results from this study have general application, at least when using a LJ gas species.

2.4. CONCLUSIONS

Both the perturbation energy and cell constant were found to be approximately linearly dependent on the values of the binary correction factors; the magnitude of the perturbation energy increases, whilst the cell constant increases with increasing binary correction factor values. It should be noted that both quantities are sensitive to small changes in k_{ij} and l_{ij}.

Different values for the binary correction factors can be calculated, depending upon which experimental data type is selected for comparison. Both k_{ij} and l_{ij} were found to have different values when either the lattice perturbation energy or the lattice constant were used for fitting. Fitting for the lattice constant

resulted in a poor value for the perturbation energy and vice versa.

The magnitude of the perturbation potential was found to correlate positively with the lattice constant. This was expected as increasing the lattice constant causes the system to deviate further from the reference state (the empty lattice) in LD theory.

REFERENCES

[1] E.D. Sloan, C.A. Koh, Clathrate Hydrates of Natural Gases, CRC Press, Boca Raton, FL, 2008.

[2] N.I. Papadimitriou, I.N. Tsimpanogiannis and A.K. Stubos, Colloids Surf. A: Physicochem. Eng. Asp. 357 (2010) 67-73.

[3] J.H. van der Waals, J.C. Platteeuw, Adv. Chem. Phys. 2 (1959) 1-57.

[4] V.T. John, G.D. Holder, J. Phys. Chem. 85 (1981) 1811-1814.

[5] V.T. John, G.D. Holder, J. Phys. Chem. 86 (1982) 455-459.

[6] V.T. John, G.D. Holder, J. Phys. Chem. 89 (1985) 3279-3285.

[7] V.T. John, K.D. Papadopoulos, G.D. Holder, AIChE J. 31 (1985) 252-259.

[8] P.M. Rodger, J. Phys. Chem. 94 (1990) 6080-6089.

[9] K.A. Sparks, J.W. Tester, J. Phys. Chem. 96 (1992) 11022-11029.

[10] B. Kvamme, A. Lund, T. Hertzberg, Fluid Phase Equilib. 90 (1993) 15-44.

[11] K.A. Sparks, J.W. Tester, Z. Cao, B.L. Trout, J. Phys. Chem. B 103 (1999) 6300-6308.

[12] Z. Cao, J.W. Tester, K.A. Sparks, B.L. Trout, J. Phys. Chem. B 105 (2001) 10950-10960.

[13] B.J. Anderson, J.W. Tester, B.L. Trout, J. Phys. Chem. B 108 (2004) 18705-18714.

[14] B.J. Anderson, M.Z. Bazant, J.W. Tester, B.L. Trout, J. Phys. Chem. B 109 (2005) 8153-8163.

[15] S.R. Zele, S.-Y. Lee, G.D. Holder, J. Phys. Chem. B 103 (1999) 10250-10257.

[16] H.A. Lorentz, Ann. Phys. 248 (1881) 127-136.

[17] D.C. Berthelot, Compt. Rend. 126 (1898) 1703-1706.

[18] T.M. Reed III, J. Phys. Chem. 59 (1955) 425-432.

[19] G.H. Hudson, J.C. McCoubrey, Trans. Faraday Soc. 56 (1960) 761-766.

[20] I.N. Tsimpanogiannis, N.I. Papadimitriou, A.K. Stubos, Mol. Phys. 110 (2012) 1213-1221.

[21] H. Docherty, A. Galindo, C. Vega, E. Sanz, J. Chem. Phys. 125 (2006) 074510.

[22] M.M. Conde, C. Vega, C. McBride, E.G. Noya, R. Ramírez, L.M. Sesé, J. Chem. Phys. 132 (2010) 114503.

[23] G.D. Holder, S. Zetts, N. Pradhan, Rev. Chem. Eng. 5 (1988) 1-70.

[24] L.S. Tee, S. Gotoh, W.E. Stewart, Ind. Eng. Chem. Fundam. 5 (1966) 356-363.

[25] G.D. Holder, S.R. Zele, R.M. Enick, C. Leblond, Ann. N.Y. Acad. Sci. 715 (1994) 344-353.

[26] J.D. Gale and A.L. Rohl, Mol. Simulat. 29 (2003) 291-341.

[27] I. Ohmine, H. Tanaka, Chem. Rev. 93 (1993) 2545-2566, and references cited therein.

[28] A. Lenz, L. Ojamäe, J. Phys. Chem. A 115 (2011) 6169-6176.
[29] W. Cochran, R.A. Cowley, J. Phys. Chem. Solids 23 (1962) 447-450.
[30] S. Baroni, S. de Gironcoli, A. Dal Corso, P. Giannozzi, Rev. Mod. Phys. 73 (2001) 515-562.
[31] J.M. Seddon, J.D. Gale, Thermodynamics and Statistical Mechanics, Royal Society of Chemistry, London, 2002.
[32] H.J.C. Berendsen, P.J.M. Postma, W.F. von Gunsteren, J. Hermans, Interaction models for water in relation to protein hydration. in Intermolecular Forces, B. Pullman, ed., Reidel, Dordrecht, 1981, p.331.
[33] J.E. Lennard-Jones, Proc. Phys. Soc. 43 (1931) 461-482.
[34] J.J. Potoff, A.Z. Panagiotopoulos, J. Chem. Phys. 109 (1998) 10914-10920.
[35] J.M. Smith, H.C. van Ness, M.M. Abbott, Introduction to Chemical Engineering Thermodynamics, 7th ed., McGraw-Hill, New York, 2005.
[36] P.P. Ewald, Ann. Phys. 369 (1921) 253-287.
[37] S. Moodley, E. Johansson, K. Bolton and D. Ramjugernath, Mol. Simulat. 38 (2012) 838-849.
[38] W.M. Deaton, E.M. Frost Jr., Gas Hydrates and Their Relation to the Operation of Natural Gas Pipelines, US Bureau of Mines Monograph 8, 1946.
[39] D.R. Marshall, S. Saito. R. Kobayashi, AIChE J. 10 (1964) 202-205.
[40] W.R. Parrish, J.M. Prausnitz, Ind. Eng. Chem. Process Des. Dev. 11 (1972) 26-35.
[41] D.Y. Peng, D.B. Robinson, Ind. Eng. Chem. Fundam. 15 (1976) 59-64.
[42] W.L. Jorgensen, J.D. Madura, C.J. Swenson, J. Am. Chem. Soc. 106 (1984) 6638-6646.
[43] M.G. Martin, J.I. Siepmann, J. Phys. Chem. B 102 (1998) 2569-2577.
[44] National Institute of Standards and Technology, Chemistry WebBook – Methane. Available at http://webbook.nist.gov/cgi/cbook.cgi?ID=C74828&Mask=4
[45] H.J.C. Berendsen, J.R. Grigera, T.P. Straatsma, J. Phys. Chem. 91 (1987) 6269-6271.
[46] W.L. Jorgensen, J.D. Madura, Mol. Phys. 56 (1985) 1381-1392.
[47] K. Katsumasa, K. Koga, H. Tanaka, J. Chem. Phys. 127 (2007) 044509.
[48] N.I. Papadimitriou, I.N. Tsimpanogiannis, A.T. Papaioannou, A.K. Stubos, J. Phys. Chem. C 112 (2008) 10294-10302.
[49] R. Shevchuk, D. Prada-Gracia, F. Rao, J. Phys. Chem. B 116 (2012) 7538-7543.
[50] W.L. Jorgensen, J. Chandrasekhar, J.D. Madura, R.W. Impey, M.L. Klein, J. Chem. Phys. 79 (1983) 926-935.
[51] H.W. Horn, W.C. Swope, J.W. Pitera, J.D. Madura, T.J. Dick, G.L. Hura, T. Head-Gordon, J. Chem. Phys. 120 (2004) 9665-9978.
[52] J.L.F. Abascal, C. Vega, J. Chem. Phys. 123 (2005) 234505
[53] M.W. Mahoney, W.L. Jorgensen, J. Chem. Phys. 112 (2000) 8910-8922.

CHAPTER THREE (BASED ON PAPER II): PHASE EQUILIBRIA OF METHANE CLATHRATE HYDRATE FROM GRAND CANONICAL MONTE CARLO SIMULATIONS

ABSTRACT

The determination of conditions at which clathrate hydrates are thermodynamically stable is important in applications such as offshore gas exploitation and energy storage. Adsorbed gas molecules occupy different cavity types within the hydrate lattice and this plays a significant role in the thermodynamic stability of clathrate hydrates. The occupancy of cavities in the hydrate lattice can be studied by undertaking Grand Canonical Monte Carlo simulations. Such simulations were performed in this study for methane clathrate hydrate with several force fields. Langmuir-type adsorption isotherms were fitted to the results of the simulations. The use of a single type of adsorption site was validated for methane clathrate hydrate. The adsorption isotherms which were fitted to the results of the simulations were used to compute the clathrate hydrate phase equilibria, which compared favourably with results from the literature.

3.1. INTRODUCTION

Clathrate hydrates are ice-like materials formed when inter-molecularly connected networks of water molecules enclathrate gas molecules, which are then trapped inside hydrogen-bonded crystal lattice structures. In nature, clathrate hydrates predominantly contain methane and can be found in permafrost or deep ocean deposits [1]. In industrial settings, clathrate hydrates form blockages in natural gas pipelines in offshore exploitation operations [2] and are a major area of concern [3]. Other areas of application of clathrate hydrates include their potential use as a storage medium for energy-carrier gases such as methane [4,5] and hydrogen [6,7], as a natural carbon sink on the Martian surface [8],and for use in industrial separation processes [9,10].

Three crystalline structures of clathrate hydrates are known: structure I (sI), structure II (sII), and structure H (sH) [1]. The sI clathrate hydrate contains two cavity types (small and large), with nominal radii of 0.395 and 0.433 nm, respectively [1]. The sII and sH clathrate hydrates have two and three cavity types, respectively. The sH clathrate hydrate has greater relative differences in cavity radii than sI or sII [1]. This is illustrated in Table 3.1 [11], which summarises the crystalline structures of the different clathrate hydrate structures. The sI or sII clathrate hydrates are usually found in nature or industry because gas molecules can readily occupy both cavity types to a reasonable extent, thereby stabilising the clathrate hydrate. The larger difference in cavity radii of the sH clathrate hydrate results

in a more pronounced size allowance for the gas molecules which can occupy the different cavity types. Therefore, only specific mixtures of small and large gas molecules can stabilize the sH clathrate hydrates, which results in this structure being less common. The use of computer simulations at the molecular level is well established as a complementary tool for research into adsorption of gases in clathrate hydrates [12–16]. An advantage of molecular simulations of clathrate hydrates over laboratory experiments is that the fractional occupancies of nanoscale cavities within the crystal lattice can be monitored directly. This is of interest as details of the physical mechanism or behaviour of clathrate hydrate formation or inhibition (depending upon the desired application) can yield improvements in industrial processes. For the case of natural gas exploitation, it is beneficial to inhibit the formation of clathrate hydrates within pipelines, thus reducing the cost to the consumer. In the case of energy storage, it is desirable to promote the formation and stability of clathrate hydrates to yield attractive materials for commercial use. Grand Canonical Monte Carlo (GCMC) simulations [17–19] in particular are useful to study gas adsorption in clathrate hydrates, as they provide information about the quantity of gas adsorbed and the spatial distribution of molecules within the crystal lattice. Moreover, purely hypothetical molecules can be investigated, providing insight into molecular behaviour of clathrate hydrates. This contribution studies adsorption of methane into sI clathrate hydrate by means of GCMC simulations, as well as phase equilibria calculated from these data. Comparisons are made with published results, and the use of GCMC simulations to study clathrate hydrate phase equilibria is illustrated.

Clathrate crystal structure	sI		sII		sH		
Crystal system	Primitive cubic		Face-centered cubic		Hexagonal		
Space group	*Pm3n*		*Fd3m*		*P6/mmm*		
Cavity type	Small	Large	Small	Large	Small	Medium	Large
Cavity description	5^{12}	$5^{12}6^2$	5^{12}	$5^{12}6^4$	5^{12}	$4^35^66^3$	$5^{12}6^8$
Cavities/unit cell	2	6	16	8	3	2	1
Cavity radius (nm)	0.395	0.433	0.391	0.473	0.391	0.406	0.571
H_2O/unit cell	46		136		34		
Unit cell formula	$2S{\cdot}6L{\cdot}46H_2O$		$16S{\cdot}8L{\cdot}136H_2O$		$3S{\cdot}2M{\cdot}1L{\cdot}34H_2O$		

Table 3.1. Summary of crystalline structures and properties of the three types of clathrate hydrate structures. In the unit cell formula S, M, and L denote small, medium, and large cavities, respectively [11].

A large fraction of adsorption sites may be occupied when using gas hydrates as an energy storage medium, since it can contain by volume, significant amounts of energy-carrier gases such as methane [4] or hydrogen [6,7,20]. Computational studies can provide occupancy data of adsorption sites directly, whereas experimental measurements are more complex or costly, and are often based on neutron diffraction [21–29]. There have been several computational studies of gas adsorption in clathrate

hydrates. These include gases such as methane [13,16], hydrogen [14], carbon dioxide [16], xenon [12], and nitrogen [30]. Such studies have considered both flexible and rigid water lattices, and although the flexible lattice is inherently more rigorous, it was found that there was little qualitative difference between the results obtained via either approach. For the sake of rigour, flexible lattices were used in this study. Adsorption characteristics of clathrate hydrates do not directly reveal the conditions at which they are thermodynamically stable. However, it was suggested that there may be "equivalence between the coexistence line on the phase diagram and the con-tour of 90% total cage occupancy, corresponding to the stable methane hydrate" [13], and that this can provide qualitative assessment of thermodynamic stability of the hydrate through adsorption simulations. Moreover, phase equilibrium calculations of the stable hydrate region, performed using van der Waals–Platteeuw (vdWP) theory, make use of a cage occupancy term. Thus, the thermodynamically stable region can be estimated if the adsorption behaviour is known. Previous studies of adsorption in the sI methane clathrate hydrate do not fully agree on the adsorption mechanism. The vdWP theory states that there are two different types of adsorption sites (small and large), and that large sites are preferentially occupied by gas species during adsorption. Computational studies by Sizov and Piotrovskaya [13] and Glavatskiy at al. [16] have suggested that there can be no distinction between small and large adsorption site types in methane clathrate hydrate (for the temperature ranges of $T < 260$ K, and $278\ K \leq T \leq 328$ K, respectively). These two studies also found that the Langmuir-type adsorption model did not fit the data. In contrast, Papadimitriou et al. [15] determined that adsorption of methane in sI clathrate hydrate can be described by adsorption in two distinct types of adsorption sites, and by Langmuir-type adsorption. Thus, this contribution examines which model can best describe the sI methane clathrate hydrate.

3.2. THEORY AND METHODS

3.2.1. CLATHRATE HYDRATE PHASE EQUILIBRIA

Phase equilibrium relations of clathrate hydrates were developed using statistical mechanics in vdWP theory [31], which describes the chemical potential of loaded clathrate hydrate in equilibrium with liquid water. There are several shortcomings of vdWP theory [32–42] due to assumptions made in its original formulation. These include the assumptions that there are no inter-molecular interactions between the gas species molecules and that there are no thermal vibrations of the water molecules in the crystal lattice. In spite of this, vdWP theory is frequently used to perform phase equilibrium calculations for clathrate hydrate systems since it yields data that is in reasonably good agreement with experimental results [43].

The internal partition function of the adsorbed methane molecules is assumed to be the same as that for the molecules in the gas phase [31]. Therefore, the phase equilibrium criterion is the equality between

the chemical potential of liquid water (μ_w^l) and water in the hydrate phase (μ_w^H):

$$\mu_W^L = \mu_W^H \tag{3.1}$$

For convenience, the chemical potential of the hypothetical empty clathrate hydrate (μ_W^β) is used as a reference state:

$$\Delta\mu_W^L = \mu_W^\beta - \mu_W^L = \Delta\mu_W^H = \mu_W^\beta - \mu_W^H \tag{3.2}$$

The fractional occupancy of cavities in the clathrate hydrate by the gas species (θ) is used to calculate the difference between the chemical potential of water in loaded hydrate and the reference state ($\Delta\mu_W^H$):

$$\Delta\mu_W^H = -R\cdot T\cdot \sum_j [\, v_j \cdot \ln(1 - \sum_i \theta_{ij})\,] \tag{3.3}$$

where index i refers to the gas species, j refers to cavity type (i.e., small, medium, large), v_j is the ratio of type j cavities to water molecules per unit cell in the hydrate lattice, and θ_{ij} is the fractional occupancy by gas species i of cavity type j. Langmuir-type adsorption [44] is often used to describe adsorption of the gas species into the cavities of the clathrate hydrate. GCMC simulations yield fractional occupancies of cavities directly. The use of this type of adsorption calculation with GCMC simulations is elaborated in section 3.2.4.

The difference in chemical potential between water in the liquid phase and the reference state ($\Delta\mu_W^L$) may be expressed as the difference in chemical potential between two pure phases at a reference state ($\Delta\mu^0$) of T_R = 273.15 K and P_R = 0 MPa, considering the temperature and pressure dependence [45]:

$$(\Delta\mu_W^L)/(R\cdot T) = (\Delta\mu^0)/(R\cdot T_R) - \int_{TR}^{T} \Delta H_W/(R\cdot T^2)\cdot dT + \int_0^P \Delta V_W/(R\cdot T)\cdot dP \tag{3.4}$$

where ΔH_W and ΔV_W are the differences in enthalpy and molar volume, respectively, between liquid water and the reference state. The volume term (ΔV_W) is assumed constant over the temperature range of interest. The enthalpy term (ΔH_W) is expressed in terms of the difference in isobaric heat capacity between liquid water and the reference state (ΔC_{PW}):

$$\Delta H_W = \Delta H_W{}^0 + \int_{TR}^{T} \Delta C_{PW}\cdot dT \tag{3.5}$$

where ΔH_W^0 is the enthalpy difference at the reference conditions of T_R= 273.15 K and P_R= 0 MPa.

The original form [45] of Equation (3.4) also includes a term correcting for the solubility of the gas species in the liquid phase. However, this term can be neglected as it is several orders of magnitude lower than the other contributions to the chemical potential [46,47]. Values used to calculate phase equilibria can be found in the literature [48].

The phase equilibria were calculated using the Nelder–Mead algorithm [49] with a tolerance of 10^{-12} to minimise the objective function, Equation (3.2), by adjusting the system pressure or temperature as required. In this way, the dissociation pressure was calculated for each temperature, and vice versa. Only sI clathrate hydrates were considered, as methane clathrate hydrates naturally occur in this form [1].

3.2.2. CLATHRATE HYDRATE CRYSTAL STRUCTURE

The usual approach to calculate gas hydrates via vdWP theory [31] considers sI clathrate hydrate as having two separate adsorption sites onto which gas molecules are adsorbed according to a Langmuir-type mechanism. These sites are located at the centres of the small and large cavities within the unit cell.

The sI unit cell itself consists of 46 water molecules, with 2 small and 6 large cavities fully enclosed by hydrogen-bonded water molecules. These cavities can be considered (geometrically) as “cages”, with the small cage being formed by 12 pentagonal rings of water molecules, and the large cage being formed by 12 pentagonal rings and two hexagonal rings of water molecules [11]. Oxygen atoms form vertices of these polygonal rings, with hydrogen atoms lying along the edges. Nominal radii of the small and large cages are 0.395 nm and 0.433 nm, respectively [2]. It should be stated that although these cages are not spherical, a spherical approximation is often used in the literature, especially when determining the Langmuir constants to describe adsorption of gas molecules. Cages in sI clathrate hydrate are arranged in a primitive cubic manner, according to the Pm3n crystallographic space group, and the cell constant is 1.203 nm [1].

Clathrate hydrates are from a class of substances known as “clathrate compounds” which consist of networks of intermolecularly connected molecules of a “host” species “enclathrating”, or trapping, a “guest” species. The sI hydrate is, in more general terms, a solution of the Kelvin problem which deals with the geometry of bubbles of equal volume which share minimum surface area when forming foam. The sI structure is the Weaire–Phelan structure [50] which is a superior solution to the previous optimal solution, the Kelvin conjecture [51]. In essence, the sI structure represents a system of cavities of roughly equal volume and thus it is reasonable to presume that in certain cases there can be guest particles which behave in a manner which suggests there is no distinction between the nominal types of

cavities.

3.2.3. SIMULATION DETAILS

Methane adsorption characteristics of sI hydrates were studied by GCMC [17,18] computer simulations making use of the Metropolis scheme [19]. The General Utility Lattice Program [52] was used to perform these computations. The GCMC ensemble specifies the chemical potential (μ), volume (V), and temperature (T) of the system. Simulations were performed for 10^7 MC moves, and the first 25% were used to reach equilibrium, since the number of adsorbed gas molecules began to plateau after about 10^6 MC moves. The following types of MC moves were considered: translation/rotation, particle creation and destruction. The probability of selecting each type of move was 33.3%. The translation/rotation moves mimic the motion of molecules within the hydrate, and the creation and destruction moves (applied solely to the gas molecules) represent adsorption and desorption processes, respectively. Flexibility was allowed for the crystal lattice, for the sake of rigour. The maximum allowed translational displacement was 0.05 nm. The value of the chemical potential (see Figure 3.1) was estimated in the isobaric-isothermal ensemble using the computer program "ms2" [53]. Chemical potential values obtained using these simulations were then used in the GCMC simulations.

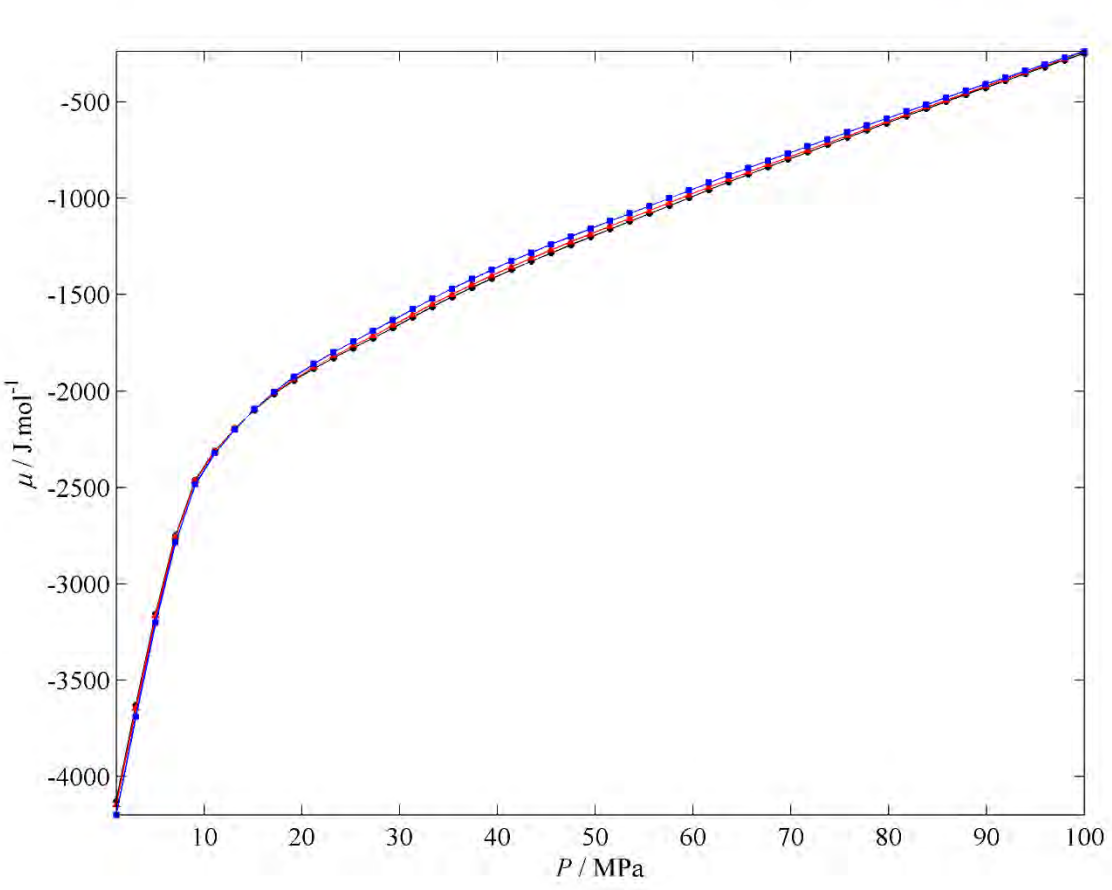

Figure 3.1. Chemical potential (μ) of methane versus pressure (P), estimated using the isobaric isothermal ensemble with Widom's method [53,54]. (-O-) T = 273.2 K, (-Δ-) T = 280 K, and (-□-) T = 300 K.

For the fluid phase MC simulations, the system consisted of 500 methane particles. Relaxation for pre-equilibration consisted of 100 MC cycles, followed by 2×10^4 NVT cycles and 5×10^4 NPT steps for equilibration. 3×10^5 MC cycles were used for data production. Widom's method [54] was used to estimate the chemical potential, using 2000 test particles. These fluid phase simulations were used to determine the chemical potential to ensure self-consistency in terms of the force fields used to describe the phases in equilibrium. In this way, any anomalous behaviour observed cannot be due to inconsistencies or discrepancies in the molecular description of the phases in equilibrium, which may be the case if, for example, an equation of state was used to determine the fluid phase chemical potential.

A single (i.e., $1 \times 1 \times 1$) unit cell of sI methane clathrate hydrate was considered in the present GCMC simulations, since extensive studies of finite size effects have found negligible differences when using either a $1 \times 1 \times 1$ or $2 \times 2 \times 2$ unit cell [14,55]. A sI lattice structure from a previous computational study [56] was used, but the lattice constant was fine-tuned to 1.20 nm.

The same force fields were used for the grand equilibrium ensemble and GCMC simulations. The water

molecules were described by the simple point charge (SPC) [57] or the TIP4P/ice [58] force fields, which allowed for comparison of the results obtained from these two models. Intermolecular dispersion forces were modelled using the Lennard-Jones (LJ) potential [59]. Two different methane force fields were used: the transferable potentials for phase equilibrium (TraPPE) [60] force field, and another in which the LJ parameters were determined from the critical properties (i.e. critical temperature T_C= 190.6 K, and critical pressure P_C= 4.60 MPa) [61,62]. The force field parameters used in this study are presented in Table 3.2. Interaction between unlike LJ pairs was determined by the Lorentz [63] and Berthelot [64] combining rules. The cut-off radius was 1 nm for the LJ interactions and Ewald [65] summation was used for electrostatic long range interactions.

Force field	Non-bonded interactions (Lennard-Jones [57])	Charges	Bond angle
SPC water [57]	ε_O / k_B = 78.21 K	q_O = -0.82 e	$\alpha_{(H\text{-}O\text{-}H)}$ = 109.47 ^{o}
	σ_O = 0.3166 nm	q_H = +0.41 e	
TIP4P/Ice water [58]	ε_O / k_B = 106.1 K	q_O = -1.1794 e	$\alpha_{(H\text{-}O\text{-}H)}$ = 104.52 ^{o}
	σ_O = 0.31668 nm	q_H = +0.5897 e	
United atom LJ methane [61,62]	ε_{CH4} / k_B = 145.27 K		
	σ_{CH4} = 0.3821 nm		
TraPPE methane [60]	ε_{CH4} / k_B = 148.0 K		
	σ_{CH4} = 0.3730 nm		

Table 3.2. Force field parameters used in this study.

3.2.4. LANGMUIR-TYPE GAS ADSORPTION

The single-site Langmuir adsorption isotherm [44] is the simplest physically plausible description of the adsorption of gases onto solid surfaces [66]. Such adsorption isotherms are dependent upon temperature and the pressure of gas being adsorbed. This description is based upon three assumptions [66]: adsorption can only proceed up to a thickness of one layer of adsorbed gas molecules; all adsorption sites are equivalent; and the adsorption ability of any molecule at any site is independent of the occupation of neighbouring sites (i.e., there is no interaction between adsorbed gas molecules).

The Langmuir adsorption isotherm, or the number of adsorbed gas molecules per unit cell (N_i) for gas species i, can be expressed in terms of gas pressure (P_i), total number of adsorption sites per unit cell (N_T), and the Langmuir constant (C_i) [44]:

$$N_i = (C_i \cdot P_i \cdot N_T) / (1 + [C_i \cdot P_i]) \quad (3.6)$$

The quantity of interest in clathrate hydrate phase equilibria, however, is not the number of gas molecules adsorbed, but the fraction of cavities which are occupied, as required in Equation (3.3). Therefore, it is necessary to express Equation (3.6) such that the fraction of occupied adsorption sites is expressed as a function of P, C_i, and T. The fractional occupancy (θ) is defined as

$$\theta = N_i / N_T \tag{3.7}$$

It should also be noted that non-ideality of gas species can be accounted for in Equation (3.6) by substitution of pressure by fugacity. For fitting the Langmuir constant and calculating phase equilibria, the fugacity was determined by the Peng–Robinson cubic equation of state [67]. This was to ensure consistency with the vdWP calculation, in which the Peng–Robinson equation of state is used in this study.

In order to determine whether Equation (3.6) provides a valid description of the adsorption observed in experiments or from simulations, a linearised form is required [68]:

$$(P_i / N_i) = [(1 / N_T) \cdot P_i] + [1 / (C_i \cdot N_T)] \tag{3.8}$$

Thus, if a plot of P_i/N_i versus P_i is linear then a single-site Langmuir-type isotherm describes the observed adsorption. It should be noted that this type of verification calculation is biased towards higher pressures [66], and is therefore well-suited to clathrate hydrate systems, which are often under high pressure.

A useful relationship which can be used to describe temperature dependence of the Langmuir constant is in terms of parameters A_i and B_i fitted to various data sources [48]:

$$C_i = (A_i / T) \cdot \exp (B_i / T) \tag{3.9}$$

It may be noted that the relationship shown above in eq. (3.9) is of the van't Hoff form. Such a temperature dependence is often used to fit experimental clathrate hydrate data [69], and in fact can be expected from general thermodynamic considerations [70,71].

3.3. RESULTS AND DISCUSSION

3.3.1. SINGLE SITE ADSORPTION

Figure 3.2 shows a snapshot for the SPC water + united-atom LJ methane clathrate hydrate system at T

= 273.2 K and P = 3 MPa, after 9310748 MC moves. Results of the GCMC simulations, expressed in the form of Equation (3.8), are presented in Figures 3.3 through 3.5. It is apparent that the results for all force fields exhibit a linear trend when considering both pressure and fugacity. This suggests that there is no significant difference whether methane is treated as an ideal or non-ideal gas under the conditions in this study. The correlation coefficients for linear trends fitted to the data for all isotherms were greater than 0.997, and all trend lines lie within the statistical uncertainties of the GCMC simulations.

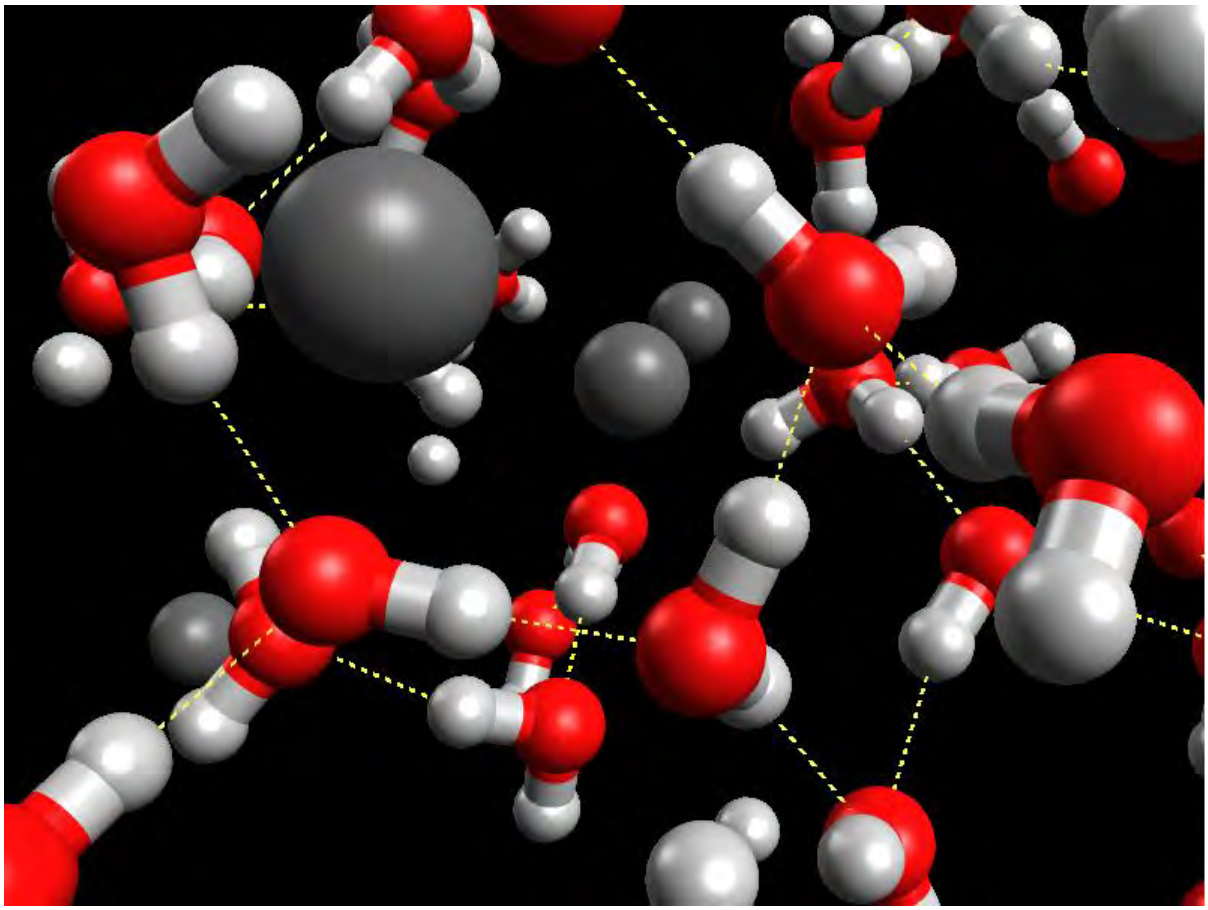

Figure 3.2. Snapshot of the SPC water + united-atom LJ methane clathrate hydrate system at T = 273.2 K and P = 3 MPa, after 9310748 MC moves. The dashed lines represent hydrogen bonds between the 3-site water molecules. Methane molecules are represented by lone, unconnected, dark grey particles inside the clathrate lattice.

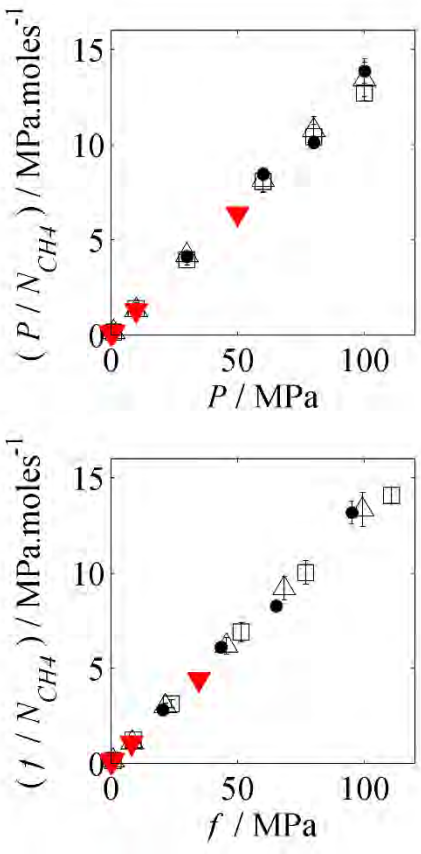

Figure 3.3. Linearised Langmuir-type adsorption isotherms for sI SPC water + united-atom LJ methane clathrate hydrate; see Equation (3.8). The upper plot employs pressure (*P*) (i.e., assumption of ideal gas behaviour for methane), and the lower plot uses fugacity (*f*) in Equation (3.8). NCH4 is the number of moles of methane adsorbed per mole of the crystal unit cell. System at: (●) *T* = 273.2 K, (Δ) *T* = 280 K, and (□) *T* = 300 K. Adsorption isotherms obtained by Papadimitriou and co-workers [15] at *T* = 273 K: (▼).

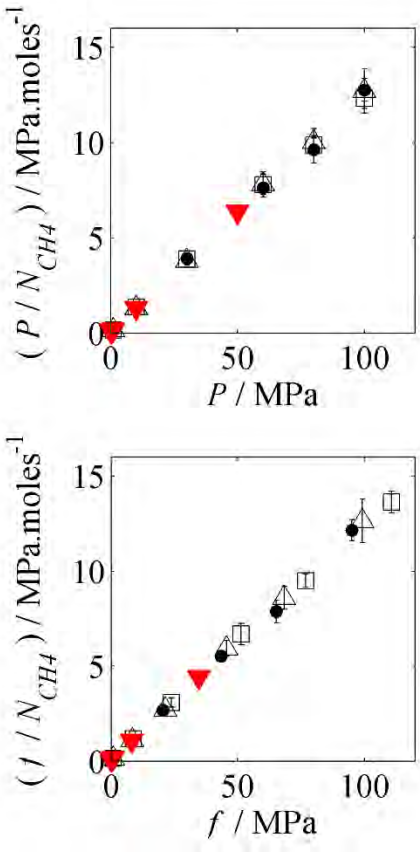

Figure 3.4. Linearised Langmuir-type adsorption isotherms for sI SPC water + TraPPE methane clathrate hydrate; see Equation (3.8). The upper plot employs pressure (*P*) (i.e., assumption of ideal gas behaviour for methane), and the lower plot uses fugacity (*f*) in Equation (3.8). NCH4 is the number of moles of methane adsorbed per mole of the crystal unit cell. System at: (●) *T* = 273.2 K, (Δ) *T* = 280 K, and (□) *T* = 300 K. Adsorption isotherms obtained by Papadimitriou and co-workers [15] at *T* = 273 K: (▼).

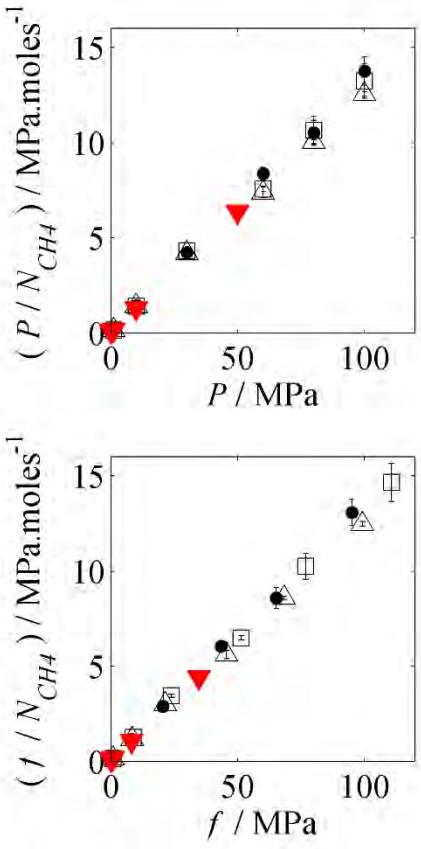

Figure 3.5. Linearised Langmuir-type adsorption isotherms for sI TIP4P/ice water + united-atom LJ methane clathrate hydrate; see Equation (3.8). The upper plot employs pressure (*P*) (i.e., assumption of ideal gas behaviour for methane), and the lower plot uses fugacity (*f*) in Equation (3.8). NCH4 is the number of moles of methane adsorbed per mole of the crystal unit cell. System at: (●) *T* = 273.2 K, (Δ) *T* = 280 K, and (□) *T* = 300 K. Adsorption isotherms obtained by Papadimitriou and co-workers [15] at *T* = 273 K: (▼).

Examination of the occupancy at the molecular level (using spatial coordinate data) showed gas molecules at all adsorption sites. Statistical uncertainties of occupancy data for the "small" cavities were substantial, and made it difficult to distinguish between adsorption at the two types of sites. For this reason, Equation (3.8) was used to further examine the plausibility of using a single type of adsorption site. It should also be noted that the reciprocals of the slopes of the linear trends described by Equation (3.8) yielded a range of $6.3 < N_T < 7.1$, which further corroborates the fact that gas molecules are adsorbed at all site (as mentioned above there are 8 sites in the unit cell used in the simulations).

The linearity present in Figures 3.3 through 3.5 suggests that adsorption of methane into sI clathrate hydrates can be described in terms of a single type of Langmuir site. This is evidenced by the linear trends in Figures 3.3 through 3.5. The correlation coefficients (R^2) for each of the linear trends (averaged for each force field combination) are shown in Table 3.3, and it is clear that all are highly linear (R^2= 0.999 in all cases, with a minimum of R^2= 0.997). The validity of a single Langmuir-type adsorption

site suggests that, from the perspective of methane molecules being adsorbed, there is no clear distinction between cavity types in the hydrate lattice. This can be due to the size of methane molecules relative to the cavities; $\sigma_{CH4} \approx 0.38$ nm (see Table 3.2), while the small and large cavity radii are 0.395 and 0.433 nm, respectively (see Table 3.1). This significant size differential between methane molecules and cavities in the hydrate lattice resulted in the probability of acceptance during the adsorption process being about the same for both small and large cavities (within the statistical uncertainties).

Force fields	A_i / K·MPa^{-1}	B_i / K	AAD / %	R^2
SPC water + united atom LJ methane	19.129	$1.3121 \cdot 10^3$	6.3	0.999
SPC water + TraPPE methane	18.276	$1.5073 \cdot 10^3$	2.7	0.999
TIP4P/Ice water + united atom LJ methane	10.392	$1.5183 \cdot 10^3$	7.3	0.999

Table 3.3. Fitted parameters for Langmuir-type adsorption isotherms [44] obtained from GCMC simulations; see Equation (3.9). AAD is the absolute average deviation of fitted adsorption isotherms to GCMC simulation results from this study, and R^2 is the average correlation coefficient of linear fits to the linearized forms of the adsorption isotherms; see eq. (3.8).

It should be noted, however, that this lack of differentiation in the adsorption of methane into the usual two cavity types can be considered as an approximation. Strictly speaking, there can be a differentiation in the adsorption of methane molecules into the cavity types. However, the statistical uncertainties of the results of the GCMC simulations of around 5-9 %, and in the results of laboratory experiments of around 2-15 % [72] should also be considered in this analysis. Therefore, results shown in Figures 3.3 through 3.5 suggest that the differentiation between cavity types in sI methane clathrate hydrates can be neglected, as this approximation is within the limits of the expected uncertainties in fractional occupancies of cavities within the hydrate lattice.

A consequence of considering only a single cavity type for certain clathrate hydrates is that in fitting Equation (3.9) to experimental data, only two parameters are required, instead of the usual two parameters per cavity type. Thus, fewer data points are needed for regression. Future GCMC simulations will focus on the size range of the gas molecules in which this simplification is valid.

3.3.2. ADSORPTION ISOTHERMS

Parameters required to estimate the Langmuir constants by Equation (3.9) are presented in Table 3.3, with average absolute deviation (AAD) of fitted equations with respect to results of GCMC simulations. Fit-ting was undertaken by comparing calculated occupancies ($\theta_{Calc.}$) and occupancies from GCMC simulations ($\theta_{Sim.}$, see Equation (3.8)), using the sum of squared errors (SSE) adjusted for uncertainties in simulations (u_i) as follows:

$$SSE = \sum_i [(\theta_{Calc.} - \theta_{Sim.})_i^2 / u_i] \quad (3.10)$$

This adjustment can limit the fitting procedure from favouring data which are associated with large uncertainties. The occupancies are considered as the fraction of the total number of adsorption sites (i.e., 8 in the sI clathrate hydrate) which are occupied by methane molecules.

It should also be mentioned that in order to describe retrograde phase behaviour of methane clathrate hydrate, an explicit pressure dependence of the Langmuir constants could be considered [74].However, pressure dependence would only influence the phase equilibria at very high pressures. The simulations considered in this study reached a maximum pressure of 100 MPa, and so this may not be applicable for the results shown. This will be investigated in future studies.

There is some disparity between the AAD values presented in Table 3.3 and the linearity (described by the R^2 values) of the Langmuir isotherm trend lines shown in Figures 3.3 through 3.5. The significantly larger absolute average deviations for the fit-ted adsorption isotherms using Equation (3.9) arise as an artefact of the temperature-dependence fitting. This is not a shortcoming of the Langmuir adsorption isotherm itself, but of the form of the temperature dependence which is commonly used.

3.3.3. PHASE EQUILIBRIA

Phase equilibria of methane clathrate hydrates are shown in Figure 3.6, expressed in terms of dissociation pressure versus temperature. The calculated phase equilibria from this study are compared to calculations using Langmuir-type isotherms reported in the literature [15,48] as well as to experimental results [75,76]. It can be seen that the present simulations agree with calculations from the literature [15], within estimated statistical uncertainties. Uncertainties were derived from the maximum fractional deviations of Langmuir-type adsorption isotherms fitted to results of GCMC simulations. It should be noted that this study uses only two adjustable parameters (A_i and B_i), as opposed to the four parameters (A_i and B_i for both the small and large cavities) from the literature [15]. Considering two types of cavities in the hydrate lattice does not result in a significant improvement of the calculated phase equilibria as compared to the assumption of a single effective cavity type.

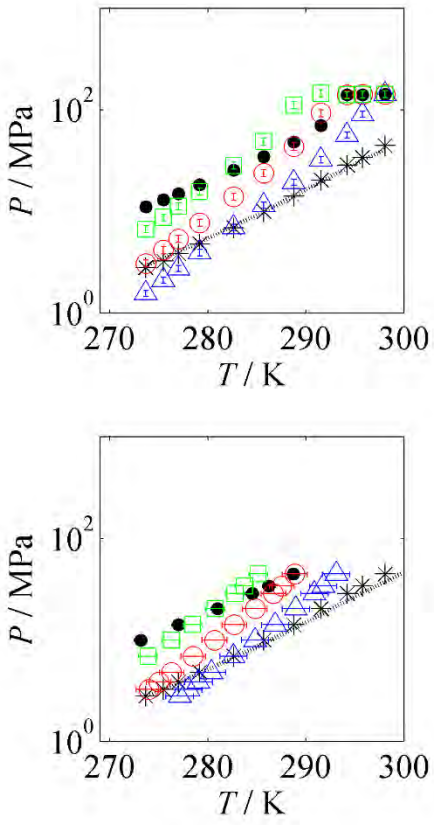

Figure 3.6. Dissociation pressure (*P*) versus temperature (*T*) for sI methane clathrate hydrate. The upper plot was determined by varying *P*, and the lower plot by varying *T* in Equation (3.2). Calculated phase equilibria based on Langmuir-type adsorption isotherms fitted to GCMC data: (●) previous study [15], (Δ) SPC water + TraPPE methane, and (O) SPC water + united atom LJ methane, (□) TIP4P/ice water + united atom LJ methane, (∗) experimental measurements [71,72], and (· · ·) calculated phase equilibria [48].

Another point of interest is the apparent convergence between calculated phase equilibria and experimental measurements at high pressures. It was previously [12] found that the free energy of clathrate hydrates calculated from GCMC simulations converges with the directly calculated free energy at high pressures. The convergence seen for the calculated phase equilibria in this study also suggests that agreement between GCMC simulations and the real clathrate hydrate systems improves at high pressures.

Figure 3.7 compares the results of this study with a previous study which used molecular dynamics (MD) simulations to determine the direct coexistence [77] for a united atom LJ methane using parameters from two sources [78,79] with several water force fields: TIP4P [80], TIP4P/2005 [81], and TIP4P/ice [58]. The influence of adjusting a binary correction factor (k_{ij}) for the Berthelot rule applied for the cross-interaction in the dispersion parameter (ε) between intermolecular LJ sites i and j is also shown. This correction factor is applied as:

$$\varepsilon_{ij} = k_{ij} \cdot (\varepsilon_i \cdot \varepsilon_j)^{0.5} \qquad (3.11)$$

The adjustment to k_{ij} shown in Equation (3.11) was performed indirectly, by fitting the excess chemical potential of dilute methane in liquid water [82].

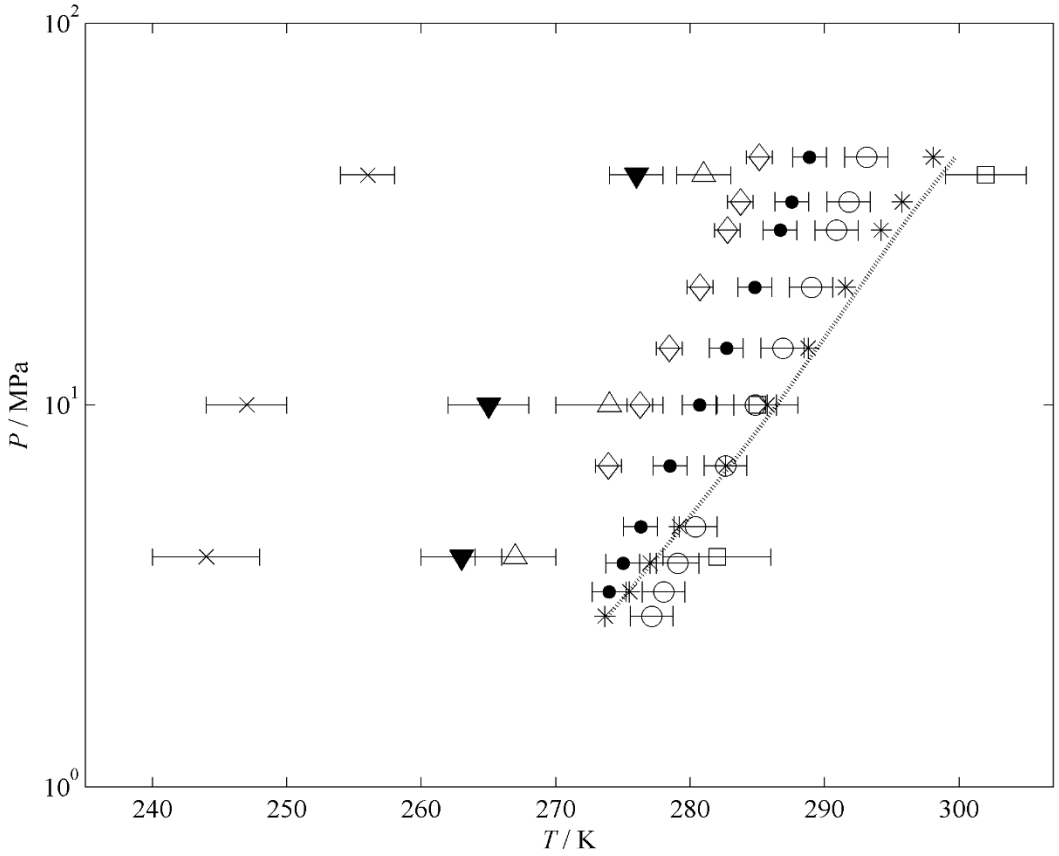

Figure 3.7. Dissociation pressure (*P*) versus temperature (*T*) for sI methane clathrate hydrate. Calculated phase equilibria based on Langmuir-type adsorption isotherms fitted to GCMC data: (●) SPC water + TraPPE methane, (o) SPC water + united atom LJ methane, (◊) TIP4P/ice water + united atom LJ methane. Direct coexistence simulations [77] using a different united atom LJ methane [78,79]: (×) TIP4P water, (▼)TIP4P/2005, (Δ) TIP4P/2005 with k_{ij} = 1.07 (see Equation (11)), (□) TIP4P/ice. (∗) experimental measurements [75,76], (· · ·) calculated phase equilibria [48].

It is apparent that the phase equilibria calculated in this study from GCMC simulations compare favourably with results of direct coexistence MD simulations. A comparison of the deviations in terms of temperature is presented in Table 3.4. In particular, only direct coexistence MD simulations performed using TIP4P/ice water performed as well as the GCMC simulations in predicting

experimental phase equilibria. Generally, the phase equilibria obtained using direct coexistence MD and GCMC simulations are comparable when using various combinations of force fields. Therefore, GCMC simulations provide a valid method to determine Langmuir-type adsorption isotherms which can then be used to calculate clathrate hydrate phase equilibria.

Figure 3.7 also shows that the force field can be fine-tuned to yield results that are in better agreement with experiment. These changes can possibly be applied to cross-interactions between methane and water LJ sites via Equation (3.11). This can be done using experimental dissociation pressures, by means of Langmuir-type adsorption isotherm fitting to the results of GCMC simulations. As stated previously, the determination of binary correction factors has been undertaken more indirectly in the past, such as via the excess chemical potential of dilute methane in liquid water [82]. For the purposes of flow assurance in offshore gas exploitation, where phase equilibria are of direct interest, it could be more useful to make a direct comparison with available experimental measurements.

It was also found that phase equilibria calculated in this study using parameters derived from GCMC simulations employing the SPC force field yielded better predictions of the experimental data than with TIP4P/ice water. The TIP4P/ice system from this study did not fit as well as a previous study using direct coexistence MD simulation. [77], which could be due to the other parameters in the phase equilibrium calculation (see Equations (3.1)–(3.5)).

Force fields	Method	Source	AAD / K	AAD / %
SPC water + united atom LJ methane	GCMC adsorption	This study	5.3	1.8
SPC water + TraPPE methane	GCMC adsorption	This study	2.4	0.8
TIP4P/Ice water + united atom LJ methane	GCMC adsorption	This study	10.8	3.7
SPC/E water + OPLS-UA methane	GCMC adsorption	[15]	10.6	3.6
TIP4P water + united atom LJ methane	Direct coexistence MD	[77]	38.0	13.2
TIP4P/2005 water + united atom LJ methane	Direct coexistence MD	[77]	19.0	6.6
TIP4P/2005 water (k_{ij} = 1.07) + united atom LJ methane	Direct coexistence MD	[77]	13.0	4.5
TIP4P/Ice water + united atom LJ methane	Direct coexistence MD	[77]	3.3	1.2

Table 3.4. Comparison of different data sets in terms of the deviation from experimental dissociation temperature of methane clathrate hydrate. AAD is the absolute average deviation of calculated (this study and [15]) and simulated [77] phase equilibria to experimental data [75,76].

3.3.4. HEAT OF DISSOCIATION

Once the phase equilibria are known, the heat of dissociation ($\Delta H_{Diss.}$) can be calculated from the Clausius–Clapeyron equation [84]:

$$\mathrm{d}\ln P / \mathrm{d}\left(1 / T \right) = - \Delta H_{Diss.} / \left(Z \cdot R \right) \qquad (3.12)$$

where Z is the compressibility factor of methane. This can be readily determined by forming a linear relationship between $\ln P$ and $1/T$. The results of this are shown in Table 3.5. For the purposes of this comparison, the compressibility factor of methane was fixed at unity. This would result in the lack of a temperature dependence for the heat of dissociation, although this is not expected to make a significant difference in the calculated value. It is apparent that the GCMC simulations overestimate the heats of dissociation, and it is therefore not always possible to obtain a close fit to the experimental phase equilibrium data (see Table 3.4) while simultaneously predicting a favourable heat of dissociation. However, it can be noted that molecular simulations generally appear to have poor predictive power when estimating the heat of dissociation of methane clathrate hydrate.

As with the calculated phase equilibria, the results from this study compare well with published values obtained via molecular simulation. The value obtained in this study for heat of dissociation for the system containing TIP4P/ice water compares favourably with a previous study [77] which also employed TIP4P/ice water, although in direct coexistence molecular dynamics simulations.

Force fields	Method	Source	$\Delta H_{Diss.}$ / kJ.mol^{-1}	AD / %
SPC water + united atom LJ methane	GCMC adsorption	This study	113.6	45.7
SPC water + TraPPE methane	GCMC adsorption	This study	115.5	48.1
TIP4P/Ice water + united atom LJ methane	GCMC adsorption	This study	102.5	31.1
SPC/E water + OPLS-UA methane	GCMC adsorption	[15]	62.5	19.9
TIP4P water + united atom LJ methane	Direct coexistence MD	[77]	95.5	22.5
TIP4P/2005 water + united atom LJ methane	Direct coexistence MD	[77]	96.9	24.3
TIP4P/2005 water (k_{ij} = 1.07) + united atom LJ methane	Direct coexistence MD	[77]	102.4	31.3
TIP4P/Ice water + united atom LJ methane	Direct coexistence MD	[77]	73.9	5.3
Experimental		[75,76]	78.0	
Calculated	vdWP calculation	[48]	73.6	5.6

Table 3.5. Heat of dissociation ($\Delta H_{Diss.}$) of methane clathrate hydrate calculated from phase equilibrium data. AD is the absolute deviation from the value calculated from experimental data. The methane gas was assumed to be ideal (i.e., Z = 1 in Equation (3.12)) for this comparison.

3.4. CONCLUSIONS

GCMC simulations were used in conjunction with a linearized Langmuir gas adsorption model to show that considering only a single gas adsorption site is valid for sI methane clathrate hydrate. A temperature dependent Langmuir-type adsorption isotherm was then fitted to the present GCMC simulation results.

Phase equilibrium calculations were performed for methane clathrate hydrate using fitted Langmuir-type adsorption isotherms. The calculated phase equilibria compared favourably with previous simulations [15,77] and experiments [75,76]. The calculated phase equilibria were then used to estimate the heat of dissociation of methane clathrate hydrate. The value obtained for the system containing TIP4P/ice water in this study compares favourably with a previous study [77] employing TIP4P/ice water in direct coexistence molecular dynamics simulations.

The results presented in this study demonstrate that GCMC simulations can be used to determine clathrate hydrate phase equilibria, and also show that using a single Langmuir-type adsorption site provides a valid description for methane clathrate hydrate.

REFERENCES

[1] E.D. Sloan, C.A. Koh, Clathrate Hydrates of Natural Gases, CRC Press, Boca Raton, 2008.

[2] E.G. Hammerschmidt, Ind. Eng. Chem. 26 (1934) 851–855.

[3] Welling and Associates, 1999 Survey, cited by N. Macintosh, Flow AssuranceStill Leading Concern among Producers, Offshore, October, 2000.

[4] S. Thomas, R.A. Dawe, Energy 28 (2003) 1461–1477.

[5] A.A. Khokhar, J.S. Gudmundsson, E.D. Sloan, Fluid Phase Equilib. 150 (1998)383–392.

[6] W.L. Mao, H.K. Mao, A.F. Goncharov, V.V. Struzhkin, Q. Guo, J. Hu, J. Shu, R.J.Hemley, M. Somayazulu, Y. Zhao, Science 297 (2002) 2247–2249.

[7] L.J. Florusse, C.J. Peters, J. Schoonman, K.C. Hester, C.A. Koh, S.F. Dec, K.N. Marsh,E.D. Sloan, Science 306 (2004) 469–471.

[8] S.L. Miller, W.D. Smythe, Science 170 (1970) 531–533.

[9] H. Kubota, K. Shimizu, Y. Tanaka, T. Makita, J. Chem. Eng. Jpn. 17 (1984) 423–429.

[10] S.P. Kang, H. Lee, Environ. Sci. Technol. 34 (2000) 4397–4400.

[11] N.I. Papadimitriou, I.N. Tsimpanogiannis, A.K. Stubos, Colloids Surf. A: Physicochem. Eng. Aspects 357 (2010) 67–73.

[12] H. Tanaka, Fluid Phase Equilib. 144 (1998) 361–368.

[13] V.V. Sizov, E.M. Piotrovskaya, J. Phys. Chem. B 111 (2007) 2886–2890.

[14] N.I. Papadimitriou, I.N. Tsimpanogiannis, A.Th. Papaioannou, A.K. Stubos, J.Phys. Chem. C 112 (2008) 10294–10302.

[15] N.I. Papadimitriou, I.N. Tsimpanogiannis, A.K. Stubos, Proceedings of the 7thInternational Conference on Clathrate Hydrates, Edinburgh, United Kingdom, 2011.

[16] K.S. Glavatskiy, T.J.H. Vlugt, S. Kjelstrup, J. Phys. Chem. B 116 (2012) 3745–3753.

[17] M.P. Allen, D.J. Tildesley, Computer Simulations of Liquids, Clarendon Press,Oxford, 1987.

[18] D. Frenkel, B. Smit, Understanding Molecular Simulation, Academic Press, SanDiego, 2002.

[19] N. Metropolis, A.W. Rosenbluth, M.N. Rosenbluth, A.H. Teller, E. Teller, J. Chem.Phys. 21 (1953) 1087–1092.

[20] W.L. Mao, H.-K. Mao, Proc. Natl. Acad. Sci. U. S. A. 101 (2004) 708–710.

[21] W.F. Kuhs, B. Chazallon, P.G. Radaelli, F. Pauer, J. Inclusion Phenom. Mol. Recog-nit. Chem. 29 (1997) 65–77.

[22] B. Chazallon, W.F. Kuhs, J. Chem. Phys. 117 (2002) 308–320.

[23] S. Sasaki, S. Hori, T. Kume, H. Shimizu, J. Chem. Phys. 118 (2003) 7892–7897.

[24] H. Itoh, J.S. Tse, K. Kawamura, J. Chem. Phys. 115 (2001) 9414–9420.

[25] H. Hirai, Y. Uchihara, Y. Nishimura, T. Kawamura, Y. Yamamoto, T. Yagi, J. Phys.Chem. B 106 (2002) 11089–11092.

[26] A.G. Ogienko, A.V. Kurnosov, A.Y. Manakov, E.G. Larionov, A.I. Ancharov, M.A.Sheromov, A.N. Nesterov, J. Phys. Chem. B 110 (2006) 2840–2846.

[27] A.Yu. Manakov, A.G. Dyadin, A.V. Ogienko, E. Kurnosov, E.G.Ya. Aladko, F.V. Lar-ionov, V.I. Zhurko, I.F. Voronin, S.V. Berger, A. Goryainov, A.I.Yu. Lihacheva, A.I.Ancharov, J. Phys. Chem. B 113 (2009) 7257–7262.

[28] H. Hirai, K. Komatsu, M. Honda, T. Kawamura, Y. Yamamoto, T. Yagi, J. Chem.Phys. 133 (2010) 124511.

[29] K.A. Lokshin, Y. Zhao, D. He, W.L. Mao, H.-K. Mao, R.J. Hemley, M.V. Lobanov, M. Greenblatt, Phys. Rev. Lett. 93 (2004) 125503.

[30] I.N. Tsimpanogiannis, N.I. Papadimitriou, A.K. Stubos, Mol. Phys. 110 (2012)1213–1221.

[31] J.H. van der Waals, J.C. Platteeuw, Adv. Chem. Phys. 2 (1959) 1–57.

[32] V.T. John, G.D. Holder, J. Phys. Chem. 85 (1981) 1811–1814.

[33] V.T. John, G.D. Holder, J. Phys. Chem. 86 (1982) 455–459.

[34] V.T. John, G.D. Holder, J. Phys. Chem. 89 (1985) 3279–3285.

[35] V.T. John, K.D. Papadopoulos, G.D. Holder, AIChE J. 31 (1985) 252–259.

[36] P.M. Rodger, J. Phys. Chem. 94 (1990) 6080–6089.

[37] K.A. Sparks, J.W. Tester, J. Phys. Chem. 96 (1992) 11022–11029.

[38] B. Kvamme, A. Lund, T. Hertzberg, Fluid Phase Equilib. 90 (1993) 15–44.

[39] K.A. Sparks, J.W. Tester, Z. Cao, B.L. Trout, J. Phys. Chem. B 103 (1999)6300–6308.

[40] Z. Cao, J.W. Tester, K.A. Sparks, B.L. Trout, J. Phys. Chem. B 105 (2001)10950–10960.

[41] B.J. Anderson, J.W. Tester, B.L. Trout, J. Phys. Chem. B 108 (2004)18705–18715.

[42] B.J. Anderson, M.Z. Bazant, J.W. Tester, B.L. Trout, J. Phys. Chem. B 109 (2005)8153–8163.

[43] P. Englezos, Ind. Eng. Chem. Res. 32 (1993) 1251–1274.

[44] I. Langmuir, J. Am. Chem. Soc. 38 (1916) 2221–2295.

[45] G.D. Holder, S. Zetts, N. Pradhan, Rev. Chem. Eng. 5 (1988) 1–70.

[46] L. Jensen, Experimental Investigation and Molecular Simulation of Gas Hydrates (Ph.D. Thesis), Technical University of Denmark, 2010.

[47] L. Jensen, K. Thomsen, N. von Solms, S. Wierzchowski, M.R. Walsh, C.A. Koh, E.D. Sloan, D.T. Wu, A.K. Sum, J. Phys. Chem. B 114 (2010) 5775–5782.

[48] W.R. Parrish, J.M. Prausnitz, Ind. Eng. Chem. Process Des. Dev. 11 (1972) 26–34.

[49] J.A. Nelder, R. Mead, Comput. J. 7 (1965) 308–313.

[50] D. Weaire, R. Phelan, Philos. Mag. Lett. 69 (1994) 107–110.

[51] W. Thompson, Lord Kelvin, Philos. Mag. 24 (1887) 503–514.

[52] J.D. Gale, A.L. Rohl, Mol. Simulat. 29 (2003) 291–341.

[53] S. Deublein, B. Eckl, J. Stoll, S.V. Lishchuk, G. Guevara-Carrion, C.W. Glass, T. Merker, M. Bernreuther, H. Hasse, J. Vrabec, Comput. Phys. Commun. 182 (2011)2350–2367.

[54] B. Widom, J. Chem. Phys. 39 (1963) 2808–2812.

[55] N.I. Papadimitriou, I.N. Tsimpanogiannis, A.Th. Papaioannou, A.K. Stubos, Mol.Sim. 34 (2008) 1311–1320.

[56] A. Lenz, L. Ojamäe, J. Phys. Chem. A 115 (2011) 6169–6176.

[57] H.J.C. Berendsen, P.J.M. Postma, W.F. van Gunsteren, J. Hermans, in: B. Pullman (Ed.), Intermolecular Forces, Reidel, Dordrecht, 1981, pp. 331–342.

[58] J.L.F. Abascal, E. Sanz, R.G. Fernandez, C. Vega, J. Chem. Phys. 122 (2005) 234511.

[59] J.E. Lennard-Jones, Proc. Phys. Soc. 43 (1931) 461–482.

[60] M.G. Martin, J.I. Siepmann, J. Phys. Chem. B 102 (1998) 2569–2577.

[61] J.M. Smith, H.C. Van Ness, M.M. Abbott, Introduction to Chemical Engineering Thermodynamics, 7th ed., McGraw-Hill, New York, 2005.

[62] J.J. Potoff, A.Z. Panagiotopoulos, J. Chem. Phys. 109 (1998) 10914–10920.

[63] H.A. Lorentz, Ann. Phys. 12 (1881) 127–136.

[64] D.C. Berthelot, Compt. Rend. 126 (1898) 1703–1706.

[65] P.P. Ewald, Ann. Phys. 64 (1921) 253–287.

[66] P. Atkins, J. de Paula, Atkins' Physical Chemistry, 7th ed., Oxford University Press, New York, 2002.

[67] D.-Y. Peng, D.B. Robinson, Ind. Eng. Chem. Fundam. 15 (1976) 59–64.

[68] I. Langmuir, J. Am. Chem. Soc. 40 (1918) 1361–1368.

[69] K.A. Sparks, Configurational Properties of Water Clathrates Through Molecular Simulations (Ph.D. thesis), Massachusetts Institute of Technology, 1991.

[70] M.Z. Bazant, B.L. Trout, Physica A 300 (2001) 139-173.

[71] J.W. Tester, M. Modell, Thermodynamics and Its Applications, 3rd ed., Prentice Hall, Upper Saddle River, 1997.

[72] T. Uchida, T. Hirano, T. Ebinuma, H. Narita, K. Gohara, S. Mae, R. Matsumoto, AIChE J. 45 (1999) 2641–2645.

[73] M.-K. Hsieh, W.-Y. Ting, Y.-P. Chen, P.-C. Chen, S.-T. Lin, L.-J. Chen, Fluid Phase Equilib. 325 (2012) 80–89.

[74] W.M. Deaton, E.M. Frost Jr., Gas Hydrates and Their Relation to the Operation of Natural Gas Pipelines, U.S. Bureau of Mines Monograph 8, 1946.

[75] D.R. Marshall, S. Saito, R. Kobayashi, AIChE J. 10 (1964) 202–205.

[76] M.M. Conde, C. Vega, J. Chem. Phys. 133 (2010) 064507.

[77] B. Guillot, Y. Guissani, J. Chem. Phys. 99 (1993) 8075–8095.

[78] D. Paschek, J. Chem. Phys. 120 (2004) 6674–6690.[77] W.L. Jorgensen, J.D. Madura, Mol. Phys. 56 (1985) 1381–1392.

[79] H.W. Horn, W.C. Swope, J.W. Pitera, J.D. Madura, T.J. Dick, G.L. Hura, T. Head-Gordon, J. Chem. Phys. 120 (2004) 9665–9678.

[80] H. Docherty, A. Galindo, C. Vega, E. Sanz, J. Chem. Phys. 125 (2006) 074510.

[81] E.D. Sloan, F. Fleyfel, Fluid Phase Equilib. 76 (1992) 123–140.

CHAPTER FOUR (BASED ON PAPER III): INFLUENCE OF UNLIKE DISPERSION INTERACTIONS IN MODELING METHANE CLATHRATE HYDRATE

ABSTRACT

Studies of the thermodynamic stability of clathrate hydrates of natural gas (mostly methane) is important in fields such as offshore gas exploitation and energy storage. Two approaches were used to study the effect of unlike dispersion interactions on methane clathrate hydrates: grand canonical Monte Carlo simulations (which yield adsorption data directly and can be used to infer phase equilibria), and estimation of the heat of dissociation coupled with the Clausius-Clapeyron equation (to calculate the phase equilibria, at the expense of providing no information about the adsorption behaviour). It was found that the adsorption isotherm parameters change monotonically with respect to unlike dispersion interactions, although a perfect fit to experimentally-derived values may not be possible, at least using the force fields considered in this study. The heat of dissociation changes monotonically due to changes in the unlike dispersion interaction, and a best fit value of the Berthelot correction factor is achieved.

4.1. INTRODUCTION

Clathrate hydrates resemble ice, and form from a gas species trapped within a network of hydrogen-bonded water molecules. Naturally occurring clathrate hydrates contain primarily methane as the guest molecule, and are found in the deep ocean or permafrost [1]. Methane hydrates are a major concern in offshore operations [2], as it frequently forms blockages in natural gas pipelines [3]. However, methane hydrates are also of interest as an energy storage medium due to the relatively low cost of the storage material, which is essentially water [4,5].

The effect of unlike dispersion interactions on adsorption in methane clathrate hydrates has not yet been studied in detail, although such a study has recently been undertaken for argon clathrate hydrates [6]. The effects of dipole moment, molecular size, and other parameters on the stability of clathrate hydrates have been studied by laboratory experiments [7,8]. However, such experiments do not allow for full control of molecular parameters, which is possible with molecular computations. By varying the molecular properties, the physical mechanisms of guest molecule adsorption can be studied directly.

The standard Lorentz [9] and Berthelot [10] combining rules are commonly used for specifying the

parameters of unlike Lennard-Jones (LJ) interactions [11] between different molecule types [12]. However, their applicability to systems containing nonpolar and polar molecules may not be optimal. For instance, gas-water interactions are not well described by these combining rules [13]. Extensive discussions on the general use of combining rules can be found in the literature [6,13-17], although there is little work with respect to clathrate hydrates. The use of the standard Lorentz and Berthelot rules for clathrate hydrate systems has only recently been discussed in the literature [18].

An extensive study was performed recently to determine the effects of the Lorentz and Berthelot combining rules on adsorption in argon clathrate hydrates [6]. Changes in the Lorentz and Berthelot combining rules resulted in significant changes in adsorption for the sII and sH clathrate hydrate structures, due to the size differential between the cages present in these structures. The effects were considered to be weak for the sI argon clathrate hydrate. It should also be noted, however, that the LJ parameters of argon were adjusted, and not the unlike interactions between argon and water.

The study focuses on the Berthelot rule, since previous studies [18—20] have shown that for spherical (e.g., argon) or approximately spherical molecules (e.g., methane), an additional 'polarizability' contribution to the guest-water interactions must be considered. This is achieved in a computationally expedient way [18] through the introduction of a correction factor to the Berthelot rule. The polarizability contribution is purely a dispersion/energetic effect, and so the size parameter remains unaffected.

4.2. THEORY AND METHODS

4.2.1. CLATHRATE HYDRATE PHASE EQUILIBRIA

Phase equilibria of clathrate hydrates are described using the van der Waals-Platteeuw theory [21]. The phase equilibrium criterion is the equality of the chemical potential of water in the hydrate and liquid phases, each relative to the hypothetical empty hydrate ($\Delta\mu_W^H$ and $\Delta\mu_W^L$, respectively). Calculation of each of these terms can be achieved by [22]:

$$\Delta\mu_W^H = - R \cdot T \cdot \sum_j [\nu_j \ln (1 - \sum_j \theta_{ij})] \qquad (4.1)$$

$$\Delta\mu_W^L = R \cdot T \cdot [\Delta\mu^0 / (R \cdot T_R) - \int_{TR}^{T} \Delta H_W / (R \cdot T^2) \cdot dT + \int_0^P \Delta V_W / (R \cdot T) \cdot dP \qquad (4.2)$$

where the indices i and j refer to the gas species and cavity type, respectively, ν_j is the ratio of water

molecules per unit cell to cavity type j, θ_{ij} is the fractional occupancy of cavity type j by gas species i, $\Delta\mu^0$ is $\Delta\mu_W^H$ at T_R = 273.15 K and P_R = 0 MPa (i.e., the reference state), and ΔH_W and ΔV_W are the differences in enthalpy and molar volume, respectively, between liquid water and the hypothetical empty hydrate in the reference state. Therefore, once the dependence of the fractional occupancy on temperature and pressure is known, phase equilibria can be estimated using the above relationships.

The fractional occupancy, θ, is the number of adsorbed methane molecules per unit cell divided by the total number of adsorption sites per unit cell, N/N_T, and is calculated by using the Langmuir adsorption constant C and the fugacity of the gas species f:

$$\theta = C \cdot f / (1 + C \cdot f) \tag{4.3}$$

Pressure can be substituted for fugacity in eq. (3), since the deviation is not great [23] over the range of experimental data [24,25] for methane clathrate hydrates. A temperature dependence relationship for the Langmuir adsorption constant [26] was fitted [27] to the simulated adsorption isotherms using two parameters A and B:

$$C = (A / T) \cdot \exp (B / T) \tag{4.4}$$

In order to estimate the phase equilibria, eq. (4) can be combined with eqs. (1) through (3).

It was recently found [28,29] that in order to accurately simulate hydrates under equilibrium, the water force field should reproduce the experimental value for the melting point of ice I_h. However, GCMC simulations assume a priori that the hydrate structure is stable under the conditions considered, and moreover, phase equilibrium is not simulated directly using GCMC simulations. GCMC simulations only consider the phenomenon of adsorption into a stable clathrate lattice, and so can only directly provide information on the loading behaviour of clathrate hydrates. Once the loading behaviour is known, the influence of pressure and temperature on occupancy can be ascertained. Since van der Waals-Platteeuw theory [21] can be used to express the chemical potential of the hydrate phase using the occupancy, the dissociation pressure can then be estimated using adsorption isotherms fitted to experimental data [30]. Thus, the phase equilibria are inferred using the pressure- and temperature-dependence of the occupancies.

By expressing the natural logarithm of the dissociation pressure as a function of the reciprocal of temperature, the heat of dissociation ($\Delta H_{Diss.}$) can be related to the slope of the dissociation pressure

curve by the Clausius-Clapeyron equation [31]:

$$d \ln P / d (1 / T) = - \Delta H_{Diss.} / (Z \cdot R) \quad (4.5)$$

where Z is the compressibility factor of methane. Methane was considered as an ideal gas when employing eq. (4.5) in this study, since over the range of experimental temperature and pressure values, the deviation from ideality is not significant [23]. In the case of using GCMC simulations (the first approach considered in this study), the heat of dissociation can only be inferred by examining the effect of adsorption isotherm parameters on the slope of the dissociation pressure curve. In the second approach in this study, the heat of dissociation itself was estimated directly by computing the enthalpies of the hydrate phase, gaseous methane, and liquid water. These calculated values were subsequently used in the integrated form of eq. (4.5) to determine the dissociation pressure curve.

4.2.2. INTERMOLECULAR INTERACTIONS

The LJ potential is frequently used to describe intermolecular interactions [30]. In this work, the adsorption isotherms and the heat of dissociation of methane clathrate hydrate were studied directly for different values of the unlike LJ well depth, ε_{ij}. This was achieved through application of a binary correction factor, k_{ij}, to the Berthelot rule:

$$\varepsilon_{ij} = k_{ij} \cdot (\varepsilon_{ii} \cdot \varepsilon_{jj})^{0.5} \quad (4.6)$$

where ε_{ii} and ε_{jj} are for the intermolecular interactions between like LJ sites. The reference case is k_{ij} = 1.0 (i.e., the Berthelot rule).

It can be noted that the Berthelot rule is a special case of a more general formulation by Reed [33] and extended upon by Hudson and McCoubrey [34], which makes use of both the molecular size parameters and ionization potentials when calculating ε_{ij}. The Berthelot rule is returned from the Hudson and McCoubrey rule when the two molecules possess similar sizes and ionization potentials. Therefore, it is not surprising that the unmodified Berthelot rule may be insufficient to describe interactions between methane and water in clathrate hydrate systems [35].

The LJ parameters (ε_{ii}/k_B = 145.27 K and σ_{ii} = 0.3821 nm) of the united atom (UA) methane were calculated [36] from the critical properties [37], and the Simple Point Charge (SPC) water force field [38] was chosen since it has successfully been used in describing clathrate hydrates (albeit without

directly considering phase equilibria) [27,39]. Since the structure-forming properties of water systems obtained from simulations using different force fields are similar [40], and since methane force field parameters are not significantly different [18], it is expected that trends observed in this study should be similar for other force field combinations. Ewald summation [41] was used for the long-range electrostatic interactions up to a real space cut-off distance of 1 nm, and the LJ interactions were truncated at 1 nm. The force field parameters are shown in Table 4.1.

Force field	Non-bonded interactions (Lennard-Jones [11])	Charges	Bond angle	Bond length
United atom LJ methane [34,35]	ε_{CH4} / k_B = 145.27 K σ_{CH4} = 0.3821 nm			
SPC water [36]	ε_O / k_B = 78.21 K σ_O = 0.3166 nm	q_O = -0.82 e q_H = +0.41 e	$\alpha_{(H\text{-}O\text{-}H)}$ = 109.47 °	$r_{O\text{-}H}$ = 0.1 nm

Table 4.1. Force field parameters used in this study.

4.2.3. GRAND CANONICAL MONTE CARLO SIMULATIONS

The General Utility Lattice Program (GULP) [42] was employed to perform grand canonical Monte Carlo (GCMC) computer simulations [43,44], using the Metropolis scheme [45]. The chemical potential values required as input for the grand canonical ensemble simulations were estimated using Monte Carlo (MC) simulations via the computer program "ms2" [46]. For these simulations, the system consisted of 500 methane molecules and the ratio of translation:volume change moves was 98:2 [47]. The system was relaxed for 100 MC cycles, followed by equilibration in two stages (using the NVT ensemble for $2 \cdot 10^4$ cycles, and then the NPT ensemble for $5 \cdot 10^4$ cycles). $3 \cdot 10^5$ cycles were then used for data production, and Widom's method [48] was employed to estimate the chemical potential using 2000 test particles in every cycle. This procedure was employed previously in conjunction with GCMC simulations [27]. One cycle consists of N moves, where N is the number of molecules in the system.

A single GCMC simulation consisted of 10^7 MC moves (about $1.85 \cdot 10^5$ cycles). The first 25 % of moves were needed to reach equilibrium, since the number of adsorbed gas molecules usually began to plateau after the first 10 % of the simulation. The following types of MC moves were considered: translation/rotation, particle creation, and particle destruction. The translation/rotation moves mimic the thermal motion of molecules within the clathrate hydrate. The creation and destruction moves (which were only allowed for the gas particles) were analogues for the adsorption and desorption of gas molecules, respectively. Each type of move had an equal probability of occurrence (i.e. 33 %), with

translation/rotation moves being equally split within their 33 %. For the sake of rigor, the water molecules were allowed to move (i.e., undergo translation/rotation). The maximum allowed displacement for the translation move was 0.05 nm while no angular limit was set for rotation moves.

A 1x1x1 sI crystal unit cell consisting of 46 water molecules (with periodic boundary conditions) was used, since previous work done with systems of this size [49,50] showed no effects due to finite size or periodicity in GCMC simulations of clathrate hydrate systems. The crystal structure was taken from a previous computational study [51]. The unit cell parameters for the crystal were: $a = b = c = 1.20$ nm and $\alpha = \beta = \gamma = 90^{o}$ [5].

The thermodynamic conditions considered were T = {273.2 K, 280 K, 300 K} and P = {1 MPa, 10 MPa, 60 MPa, 100 MPa}. This ensures that all of the temperature and pressure values along the dissociation curve above the ice-point were studied. Gas adsorption was described using a linearized form [52] of the Langmuir [53] adsorption isotherm:

$$(P / N) = (1 / N_T) \cdot P + 1 / (C \cdot N) \qquad (4.7)$$

where P is the system pressure, N is the number of gas molecules adsorbed per crystal unit cell, C is the Langmuir adsorption constant, and N_T is the total number of possible adsorption sites per crystal unit cell. Thus a plot of (P/N) versus P yields a straight line for an ideal Langmuir adsorption isotherm.

The range of k_{ij} values considered in the GCMC simulations was {0.80, 0.85, 0.95, 1.05, 1.07, 1.10, 1.25}. The results for $k_{ij} = 1.0$ were taken from the literature [27]. This range includes a 'best fit' value of $k_{ij} = 1.07$ obtained from calculations of the excess chemical potential of dilute methane in water [18]. It also takes into account any weak effects that k_{ij} may have on adsorption in methane clathrate hydrate, since a previous study showed no significant effects of the unlike dispersion interaction on adsorption over the range $0.8944 < k_{ij} < 1.0954$ [6].

4.2.4. DIRECT ESTIMATION OF THE HEAT OF DISSOCIATION

Considering eq. (4.5), it is apparent that if a reference state is considered, along with a set of specified pressure values (for example), then the temperature corresponding to the desired dissociation pressure can be calculated.

In order to make use of eq. (4.5), MC simulations were performed using the computer program "ms2" [45] for the fluid phases, in order to estimate the enthalpies of pure liquid water and gaseous methane

at the reference conditions (in this case, P = 2.80 MPa and T = 273.7 K; the experimental data point closest to the ice point of water). For these MC simulations, the parameters were the same as for the simulations used to determine the chemical potential of pure methane (see section 4.2.3), albeit without any use of Widom's method (since it was unnecessary in this case). The same force fields were used as for the GCMC simulations.

For the hydrate phase, GULP [42] was used to calculate the solid phase enthalpy for each k_{ij} value. Since the fluid phases were assumed to be pure, due to the low solubility of gaseous methane in water (and low water content of pure methane gas) over the conditions of interest [54], fluid phase simulations were only required for k_{ij} = 1.0. The starting crystal structure was taken from the literature [51], and the structure was optimized to achieve the lowest energy at constant pressure, following a similar procedure used previously [55].

Once energy of the crystal structure had been minimized, the enthalpy H was computed using for externally specified pressure P and cell volume V, along with the static and vibrational contributions to the internal energy, $U_{Stat.}$ and $U_{Vib.}$, respectively:

$$H = U_{Stat.} + U_{Vib.} + P \cdot V \tag{4.8}$$

The static contribution to the internal energy was calculated from the force field using the spatial coordinates of the interaction sites. The vibrational contribution was calculated using the vibrational frequencies of the lattice, determined from the Hessian matrix. The vibrational frequencies ω were then used to determine $U_{Vib.}$ [56]:

$$U_{Vib.} = \sum_m \sum_k w_k \cdot (0.5 \cdot \omega + h \cdot \omega / (\exp(h \cdot \omega / (k_B \cdot T)) - 1) \tag{4.9}$$

The computation proceeds over m vibrational modes for each point k in reciprocal space, using weights w_k. h and k_B are Planck's and Boltzmann's constants, respectively. For the crystal calculations, the electrostatic charges were included using the Born effective charges [57,58]. It is important to point out that this calculation procedure only applies to the solid hydrate phase, and not to the fluid phases (i.e., gaseous methane and liquid water). For the fluid phases, a similar procedure was used as for the estimation of the chemical potential of methane gas, as described in section 4.2.3.

Once the enthalpies are calculated for the fluid phases and the hydrate crystal, the heat of dissociation can be estimated using the following reaction:

$$5.75\ H_2O \cdot CH_{4(S)} \rightarrow CH_{4(G)} + 5.75\ H_2O_{(L)} \tag{4.10}$$

The hydration number was set to 5.75 since a completely filled methane clathrate hydrate crystal (i.e., $\theta = 1$) forms the basis for the solid phase enthalpy calculation (in the fully occupied methane clathrate hydrate crystal there are 46 water molecules to 8 methane molecules). The heat of dissociation was determined from the differences in enthalpy of the combined hydrate phase, the gaseous methane, and liquid water [59].

For the approach discussed in this section, $k_{ij} = \{1, 1.01, 1.02, 1.025, 1.028, 1.029\ 1.03\}$. This range was selected based on the results of a previous study, which obtained 'best fit' values for methane clathrate hydrate of $1.01 < k_{ij} < 1.03$ [55], depending on whether the lattice constant or a perturbation energy term was considered.

4.3. RESULTS AND DISCUSSION

4.3.1. GRAND CANONICAL MONTE CARLO SIMULATIONS

Changing the unlike dispersion interactions does not significantly change the linearity of the adsorption isotherms at any of the temperatures investigated. In all cases, the adsorption isotherms are linear ($R^2 > 0.98$) when represented in the form of eq. (4.7), thus indicating that the use of a single site Langmuir-type behaviour is reasonable for different values of k_{ij}.

Averaged over all data points in this study, increasing the unlike dispersion interactions resulted in an increased quantity of adsorbed methane relative to the reference state of $k_{ij} = 1.0$ (about 2.5 % for $k_{ij} = 1.10$). Fig. 4.1 shows a plot of the occupancy θ (see eq. (4.3)) as a function of pressure at $T = 273.2$ K for all values of k_{ij} considered in this study (this was done to show a representative data set, since the significant statistical uncertainties make it difficult to discern trends in the raw data). The results for $T = \{280, 300\}$ K can be found in the supplementary material. There is a weak effect of deviation from the standard Berthelot rule (i.e., $k_{ij} = 1.0$) on the adsorption of methane into the clathrate hydrate lattice, especially when the uncertainties in the results of the simulations are considered. This observation concurs with results for sI argon clathrate hydrate obtained by GCMC simulations [6].

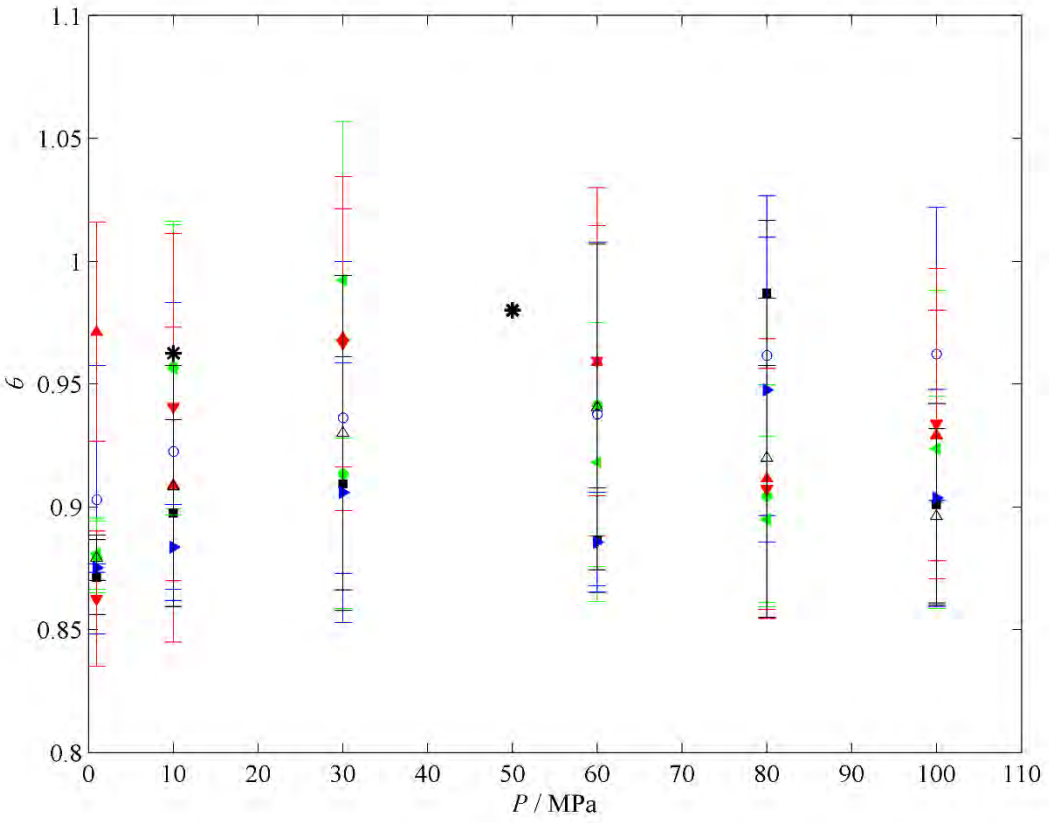

Figure 4.1. Plot of overall fractional occupancy θ (see Equation (4.6)) versus pressure P for sI methane clathrate hydrate at T = 273.2 K. (●) k_{ij} = 0.80, (o) k_{ij} = 0.85, (▲) k_{ij} = 0.95, (■) k_{ij} = 1 [27], (◀) k_{ij} = 1.05, (▶) k_{ij} = 1.07, (▼) k_{ij} = 1.10, (Δ) k_{ij} = 1.25. (*) simulated adsorption data obtained by Papadimitriou and co-workers [23] at T = 273 K.

The adsorption isotherm parameters A and B (see eq. (4.4)) fitted to the results of the GCMC simulations are shown in Table 4.2. There are monotonic trends with respect to both A and B (if the absolute average deviations are considered), which suggest that these parameters, instead of the adsorption isotherm simulation data themselves, can be used to determine a 'best fit' k_{ij} to parameters determined by regression with experimental phase equilibrium data. A is more strongly influenced by unlike dispersion interactions than B.

k_{ij}	A / K.MPa^{-1}	B / 10^3 K	AAD / %
1.25	279	0.564	7.9
1.10	67.0	1.00	4.2
1.07	58.8	0.993	7.5
1.05	27.1	1.31	7.9
1 [27]	19.1	1.31	6.3
0.95	12.2	1.45	8.5
0.85	11.2	1.50	6.8
0.80	9.92	1.50	8.0

Table 4.2. Fitted adsorption isotherm parameters obtained from GCMC simulations; see Equation (4.3). AAD is the absolute average deviation of fitted adsorption isotherms to GCMC simulation results.

It can be noted that sampling larger systems may lead to lower statistical uncertainties (this study employed 1x1x1 crystal unit cells). However, GCMC simulations of clathrates employing 2x2x2 unit cells [6] still encountered sizeable uncertainties (about 2 %, on average, for sI argon clathrate hydrates [6]). This can obscure the presence of any effect of changing the unlike dispersion interaction on gas adsorption in methane clathrate hydrates. However, when considering the adsorption isotherm parameters A and B, there are monotonic trends, which appears to be at odds with the small effect observed for the adsorption isotherms themselves. Importantly, the adsorption isotherms were determined directly, whereas the parameters A and B were fitted to aggregated sets of adsorption isotherm data, and so may more readily capture trends amongst the simulation results as a whole.

The use of a flexible water lattice in this study, while more rigorous than assuming a static crystal structure, results in significantly larger statistical uncertainties (about 4 % on average for the quantity of adsorbed methane), due to the possibility of water molecules occasionally reducing the accessible volume of the cavities within the clathrate lattice, and thus introducing more uncertainty in the acceptance or rejection of insertion of new methane particles as compared to using a rigid lattice.

An additional point to consider is the solution space of the methane clathrate hydrate phase equilibrium calculation. In other words, what sets of A and B values can be fitted to the experimental data, and how do these parameters influence the dissociation pressure curve? To study this, a linearized form of the dissociation pressure curve was considered:

$$\log_{10}(P) = (slope) \cdot T + (intercept) \tag{4.11}$$

The phase equilibria of methane clathrate hydrates over the range of interest are highly linear (R^2 >

0.99), and so it is possible to describe the dissociation pressure curve well using only the slope and intercept of eq. (4.11). Fig. 4.2 shows the slopes, and Fig. 4.3 shows the intercepts of the dissociation curves associated with each pair of A and B values. While there are trends in terms of B versus A for the parameters fitted to the results of GCMC simulations, it is apparent that this trend line would not cut the 'best' fit set of (A,B) values and thus it is not possible to produce a perfect fit to experimental data. The nearest approach to the experimental data (shown by the asterisks in the figures) occurs in the range $1.05 \leq k_{ij} \leq 1.07$, which is near the value of $k_{ij} = 1.07$ obtained previously for the methane-water system [18]. However, the hyperbolic relationship between A and B can never satisfy both the slope and intercept values of the experimental data simultaneously.

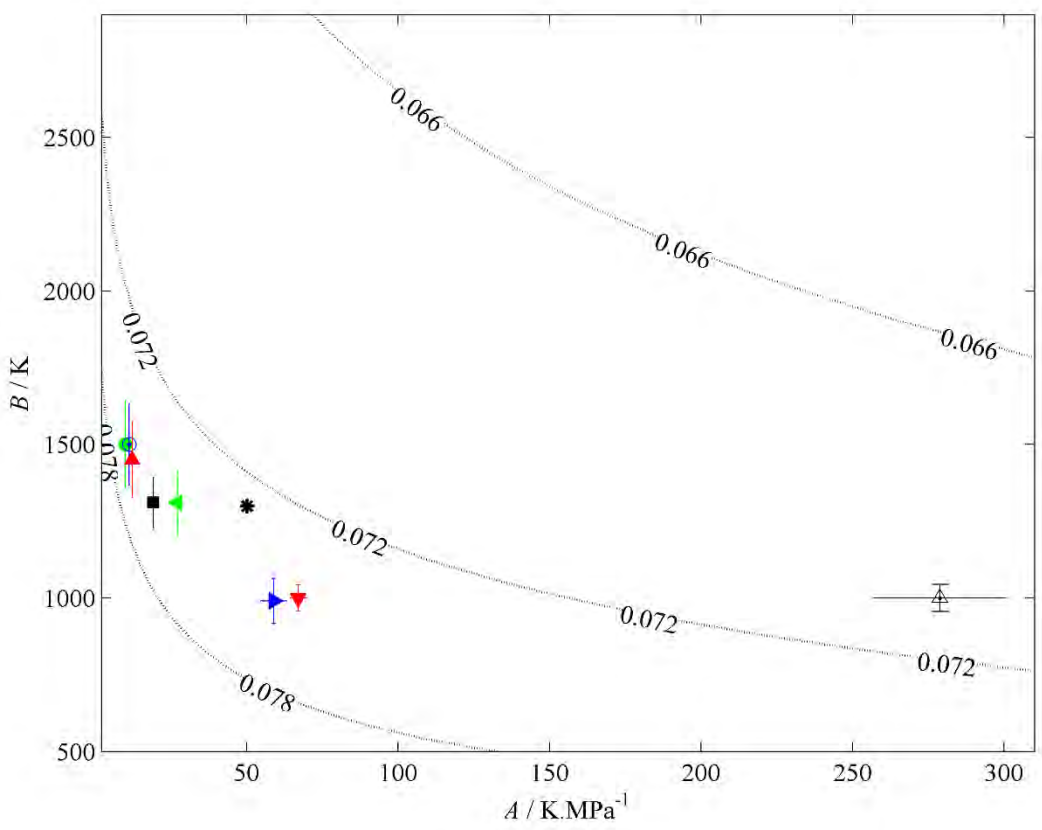

Figure 4.2. Plot of the solution space for the slope of the dissociation pressure curve; see Equation (4.11). (···) lines of constant slope (in K^{-1}), (*) adsorption isotherm parameters fitted to experimental data [24,25]. Adsorption isotherm parameters fitted to GCMC results: (●) k_{ij} = 0.80, (o) k_{ij} = 0.85, (▲) k_{ij} = 0.95, (■) k_{ij} = 1 [27], (◀) k_{ij} = 1.05, (▶) k_{ij} = 1.07, (▼) k_{ij} = 1.10, (Δ) k_{ij} = 1.25.

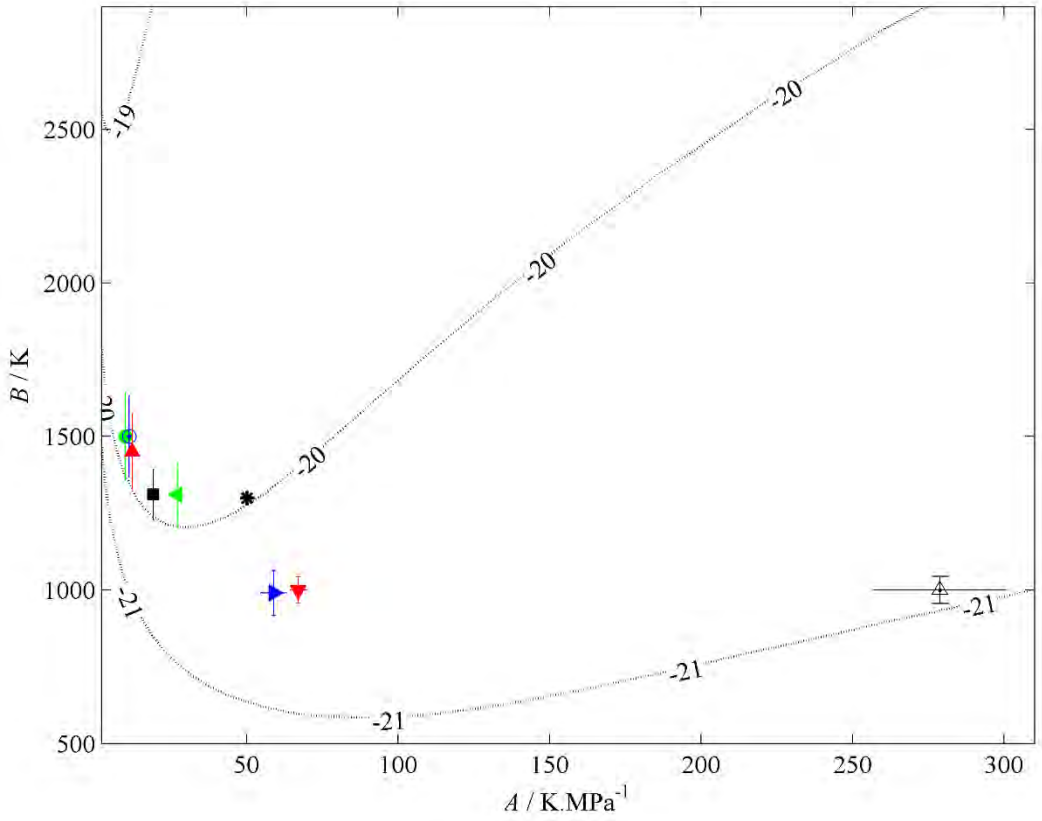

Figure 4.3. Plot of the solution space for the intercept of the dissociation pressure curve; see Equation (4.11). (···) lines of constant intercept (dimensionless), (*) adsorption isotherm parameters fitted to experimental data [24,25]. Adsorption isotherm parameters fitted to GCMC results: (●) k_{ij} = 0.80, (o) k_{ij} = 0.85, (▲) k_{ij} = 0.95, (■) k_{ij} = 1 [27], (◄) k_{ij} = 1.05, (►) k_{ij} = 1.07, (▼) k_{ij} = 1.10, (Δ) k_{ij} = 1.25.

Due to the hyperbolic nature of the trend connecting the values for A and B shown in Figs. 4.2 and 4.3, a similar intercept to that found in experiments [24,25]is achieved for $0.80 < k_{ij} < 0.95$. However, the slope and intercept of the dissociation pressure curve are not achieved simultaneously, and so the calculated phase equilibria cannot match the experimental data. With regard to the interval $1.10 < k_{ij} < 1.25$, the same slope can be achieved as was observed for the experimental data, but the intercept does not match the experimental data. In other words, A is hyperbolically related to B, and this hyperbole never cuts the slope and intercept isolines relating to the experimental data simultaneously, although it cuts one or the other for $0.80 < k_{ij} < 0.95$ and $1.10 < k_{ij} < 1.25$.

Since the slope of the dissociation pressure curve is related to the heat of dissociation (see eq. (4.5)), any effects of unlike dispersion interactions can also be examined via Fig. 4.2. For the range of k_{ij} values in this study, the unlike dispersion interaction does not significantly influence the heat of dissociation. This is evidenced by the fact that the hyperbolic trend connecting all of the values in Fig. 4.2 correlates fairly well with the isoline corresponding to a slope of approximately 0.072 K^{-1}. Therefore, it may not

be possible to fit the heat of dissociation inferred from the results of GCMC simulations using k_{ij}, at least using the force fields considered in this study.

The observations regarding the behaviour of the adsorption isotherm parameters can be considered in relation to a previous study on the argon clathrate hydrates concerning deviations from the Lorentz and Berthelot combining rules [6]. The fact that there are monotonic trends in both A and B with respect to k_{ij}, coupled with the lack of a similar trend in the adsorption of methane into the clathrate hydrate lattice, suggests that the adsorption isotherms of the methane clathrate hydrate 'warp' around the reference state of $k_{ij} = 1.0$. In other words, for a decrease in the unlike dispersion interaction at lower pressures, less adsorption occurred, while at higher pressures, more adsorption occurred (the converse was true for the case of increasing the unlike dispersion interaction). Such behaviour was also observed for the argon clathrate hydrates [6].

In addition to gas adsorption, the relationship between the free energy of the hydrate and the strength of gas-water interactions relative to the water-water interactions should be considered. A thorough study of a variety of hydrates, considering both sI and sII hydrates, showed that if the guest species molecules interact too strongly with the water constituting the hydrate lattice, the hydrogen-bond networks can be disrupted by gas-water interactions [60]. Significantly, the previous study showed that there was a minimum in the residual free energy differences between the hydrate systems with respect to the size parameter, σ_{ii}. In other words, if a gas particle was too small or too large, it would disrupt the water-water interactions that stabilise the clathrate structure. Similarly, the results of the present study show that increasing ε_{ij} can also disrupt the water-water interactions, as evidenced by the decrease in thermodynamic stability shown for $k_{ij} = 1.10$ as compared to $k_{ij} = 1.05$. Therefore, while increasing the unlike dispersion interaction can produce a more realistic description of the methane clathrate hydrate, this effect can only be achieved up to a point, beyond which increasing the gas-water interaction strength will disrupt water-water bonding.

In order to ascertain whether free energy effects play a role in the simulated adsorption of methane, additional calculations were done using GULP. Using geometric coordinate data from the GCMC simulations, Gibbs free energy calculations were done at $T = 280$ K and $P = 10$ MPa (for the sake of comparison), for $k_{ij} = \{1, 1.05, 1.07, 1.1\}$. This set of temperature and pressure values was selected since it lies above the hydrate dissociation line for all values of k_{ij} considered in this study. The Gibbs free energy, G, was estimated by first determining the Helmholtz free energy, A:

$$G = A + P \cdot V \tag{4.12}$$

$$A = U - T \cdot S \tag{4.13}$$

where S is the entropy, which was estimated using the vibrational partition function [56] (see section 2.3.3), and the internal energy U was estimated as before (see section 4.2.4.). It can be noted that vibrational contributions to thermodynamic properties are due to thermal effects, whilst 'static' effects arising from the positioning of molecules are temperature-independent. When calculating the Gibbs free energy, the entropy equal to zero for solid materials when temperature effects are not considered (i.e., at T = 0 K) [61,62].

The results of the free energy calculations are plotted in Fig. 4.4 near the closest fit range observed in Figs. 4.2 and 4.3. Free energies were also calculated from spatial coordinates obtained from additional GCMC simulations at T = 280 K and P = 10 MPa for k_{ij} = {1.06, 1.08} to further examine this range, and are included in Fig. 4.4. A linear trend fitted to the data shows a slight decrease in the Gibbs free energy with increasing k_{ij}, relative to the reference case. It should be noted, however, that the uncertainties are large, in relative terms, due to the fact that the absolute difference in G is less than 5 kJ·mol^{-1} over the range of k_{ij} values considered in this study. Therefore, it is unclear if the unlike dispersion interactions significantly influence the stability of methane clathrate hydrates under the conditions investigated here.

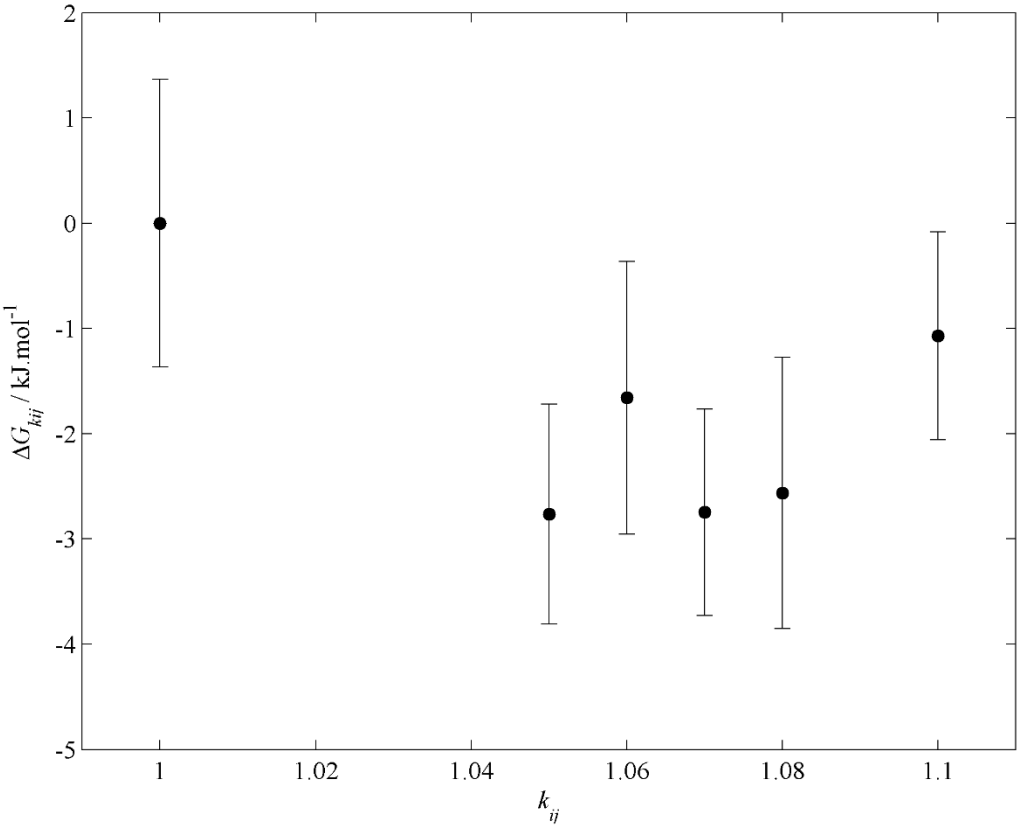

Figure 4.4. Gibbs free energy of the sI methane clathrate hydrate relative to the reference case (i.e., k_{ij} = 1) for different k_{ij} values, at T = 280 K and P = 10 MPa.

The results of the free energy analysis also suggests that, at least at T = 280 K and P = 10 MPa, increasing the amount of adsorbed methane does not produce a significantly more thermodynamically stable sI clathrate hydrate. This suggests that clathrate hydrate stability may not be governed solely by the unlike dispersion interaction.

It should be noted that although k_{ij} = {0.80, 0.95} was considered in this study, this parameter range would not be practical for describing the methane clathrate hydrate system. This is due to the fact that decreasing the unlike dispersion interactions would actually result in the simulated system deviating further from reality than it already does, since a polarizability contribution must be added to the unlike interactions. With respect to the fitted adsorption isotherm parameters (see Table 4.2 and Figs. 4.2 and 4.3), however, the trends observed continue even when decreasing k_{ij} below unity. This must be considered in conjunction with a previous analysis of the relative stability of hydrate structures (i.e., sI, sII or sH) with respect to the unlike dispersion interaction [59]. Should k_{ij} decrease sufficiently, then the most stable structure for methane clathrate hydrate can become sII (below a value of about 6.07 kJ.mol^{-1} for ε_{ij}), which is at odds with current knowledge of methane clathrate hydrate. Therefore, while the

trends may continue monotonically down to a point below $k_{ij} = 1$, it would not be desirable to impose such values for unlike dispersion interactions.

4.3.2. DIRECT ESTIMATION OF THE HEAT OF DISSOCIATION

The results of the calculations described in Section 4.2.4. for the heat of dissociation for various k_{ij} values are shown in Fig. 4.5, and are compared to experimental data obtained by calorimetry [63]. There is a monotonic trend for the heat of dissociation in terms of the unlike dispersion, which suggests that fitting to experimental data may be achieved. For methane clathrate hydrates in particular, a value best matching the calorimetric data is in the range $1.029 < k_{ij} < 1.03$.

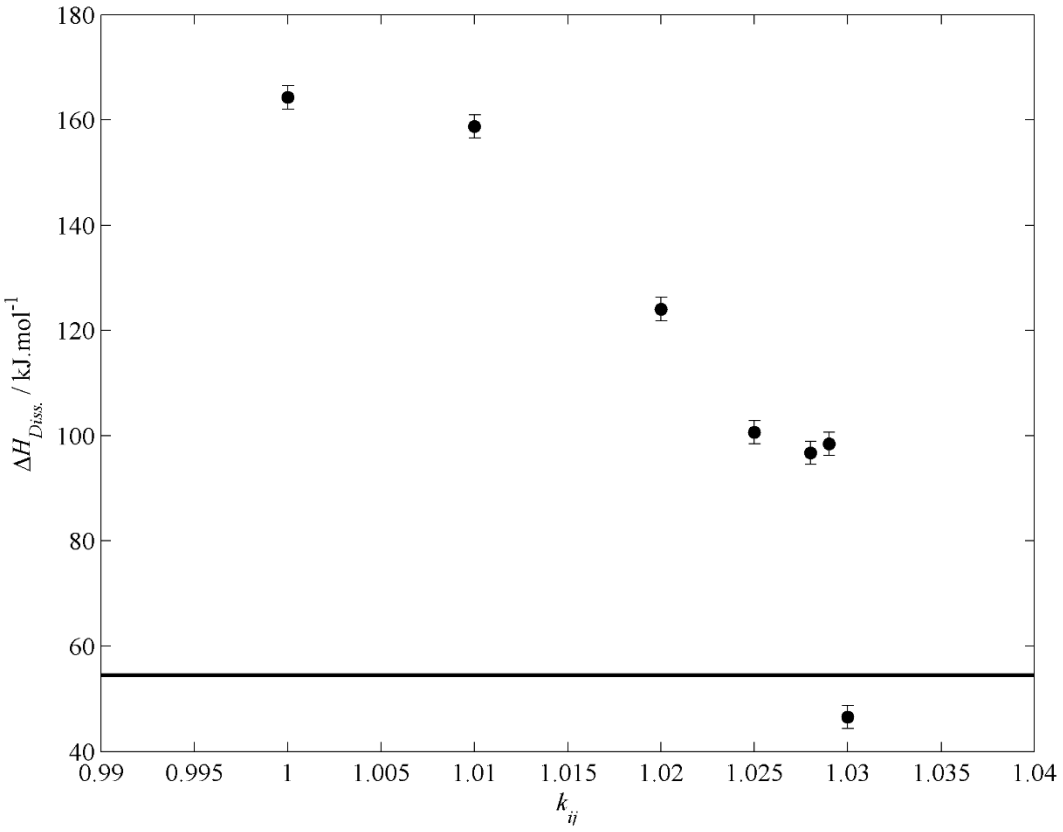

Figure 4.5. Heat of dissociation as a function of k_{ij} for methane clathrate hydrate. The solid line corresponds to a literature value of about 54.4 kJ.mol^{-1} obtained by calorimetry [63].

The decrease in the heat of dissociation with increasing k_{ij} suggests increasing the unlike dispersion interaction reduces the enthalpy difference between the solid phase and the weighted sum of the fluid phases (gaseous methane and liquid water). It is also apparent that the heat of dissociation becomes increasingly sensitive to changes in the unlike dispersion interaction as k_{ij} increases, as evidenced by

the increasingly negative slope of the curve in Fig. 4.5 for $k_{ij} > 1.02$. In a previous study [55], it was found that increasing k_{ij} moderately expands the hydrate crystal, and causes the magnitude of the internal energy of the host water lattice to increase. It can also be expected that increasing k_{ij} increases the internal energy of the combined water-methane clathrate hydrate system. Therefore, since the enthalpy consists (by definition) of internal energy and volume contributions (provided the pressure is constant), it can be expected that increasing the heat of dissociation can be more sensitive to changes in the unlike dispersion interaction than either the internal energy or the cell constant, which was observed in the present study and in the literature [55].

It can be noted that the change in the enthalpy of dissociation appears to be rather abrupt between $k_{ij} = 1.029$ and $k_{ij} = 1.030$, with a reduction in magnitude of approximately 50 %. Changes in the enthalpy of dissociation with respect to the unlike dispersion interaction are dependent only on changes in the enthalpy of the crystalline hydrate phase with respect to the unlike dispersive interactions (since the fluid phase are approximately pure). Therefore, if the crystal lattice calculations are sensitive to changes in the unlike interactions, this sensitivity can be carried through to the estimation of the enthalpy of dissociation. Previously [55], it was found that lattice-based calculations for methane clathrate hydrate can indeed display sensitivity to the unlike dispersion interaction, and therefore the preset observation with regard to the enthalpy of dissociation is not entirely unexpected.

The heat of dissociation from Fig. 4.5 was then used to compute the phase equilibria via eq. (4.5), which are shown in Fig. 4.6. As expected from the calculated heat of dissociation, the phase equilibria show a monotonic trend with respect to k_{ij}. It is also apparent that the 'best fit' value for unlike dispersion interaction obtained by this approach lies in the range $1.029 < k_{ij} < 1.03$, which concurs with the value obtained using the heat of dissociation measured by calorimetry. Previously [55], a value of $k_{ij} = 1.02$ was found to best reproduce the experimental value of the cell constant, which agrees roughly with the value obtained in the present study.

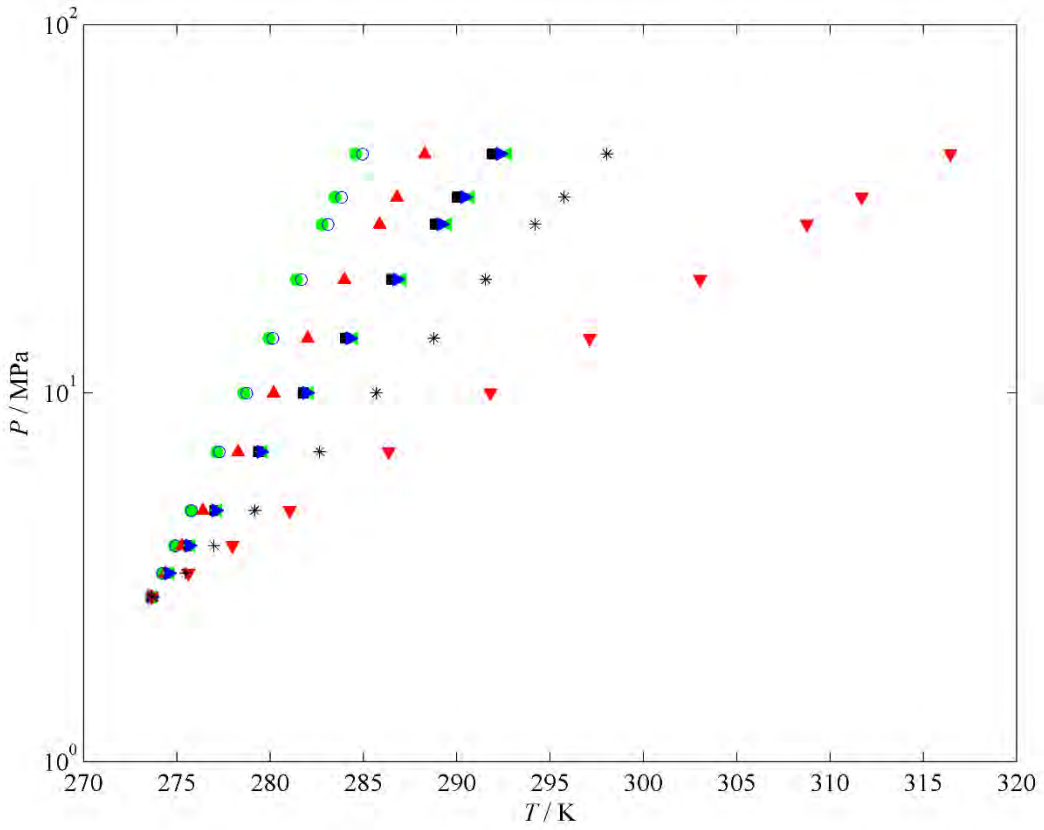

Figure 4.6. Phase equilibria of methane clathrate hydrate, estimated by computing the enthalpy of the fluid phases and the solid phase, for various k_{ij} values: (●) k_{ij} = 1, (o) k_{ij} = 1.01, (▲) k_{ij} = 1.02, (■) k_{ij} = 1.025, (◄) k_{ij} = 1.028, (►) k_{ij} = 1.029, (▼) k_{ij} = 1.03. (*) experimental data [24,25].

A significant drawback of directly estimating the heat of dissociation, as opposed to employing GCMC simulations to infer phase equilibria of clathrate hydrates, is that the occupancy behaviour cannot be computed. At best, Langmuir adsorption isotherm parameters can be fitted to the phase equilibria estimated via the Clausius-Clapeyron equation, although no details about molecular behaviour can be determined by this approach. Therefore, in order to fully study various aspects of clathrate hydrate systems by computational means, it is necessary to employ a variety of methodologies.

4.4. CONCLUSIONS

Adsorption isotherm parameters were fitted to the results of GCMC simulations for a range of k_{ij} values. These parameters change monotonically with respect to unlike dispersion interactions, although a simultaneous fit to both values regressed from experimental phase equilibria is not possible (at least using the force fields considered in this study). The closest fit to experimental data (using GCMC simulations) lies in the range $1.05 < k_{ij} < 1.07$.

The heat of dissociation was estimated directly by computing the enthalpies of the fluid phases (pure

gaseous methane and pure liquid water), and the enthalpy of the solid phase (the methane clathrate hydrate). The unlike dispersion interaction monotonically influences the calculated heat of dissociation, as well as the phase equilibria estimated via the Clausius-Clapeyron equation. A 'best fit' value for k_{ij} (using direct estimation of the heat of dissociation) was found to be in the range $1.029 < k_{ij} < 1.03$.

REFERENCES

[1] E.D. Sloan, C.A. Koh, Clathrate Hydrates of Natural Gases, CRC Press, Boca Raton, 2008.

[2] E.G. Hammerschmidt, Ind. Eng. Chem. 26 (1934) 851–855.

[3] Welling and Associates, 1999 Survey, cited by N. Macintosh, Flow Assurance Still Leading Concern among Producers, Offshore, October, 2000.

[4] S. Thomas, R.A. Dawe, Energy 28 (2003) 1461–1477.

[5] A.A. Khokhar, J.S. Gudmundsson, E.D. Sloan, Fluid Phase Equilib. 150 (1998)383–392.

[6] N.I. Papadimitriou, I.N. Tsimpanogiannis, I.G. Economou, A.K. Stubos, Mol. Phys. (2014) in press.

[7] A.R.C. Duarte, A. Shariati, C.J. Peters, J. Chem. Eng. Data 54 (2009) 1628-1632.

[8] A.T. Trueba, L.J. Rovetto, L.J. Florusse, M.C. Kroon, C.J. Peters, Fluid Phase Equilib. 307 (2011) 6-10.

[9] H.A. Lorentz, Ann. Phys. 12 (1881) 127-136.

[10] D.C. Berthelot, Compt. Rend. 126 (1898) 1703-1706.

[11] J.E. Lennard-Jones, Proc. Phys. Soc. 43 (1931) 461-482.

[12] N.I. Papadimitriou, I.N. Tsimpanogiannis, I.G. Economou, A.K. Stubos, Influence of combining rules on the cavity occupancy of clathrate hydrates: Monte Carlo simulations and van der Waals-Platteeuw-theory-based modeling, Thermodynamics 2013 conference, Manchester, United Kingdom, 2013.

[13] J. Delhommelle, P. Millie, Mol. Phys. 99 (2001) 619-625.

[14] A.J. Haslam, A. Galindo, G. Jackson, Fluid Phase Equilib. 266 (2008) 105-128.

[15] E.L. Johansson, Simulations of water clustering in vapour, hydrocarbons and polymers, PhD thesis, Chalmers University of Technology, 2007.

[16] S. Moodley, E. Johansson, K. Bolton, D. Ramjugernath, Mol. Simulat. 38 (2012) 838-849.

[17] D.-M. Duh, A. Henderson, R.L. Rowley, Mol. Phys. 91 (1997) 1143-1147.

[18] H. Doherty, A. Galindo, C. Vega, E. Sanz, J. Chem. Phys. 125 (2006) 074510.

[19] B. Guillot, Y. Guissani, J. Chem. Phys. 99 (1993) 8075-8094.

[20] D. Paschek, J. Chem. Phys. 120 (2004) 6674-6690.

[21] J.H. van der Waals, J.C. Platteeuw, Adv. Chem. Phys. 2 (1959) 1-57.

[22] G.D. Holder, S. Zetts, N. Pradhan, Rev. Chem. Eng. 5 (1988) 1-70.

[23] N.I. Papadimitriou, I.N. Tsimpanogiannis, A.K. Stubos, in Proceedings of the 7th International Conference on Clathrate Hydrates, Edinburgh, United Kingdom, 2011.

[24] W.M. Deaton, E.M. Frost Jr., Gas Hydrates and Their Relation to the Operation of Natural Gas Pipelines, U.S. Bureau of Mines Monograph 8, 1946.

[25] D.R. Marshall, S. Saito, R. Kobayashi, AIChE J. 10 (1964) 202-205.

[26] W.R. Parrish, J.M. Prausnitz, Ind. Eng. Chem. Process Des. Develop. 11 (1972) 26-34.

[27] M. Lasich, A.H. Mohammadi, K. Bolton, J. Vrabec, D. Ramjugernath, Fluid Phase Equilib. 369 (2014) 47-54.

[28] M.M. Conde, C. Vega, J. Chem. Phys. 133 (2010) 064507.

[29] M.M. Conde, C. Vega, J. Chem. Phys. 138 (2013) 056101.

[30] E.K. Karakatsani, G.M. Kontogeorgis, Ind. Eng. Chem. Res. 52 (2013) 3499-3513.

[31] E.D. Sloan, F. Fleyfel, Fluid Phase Equilib. 76 (1992) 123-140.

[32] R.J. Sadus, Molecular Simulation of Fluids, Elsevier, Amsterdam, 1999.

[33] T.M. Reed III, J. Phys. Chem. 59 (1955) 425-432.

[34] G.H. Hudson, J.C. McCoubrey, Trans. Faraday Soc. 56 (1960) 761-766.

[35] I.N. Tsimpanogiannis, N.I. Papadimitriou, A.K. Stubos, Mol. Phys. 110 (2012) 1213-1221.

[36] J.J. Potoff, A.Z. Panagiotopoulos, J. Chem. Phys. 109 (1998) 10914-10920.

[37] J.M. Smith, H.C. Van Ness, M.M. Abbott, Introduction to Chemical Engineering Thermodynamics, 7th ed., McGraw-Hill, New York, 2005.

[38] H.J.C. Berendsen, P.J.M. Postma, W.F. van Gunsteren, J. Hermans, In: B. Pullman (Ed.), Intermolecular Forces, Reidel, Dordrecht, 1981, pp. 331-342.

[39] S.R. Zele, S.-Y. Lee, G.D. Holder, J. Phys. Chem. B 103 (1999) 10250-10257.

[40] R. Shevchuk, D. Prada-Garcia, F. Rao, J. Phys. Chem. B 116 (2012) 7538-7543.

[41] P.P. Ewald, Ann. Phys. 64 (1921) 253-287.

[42] J.D. Gale, A.L. Rohl, Mol. Simulat. 29 (2003) 291-341.

[43] M.P. Allen, D.J. Tildesley, Computer Simulations of Liquids, Clarendon Press, Oxford, 1987.

[44] D. Frenkel, B. Smit, Understanding Molecular Simulation, Academic Press, San Diego, 2002.

[45] N. Metropolis, A.W. Rosenbluth, M.N. Rosenbluth, A.H. Teller, E. Teller, J. Chem. Phys. 21 (1953) 1087-1092.

[46] J. Vrabec, H. Hasse, Molecular Physics 100 (2002) 3375-3383.

[47] S. Deublein, B. Eckl, J. Stoll, S.V. Lishchuk, G. Guevara-Carrion, C.W. Glass, T. Merker, M. Bernreuther, H. Hasse, J. Vrabec, Computer Physics Communications 182 (2011) 2350-2367.

[48] B. Widom, J. Chem. Phys. 39 (1963) 2808-2812.

[49] N.I. Papadimitriou, I.N. Tsimpanogiannis, A.Th. Papaioannou, A.K. Stubos, J. Phys. Chem. C 112 (2008) 10294-10302.

[50] N.I. Papadimitriou, I.N. Tsimpanogiannis, A.Th. Papaioannou, A.K. Stubos, Mol. Simulat. 34 (2008) 1311-1320.

[51] A. Lenz, L. Ojamäe, J. Phys. Chem. A 115 (2011) 6169-6169.

[52] P. Atkins, J. de Paula, Atkins' Physical Chemistry, 7th ed., Oxford University Press, New York, 2002.

[53] I. Langmuir, J. Am. Chem. Soc. 40 (1918) 1361-1368.

[54] L. Jensen, Experimental Investigation and Molecular Simulation of Gas Hydrates (Ph.D. Thesis), Technical University of Denmark, 2010.

[55] M. Lasich, A.H. Mohammadi, K. Bolton, J. Vrabec, D. Ramjugernath, Phil. Mag. 94 (2014) 974-990.

[56] J.M. Sneddon, J.D. Gale, Thermodynamics and Statistical Mechanics, Royal Society of Chemistry, London, 2002.

[57] W. Cochran, R.A. Cowley, J. Phys. Chem. Solids 23 (1962) 447-450.

[58] S. Baroni, S. de Gironcoli, A. Dal Corso, P. Giannozzi, Rev. Mod. Phys. 73 (2001) 515-562.

[59] L.C. Jacobson, V. Molinero, J. Phys. Chem. B 114 (2010) 7302-7311.

[60] T. Miyoshi, M. Imai, R. Ohmura, K. Yasuoka, J. Chem. Phys. 126 (2007) 234506.

[61] C. Wolverton, A. Zunger, Phys. Rev. B 57 (1998) 2242-2252.

[62] M. K. Aydinol, A. F. Kohn, G. Ceder, K. Cho, J. Joannopoulos, Phys. Rev. B 56 (1997) 1354-1365.

[63] A. Gupta, J. Lachance, E.D. Sloan Jr., C.A. Koh, Chem. Eng. Sci. 63 (2008) 5848-5853.

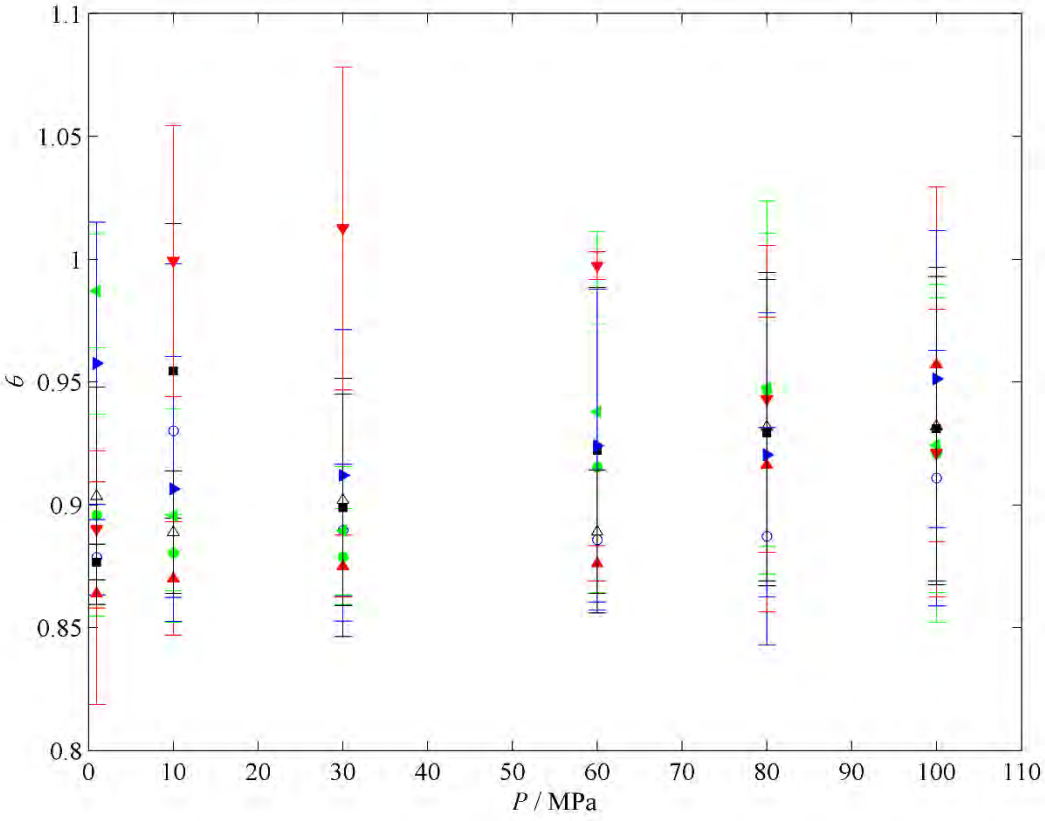

Figure 4.A1. Plot of overall fractional occupancy θ (see Equation (4.6)) versus pressure P for sI methane clathrate hydrate at T = 280 K. (●) k_{ij} = 0.80, (o) k_{ij} = 0.85, (▲) k_{ij} = 0.95, (■) k_{ij} = 1 [27], (◀) k_{ij} = 1.05, (▶) k_{ij} = 1.07, (▼) k_{ij} = 1.10, (Δ) k_{ij} = 1.25. (*) simulated adsorption data obtained by Papadimitriou and co-workers [23] at T = 273 K.

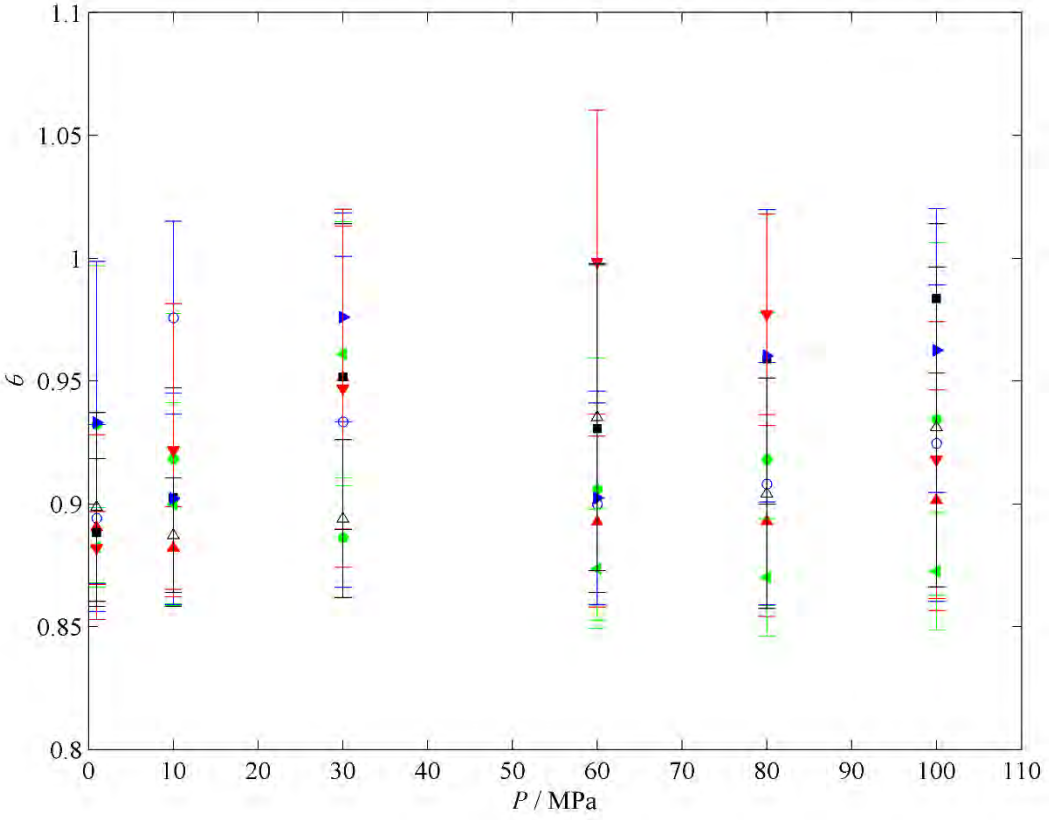

Figure 4.A2. Plot of overall fractional occupancy θ (see Equation (4.6)) versus pressure P for sI methane clathrate hydrate at T = 300 K. (●) k_{ij} = 0.80, (o) k_{ij} = 0.85, (▲) k_{ij} = 0.95, (■) k_{ij} = 1 [27], (◀) k_{ij} = 1.05, (▶) k_{ij} = 1.07, (▼) k_{ij} = 1.10, (Δ) k_{ij} = 1.25. (*) simulated adsorption data obtained by Papadimitriou and co-workers [23] at T = 273 K.

CHAPTER FIVE:
GENERAL DISCUSSION AND CONCLUSIONS

5.1. SUMMARY OF THESIS FINDINGS

The three studies in this thesis have examined the effects of altering the unlike interactions of the LJ potential of the methane clathrate hydrate on various aspects of this system: cell constant (paper I), perturbation potential (paper I), phase equilibria (papers II and III), adsorption behaviour (papers II and III), and heat of dissociation (papers II and III). Although paper I examined the effects of changing both unlike interaction parameters k_{ij} and l_{ij} (see chapter one for a description of these), it is the dispersive correction factor k_{ij} that is of primary interest. This is due to the fact that this term may account effectively for the additional polarizability contribution to the internal energy of the methane clathrate hydrate that occurs due to the water molecules forming ordered structures surrounding the 'guest' methane molecules [1-3].

Paper I showed that changing k_{ij} or l_{ij} does not significantly influence the phonons of the empty hydrate lattice (thereby suggesting that changing k_{ij} or l_{ij} does not significantly alter the physics of the system), and that there are similar trends with respect to both the cell constant and perturbation potential (the properties of interest) when either k_{ij} or l_{ij} is changed. Both quantities of interest were more sensitive to changes in k_{ij}, and the perturbation potential in particular was so sensitive as to be impractical if used to determine k_{ij} by fitting to experimental data. It was also suggested that it may not be possible to simultaneously fit both to the cell constant and to the perturbation energy. Further analysis also suggested that any fitted values could be highly sensitive to the force field parameterization of methane.

Paper I showed for the first time that use of lattice distortion theory to fit LJ interaction parameters k_{ij} and l_{ij} was infeasible, and thus other approaches were considered, as presented in papers II and III. It can also be stated that the effect of changing k_{ij} and l_{ij} on lattice distortion calculations for clathrate hydrates was unknown before the study shown in paper I.

Papers II and III are interlinked, in that paper II successfully established the use of GCMC simulations to estimate the phase equilibria and heat of dissociation of methane hydrate using fitted adsorption isotherms, and paper III used this approach to examine the effects of changing k_{ij} on all three of the aforementioned properties. Paper II also showed that for the case of the methane clathrate hydrate, the use of a single type of adsorption site obeying the Langmuir isotherm was feasible, and thus reduced the number of required adsorption parameters from four to two. It was shown as well that even without adjusting the unlike dispersion interaction, reasonably good fits to experimental phase equilibria could

be achieved. It can be stated that the simplifications to the Langmuir adsorption for methane clathrate hydrate had not been previously proposed or demonstrated, and neither had the prediction of phase equilibria from adsorption isotherms obtained from the results of GCMC simulations.

Paper III illustrated that over the moderate ranges of k_{ij} values usually used in fitting to experimental data, such as $|\Delta k_{ij}| \leq 0.1$ [3-5], there are weak effects on both phase equilibria and heat of dissociation. Due to the use of a flexible water lattice, while more theoretically rigorous, there was an increase in the statistical uncertainties of the results from the GCMC simulations, as compared to the case of a rigid lattice. This also caused difficulties in elucidating trends with respect to phase equilibria and heat of dissociation, as well as adsorption behaviour. However, trends were found with respect to the fitted adsorption isotherm parameters A and B (see papers II and III). Upon examination of the solution space for the methane clathrate hydrate described with these two parameters, it was clear that changing k_{ij} could not result in a closer fit to experimental data than simply not using it. This was due to the fact that based on the trends of A and B, the calculated phase equilibria could never satisfy both the slope and intercept of the linearised form of the dissociation pressure curve (expressed as a function of temperature). It should also be noted that while the effect of k_{ij} on the heat of dissociation is weak, there may be a monotonic trend with respect to this relationship, which was at odds with the use of A and B obtained by simulations to estimate k_{ij} by comparison with experimentally-derived values for A and B. This suggests that it would not be possible to fit to both the heat of dissociation and adsorption isotherm parameters using k_{ij}. With regard to the use of only two parameters A and B to describe a single type of adsorption site obeying the Langmuir isotherm, however, paper III showed that changing the unlike dispersive interaction does not change the fundamental behaviour of the system. It may be noted that the detailed study of the effect of changing unlike interactions on adsorption in methane clathrate hydrate had not previously been demonstrated.

The use of a flexible water lattice in GCMC simulations should be considered in the context of the statistical mechanical theory used to calculate phase equilibria [6]. This theory assumes that the clathrate hydrate crystal has a fixed volume, regardless of the size of the 'guest' molecules, which is obviously true for GCMC simulations (since μ, V, and T are fixed). However, the aforementioned theory also assumes that the water lattice is completely rigid, which was not enforced in the GCMC simulations in this thesis (although in principle it can be). The GCMC simulations were used solely to generate estimates of the occupancy behaviour by methane of the cavities within the clathrate lattice. The fact that these occupancy functions generated reasonably good estimates of the dissociation pressure curves suggests that perhaps there is not a significant difference between a fixed or a flexible lattice. This should be considered, however, together with the fact that the uncertainties for flexible lattice GCMC simulations are significantly larger than for a rigid lattice, and thus this approach yields a less precise estimate for the phase equilibria.

With regard to the sensitivity of the approaches considered in this thesis to force field parameterization, lattice distortion calculations and GCMC simulations yield different results. In paper I, the 'best fit' values of k_{ij} and l_{ij} (to both perturbation energy and cell constant) can vary substantially depending upon the choice of LJ parameters for methane ($0.999 \leq k_{ij} \leq 1.021$, and $1.003 \leq l_{ij} \leq 1.029$ over the range of size and dispersion terms considered). With regard to GCMC simulations, however, paper II showed that there is little sensitivity to the choice of force field for all properties considered (i.e., heat of dissociation, adsorption isotherm parameters, and phase equilibria).

In summary, a list of major findings from this thesis can be drawn:

1. Using the cell constant as a reference point, 'best fit' k_{ij} or l_{ij} values can be determined for methane clathrate hydrate.
2. k_{ij} and l_{ij} cannot be adjusted simultaneously to match both the cell constant and the perturbation energy.
3. Adsorption sites in methane clathrate hydrate can be considered as being of a single type that follows the Langmuir isotherm.
4. Phase equilibria can be predicted reasonably well using adsorption isotherms fitted to the results of GCMC simulations in conjunction with the standard statistical mechanical theory [6].
5. k_{ij} strongly influences adsorption isotherm parameters, and a close (but not exact) match to experimentally-derived parameter values can be achieved.
6. k_{ij} weakly influences the quantity of methane adsorbed.
7. k_{ij} strongly influences the enthalpy of the clathrate hydrate phase.
8. Lattice distortion calculations are sensitive to the choice of force fields used, whereas GCMC simulations behave similarly for different force fields.

5.2. UNLIKE INTERACTIONS AND FITTING TO PROPERTIES

There is no simple explanation on this matter, as it depends upon what quantity is of particular interest. As shown in papers I and III, it is not necessarily possible to fit to all of the desired properties at once. This may be largely due to the limitations of the LJ potential, since it merely approximates the interactions between water and methane, assuming that the interactions are similar in all directions. In reality, methane molecules are not spherical, and are instead tetrahedral and octupolar, and so there will be some deviations from a strictly spherical potential energy function.

That being said, it was possible to fit to two properties quite well, and without unreasonable sensitivity: cell constant and adsorption isotherm parameters. In the former case, $k_{ij} = 1.02$, and in the latter case, $1.05 \leq k_{ij} \leq 1.07$. Even though these k_{ij} values do not coincide, they are both larger than unity, which

concurs with previous observations regarding the need to introduce additional dispersive energy to account for polarizability [1-3]. The second value (or rather range of values) also agrees with the value of k_{ij} = 1.07 obtained using the excess chemical potential of dilute methane in water [3], and then successfully applied to methane clathrate hydrate using direct coexistence MD simulations [5]. It should also be noted that in paper I, a completely filled methane clathrate hydrate was used, whereas for papers II and III, GCMC simulations yielded more realistic occupancies, which was not possible using phonon-based lattice calculations. This feature may account for the lower k_{ij} value obtained in paper I, since more methane was present than in the clathrate hydrates in papers II or III (except for the simulated hydrates considered when directly calculating the heat of dissociation in paper III). Table 1 summarizes the main findings of this thesis in terms of both of the correction factors for the unlike interactions.

Property	k_{ij}	l_{ij}
Perturbation energy	1.002 ± 0.009	1.02 ± 0.01
Cell constant	1.02 ± 0.01	> 1.03
Adsorption isotherm parameters	1.05 – 1.07	N/A
Phase equilibrium	1.029 – 1.03 or 1.05 – 1.07	N/A
Heat of dissociation	1.029 – 1.03	N/A

Table 5.1. Summary of 'best fit' values for k_{ij} and l_{ij} for all properties considered in this thesis.

In terms of fitting both k_{ij} and l_{ij} simultaneously to experimental data, paper I showed that it may be possible to adjust one or both of these correction factors simultaneously to match a desired property. However, it must be stated that adjusting both simultaneously to fit one property would be overfitting, since it was shown in paper I to be possible to fit using only one of k_{ij} or l_{ij}. Moreover, it can also be noted that fitting multiple properties at once by simultaneously adjusting k_{ij} and l_{ij} may not be possible, since (in the case of paper I), the perturbation potential and cell constant were so closely correlated. In order to simultaneously fit several properties using force field correction factors may not be possible using such simple potentials for the intermolecular interactions.

Ultimately, once k_{ij} or l_{ij} have been determined by comparison to experimental data (whatever the quantity of interest may be), then these correction factors can be used in further simulations, with the knowledge that, at least in respect of the chosen quantity, future computations may be more realistic. Also, the magnitude of a 'best fit' value of either k_{ij} or l_{ij} can reveal some information about the methane clathrate hydrate system itself (such as the issue of k_{ij} always being larger than unity, as mentioned above), which will be discussed in the next section.

5.3. SYSTEM RESPONSES TO CHANGING UNLIKE INTERACTIONS

It is not only of interest to determine the values of k_{ij} or l_{ij} which produce an 'optimal' fit to a desired quantity, but it can be instructive to examine the response of the system itself to changes in the unlike interactions. Paper I showed that the perturbation energy decreases due to increases in either k_{ij} or l_{ij}, whereas the cell constant increases roughly linearly when increasing either k_{ij} or l_{ij}. Thus, increasing the strength of the unlike dispersion interaction results in a more negative perturbation energy and an increase in the cell constant. These two quantities are related, since if the crystal lattice expands, the system will deviate further and further from the reference state (i.e. the hypothetical empty hydrate) used in lattice distortion theory [7]. Similarly, increasing the unlike size term (by increasing l_{ij}) will also expand the crystal unit cell, and thus obviously results in a more negative perturbation energy.

Paper I also showed that the perturbation energy and cell constant are related almost linearly, and thus if the cell constant of a simulated methane hydrate system was known, its perturbation energy could be readily estimated. This suggests that the perturbation energy and cell constant are intimately related, and so it is not possible to change one without affecting the other in a predictable, but not necessarily desirable way. Such behaviour can be expected, though, since the perturbation energy is defined as the deviation in host lattice energy from the hypothetical empty hydrate due to distortion by the enclathrated gas species. Therefore, any gas species that causes any sort of distortion in the crystal structure will necessarily alter the perturbation energy considered by lattice distortion theory [7].

Paper III showed that k_{ij} has a weak or unclear effect on adsorption behavior in methane clathrate hydrate. In addition, there were significant statistical uncertainties, which could not be avoided. With respect to the adsorption isotherm parameters, however, there were visible trends. This is due to the fact that fitting these parameters to the results of the GCMC simulations considers aggregated data sets. It was also found that the unlike dispersion interaction did not significantly influence the Gibbs free energy of methane clathrate hydrate, a point which suggests that the free energy of clathrate hydrates is influenced by a multitude of factors. Therefore, it cannot be altered meaningfully by simply applying a LJ correction factor to the force field parameters.

Paper III also showed that by directly computing the heat of dissociation, k_{ij} could indeed be fitted to data measured by calorimetry, although it must be noted that in this case, k_{ij} only affects the hydrate phase (since gaseous methane and liquid water were considered to be pure). Moreover, the unlike dispersion interaction obtained by this approach concurred with the value determined by comparing phase equilibria subsequently inferred using the Clausius-Clapeyron equation. This agreement suggests that this approach is viable to estimate k_{ij} values. It can also be noted that using this approach, increasing the unlike dispersion interaction produced a more stable methane clathrate hydrate (evidenced by the

downward shift of the dissociation pressure curve with increasing k_{ij}). However, it should be stated that this approach only considers a completely filled clathrate lattice, and since the GCMC simulations in paper III showed an insignificant effect of k_{ij} on the Gibbs free energy, it can be concluded that the unlike dispersion interactions, fractional occupancy of the clathrate lattice by gas molecules, and the Gibbs free energy are intimately related to one another.

5.4. OUTLOOK AND FUTURE WORK

In the preceding sections, general conclusions were drawn from the results of this thesis, as presented in papers I, II, and III. However, the results of the studies in this work do yield further avenues of investigation, and indeed, future work can produce a more complete description of several features of methane clathrate hydrate (and perhaps clathrate hydrates in general) examined in this thesis.

Paper II showed that the use of a single Langmuir adsorption site type is a reasonable approximation for methane clathrate hydrate. However, this would obviously not be the case for all clathrate hydrate systems due to the fact that other molecules (such as ethane) may not fit easily into the small cavities of the clathrate crystals. Therefore, it can be instructive to manipulate the molecular size parameter of the adsorbed gas species to determine the threshold at which this approximation is no longer valid.

Since paper III showed that the effect of k_{ij} on gas adsorption in methane clathrate hydrate is insignificant, it can be useful to increase the range of k_{ij} values considered in subsequent studies, possibly to unrealistic values (e.g. $k_{ij} = 10$). This may yield deeper information on the role of unlike dispersion interactions in gas adsorption in clathrate hydrate systems.

The success of the second approach used in paper III (i.e., directly calculating the heat of dissociation) suggests that the validity of its more general use should be investigated. Thus, this aspect of the study can be repeated for a variety of clathrate hydrate systems, especially those consisting of gas mixtures.

REFERENCES

[1] B. Guillot, Y. Guissani, J. Chem. Phys. 99 (1993) 8075-8094.

[2] D. Paschek, J. Chem. Phys. 120 (2004) 6674-6690.

[3] H. Doherty, A. Galindo, C. Vega, E. Sanz, J. Chem. Phys. 125 (2006) 074510.

[4] E.L. Johansson, Simulations of water clustering in vapour, hydrocarbons and polymers, PhD thesis, Chalmers University of Technology, 2007.

[5] M.M. Conde, C. Vega, J. Chem. Phys. 133 (2010) 064507.

[6] J.H. van der Waals, J.C. Platteeuw, Adv. Chem. Phys., 2 (1959) 1-59.

[7] S.R. Zele, S.-Y. Lee, G.D. Holder, J. Phys. Chem. B, 103 (1999) 10250-10257.